Attorney Docket No. 9536-3 PATENT

IN THE UNITED STATES PATENT AND TRADEMARK OFFICE

In re: Vance et al.
Application No.: 10/623,930
Filed: July 21, 2003
For: *Compositions and Methods for the Modulation of Gene Expression In Plants*

Confirmation No.: 6465
Group Art Unit: 1638
Examiner: V. Kumar

Date: January 3, 2007

Mail Stop RCE
Commissioner for Patents
P.O. Box 1450
Alexandria, VA 22313-1450

Tab A

Attorney Docket No. 9536-3 PATENT

IN THE UNITED STATES PATENT AND TRADEMARK OFFICE

In re: Vance et al.
Application Serial No.: 10/623,930
Filed: July 21, 2003
For: *Compositions and Methods for the Modulation of Gene Expression In Plants*

Confirmation No.: 6465
Group Art Unit: 1638
Examiner: V. Kumar

Declaration of Vicki Bowman Vance, Ph.D.
Pursuant to 37 C.F.R. § 1.132

I, Vicki Bowman Vance, do hereby declare and say as follows:

1. I am a named inventor under United States Application No. 10/623,930 ("the '930 application") and of the subject matter claimed therein.

2. I have a Ph.D. in Plant Biology, from Washington University (St. Louis, MO). I am a Professor of Biological Sciences at the University of South Carolina, Columbia, SC. Presently, I am also serving as Program Director, National Science Foundation, Molecular and Cellular Biology Division. I am involved in research in the area of gene silencing in plants and have authored or co-authored more than 16 publications related to this area. A *curriculum vitae* is attached herewith at Appendix B.

3. The practice of this invention entails using natural plant genes that encode microRNAs (miRNAs) and modifying those genes using standard recombinant DNA technology, known in the art at the time of filing of the 093 application, so that "artificial" miRNAs are produced that target the RNAs of choice. MiRNAs are small RNAs (usually 21-24 nucleotides long) that incorporate into a large protein silencing complex and guide that complex to a particular target RNA and prevent the target RNA from producing protein, either by blocking translation or, more commonly in plants, by causing the target RNA to be cleaved. MiRNAs are not transcribed directly from their genes as 21-24 nucleotide small RNAs, but are made as longer precursor RNAs that contain a stem-loop structure in which the miRNA sequence is found within one arm or the other of the stem. The initial miRNA transcript is called a primary transcript (or the pri-miRNA) and usually contains sequences both upstream and downstream of the stem-loop structure. However,

it is the stem-loop structure that is important for the proper processing events needed to produce a mature functional miRNA.

An intermediate step in miRNA production is the production of the stem-loop structure itself, which is called the precursor miRNA or pre-miRNA. MiRNAs and the stem-loop precursors from which they are derived were well known in the art at the time of filing of the present application. The primary literature describing plant miRNA precursors is cited in the application (Reinhart et al., Genes Dev.16(13): 1616-26 (2002) and Llave et al., Plant Cell. 14(7): 1605-19 (2002); copies provided with applicants' response dated August 10, 2006). Reviews describing the structures of the precursors that are processed to produce the mature functional miRNAs have also been published (for example, Bartel and Bartel, Plant Physiol. 132(2): 709-17 (2003) and Kidner and Martienssen, Trends Genet. 19(1): 13-6 (2003); copies provided with applicants' response dated August 10, 2006). Thus, plant miRNAs and their precursors, as well as the technology used to isolate them, were well known in the art at the time of filing the '093 application.

4. The structures of 863 plant stem-loop miRNA precursors are currently available at a website described by Griffiths-Jones and colleagues (Nucleic Acids Res. 34(Database issue): D140-42006 (2006); copy enclosed at Appendix C). The first release of this database was in July of 2003 (Release 2.0). Only the stem-loop structure is reported, because the actual length of the primary transcript is not known in most cases. However, as stated above, it is the stem-loop that is the important part of the miRNA precursor. Thus, miRNAs and their precursors were well known in the art at the time of filing the present application, and this information was then and remains easily and publicly accessible.

5. The '093 invention describes a general strategy to make "designer miRNAs" (also referred to as "artificial miRNAs" or "synthetic miRNAs") that target cellular or viral RNAs making use of the natural miRNA genes cited above. Thus, the natural miRNA sequence within the natural miRNA gene is modified so that it is now the desired "artificial" miRNA. To ensure that the newly designed miRNA remains within the proper context of the natural miRNA precursor and is therefore properly processed, the sequences opposite (or complementary) to the artificial miRNA in the stem are also modified to maintain the secondary structure of the stem. The modifications needed to produce a stem-loop that is

subsequently processed into an artificial miRNA utilize straightforward recombinant DNA technologies that were standard in the art at the time of filing of the '093 application.

Further, since the filing of the present application, the invention has been successfully practiced by several independent labs, each using a different miRNA gene as the backbone. The results of the successful use of the invention have been published in highly respected scientific journals and some of these are briefly described below.

a) The Vaucheret lab successfully demonstrated the making and using of the invention by modifying one of the genes that encodes miRNA 168 (miR168) in the model plant *Arabidopsis thaliana*. The miR168 gene was modified to change the natural miR168 sequence within the precursor to one targeting a messenger RNA different from the original miR168 target. The other side of the stem structure in the precursor was modified to maintain the secondary structure of the engineered miR168 precursor, as taught in the invention. The desired target was cleaved in transgenic plants thereby demonstrating the success of the invention. This work was published in 2004 (Vaucheret et al., Genes Dev. 18(10):1187-97 (2004); copy provided with applicants' response dated August 10, 2006).

b) The use of the present invention was recently demonstrated in a more global way in the Weigel lab (Schwab et al., Plant Cell. 18(5):1121-33 (2006); copy provided with applicants' response dated August 10, 2006). These investigators used two different miRNA genes (miR172a and miR319a) as backbones to produce designer miRNAs to target specific genes as taught by the invention. They refer to the designer miRNAs produced this way as artificial miRNAs (amiRNAs). The investigators reported that both miR172a and miR319a genes worked well for producing amiRNAs and that they were able to target a variety of endogenous plant genes in a very efficient and straightforward manner using the amiRNA technology.

c) The invention was also successfully used in a publication appearing in 2006 (Alvarez et al., Plant Cell. 18(5):1134-51 (2006); copy enclosed at Appendix D). These authors used the Arabidopsis miR164b gene as the backbone of their artificial miRNA. The artificial miRNA was targeted to a set of three endogenous Arabidopsis genes by designing an artificial miRNA that was complementary to a sequence common to the expressed messenger RNAs of all three Arabidopsis RNAs. Thus, the authors

demonstrated that a single artificial miRNA could be used to target multiple RNAs. This publication concludes that "miRNAs provide a flexible, quantitative, and autonomous platform that can be employed for regulated expression of multiple related genes in diverse species."

d) A fourth publication demonstrates that the artificial miRNA invention can also be successfully employed to target viral RNAs that are required for the replication of certain plant viruses, thereby establishing resistance to the targeted virus (Niu et al., Nat Biotechnol. 24(11):1420-8 (2006); copy enclosed at Appendix E). In this published work, the authors used a miRNA gene encoding miR159 as the backbone for their artificial miRNA. As seen in the previous examples as well as in this case, the modifications to the miRNA gene, to modify the natural miRNA sequence to the desired artificial miRNA and, subsequently, to modify the opposite strand of the precursor to maintain proper secondary structure of the precursor, were techniques known in the art at the time of filing of the present application. These technologies are straightforward and successful and show that the invention works very well. These authors also point to the general applicability of the technology and the ease with which it can be used.

e) The Niu et al, 2006 reference also demonstrates the use of a "dimeric miRNA precursor" to produces two different artificial microRNAs from the same precursor. In this case, the authors first engineered two different artificial miRNA precursors using the miR159 stem-loop backbone and demonstrated the efficacy of each independently. Then they constructed a dimeric gene, which contained the two individual artificial miRNA constructs ligated together and under control of the same promoter. Thus, the two miR159 stem-loop structures, each containing a different artificial miRNA, were part of the same miRNA precursor. This dimeric precursor strategy was quite effective and allowed the investigators to produce two different artificial miRNAs in a coordinated fashion.

6. Finally, the Nui et al., 2006 publication also brings up a point that relates to the ease with which the invention can be practiced. The whole process can be pre-tested using a well-established standard transient assay called agro-infiltration. The agro-infiltration assay was developed early on for work on RNA silencing (Brigneti et al., EMBO

J. 17(22): 6739-46 (1998); Johansen and Carrington, Plant Physiol. 126(3):930-8 (2001); copies enclosed at Appendix F) and was later very successfully adapted to the evaluation of endogenous microRNAs and their targets (Llave et al, Science. 297(5589):2053-6 (2002); copy enclosed at Appendix G). This standard assay can be used both to ensure that the artificial miRNA is properly produced from the modified gene and that the artificial miRNA will work to cleave the desired target. Thus, the success of the particular artificial miRNA can be quickly and easily assayed before proceeding to make stable transgenic plants. In the transient agro-infiltration assay, the binary plasmid carrying the modified miRNA gene is transformed into Agrobacterium and then the transformed bacteria are infiltrated into the leaves of *Nicotiana benthaminiana*. The accumulation of the desired artificial miRNA can then be assayed by standard technologies such as those described in these publications and well known in the art at the time the application was filed, including Northern gel blot analysis. Similarly, to determine if the artificial miRNA will cleave the desired target, the two constructs (one expressing the artificial miRNA and the other the putative target RNA) can be co-infiltrated into the same spot on the same leaf and the cleavage of the target at the miRNA target site assayed by standard methods, including Northern gel blot analysis and 5' Rapid Amplification of cDNA Ends (5'-RACE).

7. I hereby declare that all statements made herein of my own knowledge are true and that all statements made on information and belief are believed to be true; and further that these statements were made with the knowledge that willful false statements and the like so made are punishable by fine or imprisonment, or both, under Section 1001 of Title 18 of the United States Code and that such willful false statements may jeopardize the validity of the application or any patent issued thereon.

Vicki Bowman Vance, Ph.D. 1/2/2007

Vicki Bowman Vance, Ph.D. Date

Curriculum Vitae

NAME	POSITION TITLE
Vicki Bowman Vance	Professor of Biological Sciences

EDUCATION/TRAINING

INSTITUTION AND LOCATION	DEGREE	YEAR	FIELD OF STUDY
Eastern Illinois University (Charleston, IL)	BS	1971	Botany
University of Illinois at Medical Center (Chicago, IL)	MS	1973	Microbiology
Washington University (St. Louis, MO)	Ph.D.	1983	Plant Biology

A. Positions and Honors.

Positions and Employment

1972-1973	Bacteriologist, USDA Dairy Testing Laboratory, Chicago, IL
1973-1975	Clinical Virologist, Municipal Contagious Disease Hospital, Chicago, IL
1977-1978	Lab Specialist, Department of Biology, University of Virginia, Charlottesville, VA (C.P. Emerson, Advisor)
1983-1988	Postdoctoral Research Fellow, Department of Biology, University of South Carolina, Columbia, SC (09/83-09/84, with L. Bowman, ribosomal RNA studies; 10/84-02/85, with M. R. Stallcup, *in vitro* transcription studies; 03/85-02/88, with A. Huang, plant molecular biology studies)
1988-1989	Research Assistant Professor, Dept of Biology University of South Carolina, Columbia, SC
1989-1995	Assistant Professor, Dept of Biological Sciences, University of South Carolina, Columbia, SC
1995-2000	Associate Professor, Dept of Biological Sciences, University of South Carolina, Columbia, SC
2000-present	Professor, Dept of Biological Sciences, University of South Carolina, Columbia, SC
2003-present	Wade T. Batson Jr. Professor of Botany
2005-present	Co-founder and Vice President of Research for GEOGENETICS, INC
2006-2007	Program Director, National Science Foundation, Molecular and Cellular Biology Division, Genes and Genomes Cluster

Other Experience, Professional Memberships, and Achievements

1992-present	Member, American Society of Virology
1993	Convener, Plant Virus Replication Section, American Society of Virology meeting
1996, 99, 03	Review Panel Member, USDA National Research Initiative Competitive Grants Program (Plant Pathology and Genetic Mechanisms Panels)
1997-present	Member, American Phytopathological Society
1997-1999	Virology Committee, American Phytopathological Society
1999	Principal co-inventor, US patent no. 5,939,541: "Method for Enhancing Expression of a Foreign or Endogenous Gene Product in Plants"
2000-present	Member, American Society of Plant Biologists
2001	Review Panel Member, NIH study section CDF-1 (Mar. 15-16, 2001)
2002	Inventor, US patent no. 6,395,962: "Compositions and methods for modulating gene expression in plants"
2002&2003	Review Panel member, NIH study section SSS-Y (Nov. 13-15, 2002; July 9-11, 2003)
2005	Principal co-inventor, US patent no. 6,806,400: "Method for Enhancing Pathogen Resistance in Plants"
2005	Inventor, US Patent no, 6,972,349: "Control of Post-Transcriptional Gene Silencing in Plant"
2006	NSF 2010 Review Panel Member, May 10-12, 2006

2006 NSF/USDA Joint Microbial Genome Sequencing Program Panel Member, May 29-31, 2006.

Honors

1971-1972 Graduate Fellowship, University of Illinois at Medical Center
1981-1983 Pioneer Seed Fellow, Washington University
1993 Elected "Preferred Faculty Member," University of South Carolina
2001 Invited Speaker for Council for the Advancement of Science Writers (November, 2001)
2002 Certificate of Appreciation from Patterson Hall residents, USC
2003 Appointed Wade T. Batson, Jr. Professor of Botany (August, 2003)
2004 Finalist for Michael J. Mungo Teaching Award
2006 USC Russell Research Award recipient

B. Peer-reviewed Publications; Patents

1. **Vance, V. B**. and Beachy, R.N. (1984) Translation of soybean mosaic virus RNA *in vitro*: Evidence of protein processing. *Virology* 132: 271-281.
2. **Vance, V. B**. and Beachy, R.N. (1984) Detection of genomic-length soybean mosaic virus RNA on polyribosomes of infected soybean leaves. *Virology* 138: 26-36.
3. **Vance, V. B.**, Thompson, E.F. and Bowman, L.H. (1985) Transfection of mouse ribosomal DNA into rat cells: Faithful transcription and processing. *Nucleic Acids Research* 13: 7499-7513.
4. Qu, R., Wang, S.M., Lin, Y., **Vance, V. B**. and Huang, A.H.C. (1986) Characterization and biosynthesis of membrane proteins of lipid bodies in the scutella of maize. *Biochem. J.* 235: 57-65.
5. Huang, A.H.C., Qu, R., Wang, S.M., **Vance, V. B.**, Cao, Y. and Lin, L. (1987) Synthesis and degradation of lipid bodies in the scutella of maize. In: The metabolism, structure and function of plant lipids. (P.K. Stumpf, J.B. Mudd and W.D. Nes, eds.) pp. 239-246. Plenum Press, New York.
6. **Vance, V. B.** and Huang, A.H.C. (1987) The major protein from lipid bodies of maize: Characterization and structure based on cDNA cloning. *J. Biol. Chem.* 262: 11275-11279.
7. **Vance, V. B.** and Huang, A.H.C. (1988) Expression of lipid body protein gene during maize seed development: spatial, temporal and hormonal regulation. *J. Biol. Chem.* 263: 1476-1481.
8. Qu, R., **Vance, V. B**. and Huang, A.H.C. (1990) Expression of genes encoding oleosin isoforms in the embryos of maturing maize kernels. *Plant Science* 72: 223-232.
9. **Vance, V. B.** (1991) Replication of potato virus X RNA is altered in co-infections with potato virus Y. *Virology* 182: 486-494.
10. Scott, S.W., **Vance, V. B.**, and Bachman, E.J. (1992) The use of nucleic acid probes for the detection of necrotic ringspot virus and prune dwarf virus. *Acta Horticulturae* 309: 79-84.
11. **Vance, V. B**., Jordon, R.L., Edwardson, J.R., Christie, R.G., Purciful, D.E., Turpen, T. and Falk, B.W. (1992) Evidence that pepper mottle virus and potato virus Y are distinct viruses: Analysis of the 3'untranslated and coat protein sequences of a California isolate of pepper mottle virus. *Archives of Virology* (suppl. 5): 337-345.
12. **Vance, V. B.**, Moore, D., Turpen, T.H., Bracker, A. and Hollowell, V.C. (1992) The complete nucleotide sequence of pepper mottle virus genomic RNA: Comparison of the encoded polyprotein with those of other sequenced potyviruses. *Virology* 191, 19-30.
13. Bachman, E., Scott, S., Xin, Ge and **Vance, V.B**. (1994) Complete nucleotide sequence of prune dwarf viral RNA 3: Implications for coat protein activation of genome replication in ilarviruses. *Virology* 201, 127-131.
14. **Vance, V. B**., Berger, P.H. Carrington, J.C., Hunt, A.G. and Shi, X.M. (1995). 5' proximal potyviral sequences mediate potato virus X/potyviral synergism in transgenic tobacco. *Virology* 206, 583-590.
15. Sriskanda, V., Pruss, G., Ge, X., **Vance, V. B.** (1996). An eight-nucleotide sequence in the potato virus X 3' untranslated region is required for both host protein binding and viral multiplication. *J. Virol.* 70, 5266-5271.
16. Shi, X.M., Miller, H., Verchot, J., Carrington, J.C. and **Vance, V. B.** (1997). Mutations in the region encoding the central domain of HC-Pro eliminate PVX/potyviral synergism. *Virology* 231, 35-42.
17. Pruss, G., Ge, X., Shi, X.M., Carrington, J.C. and **Vance, V. B.** (1997). Plant viral synergism: The potyviral genome encodes a broad range pathogenicity enhancer that transactivates replication of heterologous viruses. *Plant Cell.* 9, 859-868.

18. Anandalakshmi, R., Pruss, G.J., Ge, X., Marathe, R., Mallory, A.C., Smith, T.H., and **Vance, V. B.** (1998) A viral suppressor of gene silencing in plants. *PNAS USA* 95, 13079-13084. **(this article was the subject of a News and Views in Nature)
19. Marathe, R.J., Smith, T. H., Anandalakshmi, R., Bowman, L.H., Fagard, M., Mourrain, P., Vaucheret, H., and **Vance, V. B.** (2000) Plant viral suppressors of post-transcriptional silencing do not suppress transcriptional silencing. *Plant J.* 22, 51-59.
20. **Vance, V. B.** (2000) Plant Viral Synergism. In *Encyclopedia of Plant Pathology.* Edited by O. C. Maloy & T. D. Murray. New York: John Wiley and Sons.
21. Anandalakshmi, R., Marathe, R., Ge X., Herr, J.M., Mallory, A., Mau, C., Pruss, G., Bowman, L., and **Vance, V. B.** (2000) A calmodulin-related protein from tobacco suppresses post-transcriptional gene silencing. *Science* 290, 142-144.
22. Mallory, A.C., Ely, L., Smith, T. H., Marathe, R., Anandalakshmi, R., Fagard, M., Vaucheret, H., Pruss, G., Bowman, L., and **Vance, V. B.** (2001) HC-Pro suppression of transgene silencing eliminates the small RNAs but not transgene methylation or the mobile silencing signal. *Plant Cell* 13, 571-583.
23. Matzke, M.A., Matzke, A.J., Pruss, G., and **Vance, V.B.** (2001) RNA-based silencing strategies in plants. *Curr. Opin. Genet. Dev.* 11, 221-227.
24. **Vance, V.B**. and Vaucheret, H. (2001) RNA silencing in plants – defense and counterdefense. *Science* 292, 2277-2280.
25. Mlotshwa, S.,Voinnet, O., Mette, M.F., Matzke,M., Vaucheret, H., Ding, S.W., Pruss,G., and **Vance, V.B.** (2002) RNA silencing and the mobile silencing signal. *Plant Cell,* 14 supplement, S289-301.
26. Mallory, A., G. Parks, M. Endres, Baulcombe, D., Bowman, L. **Vance, V. B.** (2002) The amplicon-plus system for high-level expression of transgenes in plants. *Nature Biotechnology* 20, 622-625.
27. Mallory, A.C., Reinhart, B.J., Bartel, D., **Vance, V.B.*** and Bowman, L.H.* (2002) A viral suppressor of RNA silencing differentially regulates the accumulation of short interfering RNAs and microRNAs in tobacco. *PNAS USA* 23, 15228-15233. *these authors contributed equally to the work
28. Mallory, A.C., Mlotshwa, S., Bowman, L.H. and **Vance, V.B.** (2003) The capacity of transgenic tobacco to send a systemic RNA silencing signal depends on the nature of the inducing transgene locus. *Plant J.* 35, 82-92.
29. Pruss, G.J., Lawrence, C.B., Bass, T., Li, Q., Bowman, L.H., and **Vance, V.** (2004) The potyviral suppressor of RNA silencing confers enhanced resistance to multiple pathogens. *Virology* 320, 107-20.
30. Wang M.B., Bian X.Y., Wu L.M., Liu L.X., Smith N.A., Isenegger D., Wu R.M., Masuta C., **Vance V.B.**, Watson J.M., Rezaian A., Dennis E.S., Waterhouse P.M. (2004) On the role of RNA silencing in the pathogenicity and evolution of viroids and viral satellites. *Proc Natl Acad Sci U S A.* 101, 3275-80.
31. Roth, B.M., Pruss, G.J. and **Vance V.B.** (2004) Plant viral suppressors of RNA silencing. *Virus Res.* 102, 97- 108.
32. Adai, A., Johnson, C., Mlotshwa, S., Archer-Evans, S., Manocha, V., **Vance, V.** and Sundaresan, V. (2005) Computational prediction of miRNAs in Arabidopsis thaliana. *Genome Res.* 15, 78-91.
33. Mlotshwa, S., Schauer, S., Smith, T. H., Mallory, A., Herr, J.M., Roth, B., Merchant, D., Ray, A., Bowman, L. and **Vance, V.** (2005) Ectopic DICER-LIKE1 Expression in P1/HC-Pro Arabidopsis Rescues Phenotypic Anomalies but not Defects in MicroRNA and Silencing Pathways. *Plant Cell* 17, 2873-85.
34. Johnson, C., Bowman, L., Adai, A.T., **Vance, V.** and Sundaresan, V. (2006) CSRDB: A Small RNA Integrated Database and Browser Resource for Cereals. Nucleic Acids Research, epub ahead of print December 14.
35. Mlotshwa, S., Li J., Chen, X., Poethig, S., Bowman, L.H. and **Vance, V.B.** (2006) Required Roles for *Arabidopsis* DICER-LIKE2 and DICER-LIKE4 in RNA Silencing. In Preparation.

Patents

Issued US Patents

- Inventor, US patent no. 6,395,962: "Compositions and methods for modulating gene expression in plants"

- Principal co-inventor, US patent no. 5,939,541: "Method for Enhancing Expression of Foreign or Endogenous Gene Products in Plants"
- Principal co-inventor, US patent no. 6,806,400: "Method for Enhancing Resistance in Plants"
- Inventor, US patent no. 6,972,349: "Control of Post-Transcriptional Gene Silencing"

Patents Pending

- Principal co-inventor, "Compositions and Methods for Modulation of Gene Expression in Plants", filed July, 2003, pending.
- Principal co-inventor, "An Endogenous Regulator of RNA Silencing in Plants", filed June 2005, pending.

C. Invited Presentations (2003-2006)

Seminars at Research Level

- East Carolina Medical School, Greenville, NC January 2003
- University of California, Davis: student invited seminar speaker, February 2003
- Wayne State University, Detroit Michigan, March 2003
- University of Maryland, College Park, Maryland, April, 2003
- Maxygen Inc., Santa Clara, California, July 2003
- Michigan State University, East Lansing, Michigan, September 2003
- University of Minnesota, St. Paul, MN, June 2-4, 2004
- Monsanto Company, St. Louis, MO, June 14-15, 2005.
- University of South Carolina, Aiken, September 14, 2005.
- Syngenta Biotechnology, Inc., November 14, 2005.

Seminars Given for General Audience

- Preston Lecture, Preston Residential College, April 9, 2003.
- Regional InnoVenture, Columbia, SC, July 14, 2005.
- Mentor Presentation to Howard Hughes Academic Year Scholars and NSF Plant Genome Scholars, November 11, 2005

Invited Conference Presentations (2003-2006)

- 45th Annual Maize Genetics Conference, Lake Geneva, Wisconsin, March 13-16, 2003.
- 4th Annual Arabidopsis Minisymposium, Keynote Speaker, University of Maryland, April 12-13, 2003.
- University of Florida, Plant Molecular and Cellular Biology 2003 Workshop, Keynote Speaker, Daytona Beach, Florida, May 9-10, 2003.
- Gordon Conference, Viruses and Cells, Il Ciocco Italy, Session Chair, May 18-23, 2003.
- EMBO Workshop-Genomic Approaches in Plant Virology. Keszthely, Hungary May 28-31, 2003.

- American Society of Virology, Plenary Speaker, UC Davis, July 12-16, 2003.
- Plant Genetics 2003: Mechanisms of Genetic Variation, Snowbird, Utah, October 22-26, 2003.
- National Congress of Plant Biochemistry and Molecular Biology, Acapulco, Mexico, November 3-7, 2003.
- US-Egypt Partnership, Science and Technology Agreement, NSF Workshop on Genetic Engineering and Genomics, Mubarak City, Egypt, Dec. 5-8, 2003.
- The 25th Annual Lorne Genome Conference, The Organization and Expression of the Genome, Lorne, Victoria, Australia, 2/15/2004.
- Sackler Colloquium, RNAi, National Academy of Sciences, Washington DC, 5/16/2004-5/18/2004
- 2004 World Congress on In Vitro Biology, San Francisco, CA, 5/22/2004-5/25/2004.
- American Society of Virology, Montreal, Canada, 7/9/2004-7/11/2004.
- Banbury Center Meeting, "RNAi-Related Processes in Plants: Chromatin, Development and Defense", Cold Spring Harbor, NY, 8/15/2004-8/18/2004.
- 2004 SC EMBER Conference on Life Sciences, Isle of Palms, SC 10/18/2004-10/19/2004.
- Conference on Plant-Made Pharmaceuticals, Montreal, Canada, 1/30/04-2/03/05.
- Noble Foundation Virology Mini-Retreat, Ardmore, Oklahoma, 4/1/05-4/3/05.
- 22nd Annual Stony Brook Symposium, Stony Brook University, 5/22/05-5/24/05.
- The 5th Symposium of Post-transcriptional Regulation of Plant Gene Expression, University of Texas at Austin, 6/8/05-6/12/05.
- 8th Annual Awardee Meeting, Plant Genome Research Project, National Science Foundation, September 8-9, 2005.
- XII International Molecular Plant Microbe Interactions Congress, Keynote Speaker, Merida, Yucatan, Mexico, December 14-18, 2005.
- RESISTVIR IVth Meeting entitled "Advances on sources, mechanisms and durability of resistance to plant viruses/vectors", Alicante, Spain, February 2-5.

- InnoVenture 2006, Selected Presenter for GeoGenetics, Inc., March 28-29.
- 16th Penn State Plant Physiology Symposium entitled "RNA Biology: Novel Insights from Plant Systems", Pennsylvania State University, University Park, PA, May18-20.
- 9th Annual Awardee Meeting, Plant Genome Research Project, National Science Foundation, September 7, 2006.
- Symposium on Plant Regulatory RNAs, Institute of Plant and Microbial Biology, Academia Sinica, Taipei, Taiwan, September 8-9, 2006.
- Joint US/India Workshop on Agricultural Biotechnology for the Global Public Good, Chennai, India, Organized by the National Academy of Sciences on behalf of the US State Department, October 5-8, 2006

D140–D144 Nucleic Acids Research, 2006, Vol. 34, Database issue
doi:10.1093/nar/gkj112

miRBase: microRNA sequences, targets and gene nomenclature

Sam Griffiths-Jones*, Russell J. Grocock, Stijn van Dongen, Alex Bateman and Anton J. Enright

The Wellcome Trust Sanger Institute, Wellcome Trust Genome Campus, Hinxton, Cambridge CB10 1SA, UK

Received September 12, 2005; Revised and Accepted October 18, 2005

ABSTRACT

The miRBase database aims to provide integrated interfaces to comprehensive microRNA sequence data, annotation and predicted gene targets. miRBase takes over functionality from the microRNA Registry and fulfils three main roles: the miRBase Registry acts as an independent arbiter of microRNA gene nomenclature, assigning names prior to publication of novel miRNA sequences. miRBase Sequences is the primary online repository for miRNA sequence data and annotation. miRBase Targets is a comprehensive new database of predicted miRNA target genes. miRBase is available at http://microrna.sanger.ac.uk/.

INTRODUCTION

MicroRNAs (miRNAs) are a class of non-coding RNA gene whose final product is a ~22 nt functional RNA molecule. They play important roles in the regulation of target genes by binding to complementary regions of messenger transcripts to repress their translation or regulate degradation (1–3). miRNAs have been implicated in cellular roles as diverse as developmental timing in worms, cell death and fat metabolism in flies, haematopoiesis in mammals, and leaf development and floral patterning in plants [reviewed in (4,5)]. Recent reports have suggested that miRNAs may play roles in human cancers (6–8).

The biogenesis of miRNA sequences has been largely elucidated [reviewed in (9)]. The mature miRNA (often designated miR) is processed from a characteristic stem–loop sequence (called a pre-mir), which in turn may be excised from a longer primary transcript (or pri-mir). Only a handful of primary transcripts have been fully described, but evidence suggests that miRNAs are transcribed by RNA polymerase II, and that the transcripts are capped and polyadenylated.

Since the discovery of the founding members of the miRNA class, lin-4 and let-7 in *Caenorhabditis elegans* [reviewed in (10)], over 2000 miRNA sequences have been described in vertebrates, flies, worms and plants, and even in viruses. However, the functions of only a handful of these miRNAs have been experimentally determined. In parallel with novel gene identification efforts, the miRNA community is therefore focused on predicting and validating miRNA gene targets.

The miRBase database brings together the gene naming and sequence database roles previously fulfilled by the microRNA Registry (11), with the first automated pipeline for predicting miRNA target genes in multiple animal genomes. These three functions are briefly discussed in turn.

miRBase REGISTRY

The rapid growth of the miRNA field has been facilitated by the adoption of a consistent gene naming scheme, which has been applied since the first large-scale miRNA discoveries (12–14). The miRNA Registry (11) has acted as an independent arbiter of gene names, and this function is continued by the miRBase Registry. Names are assigned by the Registry based on guidelines agreed by a number of prominent miRNA researchers and discussed elsewhere (15). In order to minimize the gaps in the naming scheme and to take advantage of the peer review process to assess the validity of submitted miRNAs, names are assigned after a manuscript describing their discovery is accepted for publication. Official gene names should be incorporated into the final version of a manuscript. The nomenclature guidelines require that novel miRNA genes are experimentally verified by cloning or with evidence of expression and processing. Homologous miRNAs from related organisms that are identified by sequence analysis methods may be named without the need for further experimental evidence.

miRNAs are assigned sequential numerical identifiers. The database uses abbreviated 3 or 4 letter prefixes to designate the species, such that identifiers take the form hsa-miR-101 (in *Homo sapiens*). The mature sequences are designated 'miR' in the database, whereas the precursor hairpins are labelled 'mir'. The gene names are intended to convey limited information about functional relationships between mature miRNAs. For example, hsa-miR-101 in human and mmu-miR-101 in mouse

*To whom correspondence should be addressed. Tel: +44 1223 834244; Fax: +44 1223 494919; Email: sgj@sanger.ac.uk

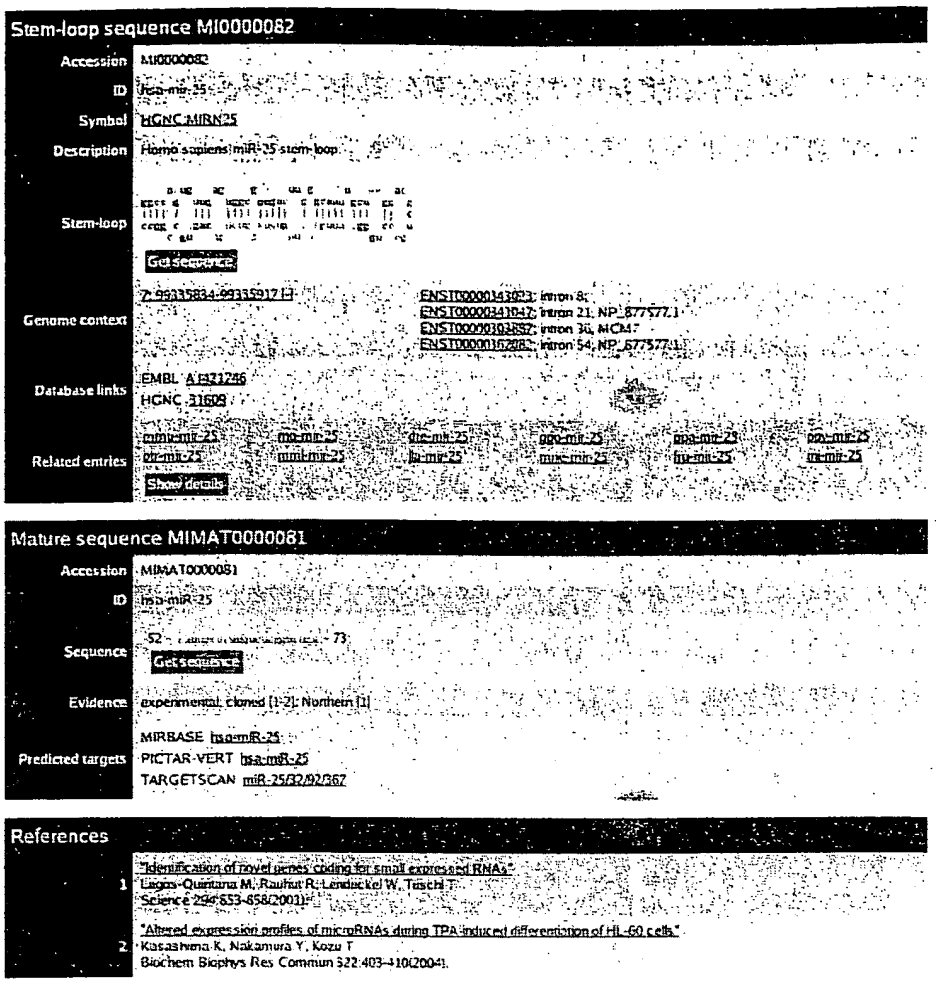

Figure 1. The sequence database entry for hsa-mir-25. The three sections of the page describe the predicted stem–loop hairpin, mature sequences and primary references. The genomic coordinates and contextual information link to the Ensembl database. Each mature miRNA contains an evidence field, and links are provided to predicted target pages.

are orthologous. Paralogous sequences whose mature miRNAs differ at only one or two positions are given lettered suffixes—for example, mmu-miR-10a and mmu-miR-10b in mouse. Distinct hairpin loci that give rise to identical mature miRNAs have numbered suffixes (e.g. dme-mir-281-1 and dme-mir-281-2 in *Drosophila melanogaster*). It should be noted that plant and viral naming schemes differ subtly.

However, miRNA names should not be relied upon to convey complex relationship information. Naming criteria may be subtly redefined over time, and opinion on the degree of conservation of mature sequence required for functional redundancy varies—some recent studies suggest that only the 5′ so-called seed region of the sequence forms a tight duplex with the target mRNA (16). Related hairpin precursor sequences may give rise to mature sequences with only marginal similarity and different miRNA numbers. The naming scheme is also complicated by instances where two different mature miRNA sequences appear to be excised from opposite arms of the same hairpin precursor. Such mature sequences are currently named of the form miR-17-5p (5′ arm) and miR-17-3p (3′ arm). Complex sequence relationships and names are discussed with the submitting author on a case by case basis.

miRBase SEQUENCES

In parallel with the miRNA community's need for a consistent naming scheme, miRNA research and informatics has benefited greatly from a dedicated database of miRNA sequences and annotation. The miRBase Sequence database takes over from the microRNA Registry database as the primary repository for miRNA data. We briefly describe recent growth and database improvements.

Rapid database growth

The miRBase Sequence database contains sequences of all published mature miRNA sequences, together with their predicted source hairpin precursors and annotation relating to their discovery, structure and function. The database has grown rapidly in the past 2 years, from 506 entries representing miRNA hairpin precursors in six species (release 2.0, June 2003) to 2909 entries in 36 species (release 7.0, June 2005).

Stable accessions

miRNA names may change in time to reflect newly discovered relationships between sequences. Stable database accession

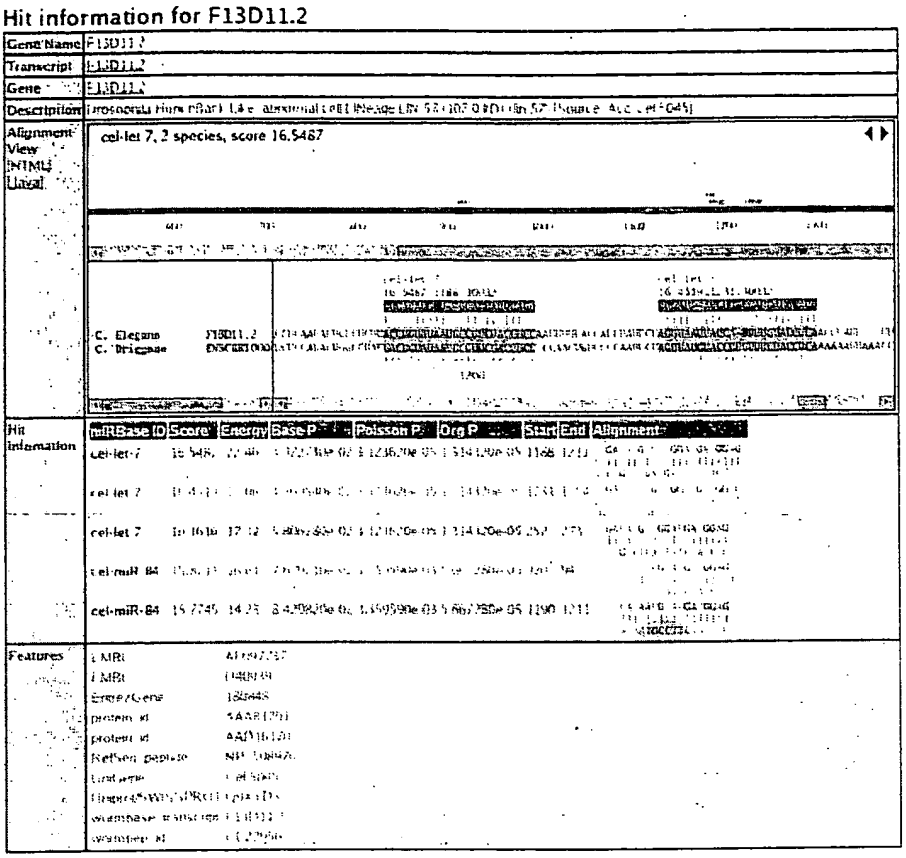

Figure 2. miRBase Target view page for transcript F13D11.2. The alignment view shows the alignment of miRNA binding sites in orthologous 3′-UTRs. Bits scores, *P*-values, folding energies and alignments are shown for each miRNA match.

numbers are therefore assigned to both hairpin (e.g. MI0000015) and mature (e.g. MIMAT0000029) sequences to enable tracking of sequence entities. A summary of the differences between releases is available. In addition, human and mouse gene symbols are provided in consultation with the Genome Nomenclature Committees (HGNC and MGNC).

Evidence tracking

The database contains miRNAs from two fundamentally different sources. Experimentally verified mature miRNAs are annotated with primary literature references and the experimental method used for discovery. The database also contains sequences that are predicted homologs of miRNAs verified in a related organism. For example, 223 of 313 distinct mature miRNA sequences from human (71%) have experimental evidence in human, while the remainder are clearly identifiable homologs of verified miRNAs from mouse, rat and zebrafish. Homologs are predicted based on sequence similarity and folding characteristics of the precursor hairpin, synteny analysis and conservation of the mature miRNA. The source of every miRNA is clearly annotated on the miRNA entry page (Figure 1) and distributed in the flat file downloads. The miRBase Sequence database does not currently contain predicted miRNAs that are without experimental evidence in any related organism.

Genomic context

For organisms with an assembled genome sequence we provide coordinates of the genomic position of each miRNA sequence on the entry page (Figure 1) and also in GFF format on the FTP site. miRNA genes may be located within other genes, both protein-coding and non-coding (17,18), and the context of the genomic location with respect to Ensembl genes is also annotated (Figure 1). 35% of mammalian miRNA loci overlap annotated genes—over 90% of these are located in introns. In comparison, ~14% of worm and fly miRNAs are intronic. Distributed annotation system (DAS) sources provide easy access to miRNA genomic locations, and the data are available for viewing within the Ensembl (19) and UCSC browsers (20).

miRBase TARGETS

As focus shifts from miRNA gene identification to functional characterization, miRBase includes not only miRNA sequence data but also information about their genomic targets. The function of a specific miRNA can be thought of as a product of the genes that it regulates. Although large-scale experimental detection of targets is currently difficult, a number of computational techniques exist for the prediction of miRNA targets in mRNA sequences (16,21–27). These methods can be used both to predict potential targets for miRNAs

and for the selection of targets for experimental validation. For the most part, computational methods rely on first detecting potential binding sites (with a large degree of complementarity to the miRNA), followed by filtering out those sites that do not appear to be conserved in multiple species. This approach appears to work well, at least for species that have clearly defined orthologs in closely related species (e.g. human, mouse and rat). However, the conservation criterion is poor for those species for which we do not have closely neighbouring genome sequences.

The miRBase Targets database uses a novel fully automated pipeline (which will be described in detail elsewhere) to address some of these issues. All animal miRNA sequences from the miRBase Sequence database are scanned against 3′-untranslated regions (3′-UTRs) predicted from all available species in Ensembl (19) along with *Caenorhabditis briggsae* and *Drosophila pseudoobscura*. The core algorithm assigns *P*-values to individual miRNA–target binding sites, multiple sites in a single UTR, and sites that appear to be conserved in multiple species based on robust statistical models (22). The interface connects each miRNA to a list of predicted gene targets. The detailed target view page (Figure 2) illustrates individual binding sites for one or more miRNAs and their target in an orthologous 3′-UTR alignment. We are in the process of including annotation of experimentally validated miRNA targets.

The miRBase Target database is designed with two main aims: to make available high-quality targets in a timely manner, and to remain as inclusive as possible with respect to the target prediction community. To this end, we provide a core set of predictions that are updated concurrently with the rest of the miRBase system. We also intend to provide a mechanism for viewing and comparing third-party target predictions contributed via DAS. The core predictions are generated in-house using the miRanda algorithm (v3.0) (21). The strengths of miRanda are that it is open source, scalable and incorporates robust statistical models. The provision of a *P*-value for each miRNA–target assignment allows the user to assess the confidence in the prediction. In addition, the method does not assume that the miRNA binding sites *must* be conserved, although in practice the most highly significant *P*-values tend to represent miRNA–target interactions that are conserved across multiple species. As new insights into miRNA–target binding mechanisms and improved prediction algorithms become available, they will be integrated into the system to provide the highest-quality target predictions to the user. In parallel with the miRBase Target pipeline, miRNA sequence entries also provide links to third-party target prediction websites (Figure 1).

AVAILABILITY

The miRBase database is freely available to all for online searching at http://microrna.sanger.ac.uk/. Sequences and annotation are also available for download from the FTP site in a number of formats, including FASTA format sequences and relational database dumps for easy upload to a MySQL or other database. Queries, feedback and data submissions and revisions are welcome by email to microrna@sanger.ac.uk.

ACKNOWLEDGEMENTS

We thank Mhairi Marshall and John Tate for website design, and are grateful to David Bartel and Tom Tuschl for ongoing nomenclature discussion. We also thank Michel Weber for assistance in providing data for viewing in the UCSC genome browser, Marc Rehmsmeier for discussion of *P*-value statistics and Antonio Giraldez for experimental work on target verification. Work at the Sanger Institute is supported by the Wellcome Trust. Funding to pay the Open Access publication charges for this article was provided by the Wellcome Trust.

Conflict of interest statement. None declared.

REFERENCES

1. Bartel,D.P. (2004) MicroRNAs: genomics, biogenesis, mechanism, and function. *Cell*, **116**, 281–297.
2. Filipowicz,W., Jaskiewicz,L., Kolb,F.A. and Pillai,R.S. (2005) Post-transcriptional gene silencing by siRNAs and miRNAs. *Curr. Opin. Struct. Biol.*, **15**, 331–341.
3. Sontheimer,E.J. and Carthew,R.W. (2005) Silence from within: endogenous siRNAs and miRNAs. *Cell*, **122**, 9–12.
4. Ambros,V. (2004) The functions of animal microRNAs. *Nature*, **431**, 350–355.
5. Kidner,C.A. and Martienssen,R.A. (2005) The developmental role of microRNA in plants. *Curr. Opin. Plant Biol.*, **8**, 38–44.
6. He,L., Thomson,J.M., Hemann,M.T., Hernando-Monge,E., Mu,D., Goodson,S., Powers,S., Cordon-Cardo,C., Lowe,S.W., Hannon,G.J. and Hammond,S.M. (2005) A microRNA polycistron as a potential human oncogene. *Nature*, **435**, 828–833.
7. Lu,J., Getz,G., Miska,E.A., Alvarez-Saavedra,E., Lamb,J., Peck,D., Sweet-Cordero,A., Ebert,B.L., Mak,R.H., Ferrando,A.A. *et al.* (2005) MicroRNA expression profiles classify human cancers. *Nature*, **435**, 834–838.
8. O'Donnell,K.A., Wentzel,E.A., Zeller,K.I., Dang,C.V. and Mendell,J.T. (2005) c-Myc-regulated microRNAs modulate E2F1 expression. *Nature*, **435**, 839–843.
9. Kim,V.N. (2005) MicroRNA biogenesis: coordinated cropping and dicing. *Nature Rev. Mol. Cell Biol.*, **6**, 376–385.
10. Pasquinelli,A.E. and Ruvkun,G. (2002) Control of developmental timing by microRNAs and their targets. *Annu. Rev. Cell Dev. Biol.*, **18**, 495–513.
11. Griffiths-Jones,S. (2004) The microRNA Registry. *Nucleic Acids Res.*, **32**, D109–D111.
12. Lagos-Quintana,M., Rauhut,R., Lendeckel,W. and Tuschl,T. (2001) Identification of novel genes coding for small expressed RNAs. *Science*, **294**, 853–858.
13. Lau,N.C., Lim,L.P., Weinstein,E.G. and Bartel,D.P. (2001) An abundant class of tiny RNAs with probable regulatory roles in *Caenorhabditis elegans*. *Science*, **294**, 858–862.
14. Lee,R.C. and Ambros,V. (2001) An extensive class of small RNAs in *Caenorhabditis elegans*. *Science*, **294**, 862–864.
15. Ambros,V., Bartel,B., Bartel,D.P., Burge,C.B., Carrington,J.C., Chen,X., Dreyfuss,G., Eddy,S.R., Griffiths-Jones,S., Marshall,M. *et al.* (2003) A uniform system for microRNA annotation. *RNA*, **9**, 277–279.
16. Lewis,B.P., Burge,C.B. and Bartel,D.P. (2005) Conserved seed pairing, often flanked by adenosines, indicates that thousands of human genes are microRNA targets. *Cell*, **120**, 15–20.
17. Rodriguez,A., Griffiths-Jones,S., Ashurst,J.L. and Bradley,A. (2004) Identification of mammalian microRNA host genes and transcription units. *Genome Res.*, **14**, 1902–1910.
18. Weber,M.J. (2005) New human and mouse microRNA genes found by homology search. *FEBS J.*, **272**, 59–73.
19. Hubbard,T., Andrews,D., Caccamo,M., Cameron,G., Chen,Y., Clamp,M., Clarke,L., Coates,G., Cox,T., Cunningham,F. *et al.* (2005) Ensembl 2005. *Nucleic Acids Res.*, **33**, D447–D453.
20. Karolchik,D., Baertsch,R., Diekhans,M., Furey,T.S., Hinrichs,A., Lu,Y.T., Roskin,K.M., Schwartz,M., Sugnet,C.W., Thomas,D.J. *et al.* (2003) The UCSC Genome Browser Database. *Nucleic Acids Res.*, **31**, 51–54.

21. Enright,A.J., John,B., Gaul,U., Tuschl,T., Sander,C. and Marks,D.S. (2003) MicroRNA targets in *Drosophila*. *Genome Biol.*, 5, R1.
22. Rehmsmeier,M., Steffen,P., Hochsmann,M. and Giegerich,R. (2004) Fast and effective prediction of microRNA/target duplexes. *RNA*, 10, 1507–1517.
23. Stark,A., Brennecke,J., Russell,R.B. and Cohen,S.M. (2003) Identification of *Drosophila* microRNA targets. *PLoS Biol*, 1, E60.
24. Rajewsky,N. and Socci,N.D. (2004) Computational identification of microRNA targets. *Dev Biol.*, 267, 529–535.
25. Lewis,B.P., Shih,I.H., Jones-Rhoades,M.W., Bartel,D.P. and Burge,C.B. (2003) Prediction of mammalian microRNA targets. *Cell*, 115, 787–798.
26. Brennecke,J., Stark,A., Russell,R.B. and Cohen,S.M. (2005) Principles of microRNA–target recognition. *PLoS Biol.*, 3, e85.
27. Krek,A., Grun,D., Poy,M.N., Wolf,R., Rosenberg,L., Epstein,E.J., MacMenamin,P., da Piedade,I., Gunsalus,K.C., Stoffel,M. and Rajewsky,N. (2005) Combinatorial microRNA target predictions. *Nature Genet.*, 37, 495–500.

The Plant Cell, Vol. 18, 1134–1151, May 2006, www.plantcell.org © 2006 American Society of Plant Biologists

Endogenous and Synthetic MicroRNAs Stimulate Simultaneous, Efficient, and Localized Regulation of Multiple Targets in Diverse Species[W]

John Paul Alvarez,[a,b] Irena Pekker,[a] Alexander Goldshmidt,[a] Eyal Blum,[a] Ziva Amsellem,[a] and Yuval Eshed[a,1]

[a] Department of Plant Sciences, Weizmann Institute of Science, Rehovot, 76100, Israel
[b] School of Biological Sciences, Monash University, Victoria 3800, Australia

Recent studies demonstrated that pattern formation in plants involves regulation of transcription factor families by microRNAs (miRNAs). To explore the potency, autonomy, target range, and functional conservation of miRNA genes, a systematic comparison between plants ectopically expressing pre-miRNAs and plants with corresponding multiple mutant combinations of target genes was performed. We show that regulated expression of several *Arabidopsis thaliana* pre-miRNA genes induced a range of phenotypic alterations, the most extreme ones being a phenocopy of combined loss of their predicted target genes. This result indicates quantitative regulation by miRNA as a potential source for diversity in developmental outcomes. Remarkably, custom-made, synthetic miRNAs vectored by endogenous pre-miRNA backbones also produced phenocopies of multiple mutant combinations of genes that are not naturally regulated by miRNA. *Arabidopsis*-based endogenous and synthetic pre-miRNAs were also processed effectively in tomato (*Solanum lycopersicum*) and tobacco (*Nicotiana tabacum*). Synthetic miR-ARF targeting *Auxin Response Factors 2*, *3*, and *4* induced dramatic transformations of abaxial tissues into adaxial ones in all three species, which could not cross graft joints. Likewise, organ-specific expression of miR165b that coregulates the *PHABULOSA-like* adaxial identity genes induced localized abaxial transformations. Thus, miRNAs provide a flexible, quantitative, and autonomous platform that can be employed for regulated expression of multiple related genes in diverse species.

INTRODUCTION

A major component of pattern formation in plants involves complex interplay between transcription factors (TFs) expressed in precise temporal and spatial domains and modifiers that act to maintain and refine their expression boundaries. TFs are usually expressed at low levels and guide the activity of many downstream effectors. Evolutionary expansion of TF families in plants (Riechmann et al., 2000) has meant that functional redundancy is a common theme in plant genomes. The majority of recently identified plant microRNAs (miRNAs) impose sequence-based simultaneous downregulation of developmentally important TFs (Llave et al., 2002a; Rhoades et al., 2002). Indirect evidence suggests that plant miRNAs have the potential to act efficiently to eliminate or clear cells of their target gene activities (Bartel, 2004). For instance, a large reduction in the activity of miRNA-regulated targets, either at the RNA or protein level, is evident upon ectopic miRNA expression (Aukerman and Sakai, 2003; Palatnik et al., 2003; Achard et al., 2004; Chen, 2004; Li et al., 2005; Schwab et al., 2005). Complementing these observations, strong dominant phenotypes are induced by target genes upon release of miRNA-guided regulation by mutations in their miRNA binding sites, and misexpression of miRNA-resistant targets with mutations at the miRNA binding site results in much stronger phenotypes than those obtained with native transcripts (reviewed in Chen, 2005). However, there is also evidence for quantitative action of plant miRNAs in quenching, as opposed to clearing, of the target gene activity. Thus, miRNA-resistant mutants are inherited in an incompletely dominant manner and are still subject to some miRNA-directed cleavage (Tang et al., 2003; Mallory et al., 2004a), and mutations in miRNA genes can result in increased levels of target gene expression (Baker et al., 2005).

Despite molecular indications that miRNAs can be very efficient, direct phenotypic evidence derived from comparing multiple mutant combinations with the effects of ectopic expression of the corresponding miRNA is limited. Unlike animal miRNAs, which simultaneously negatively regulate dozens of targets (Lim et al., 2005), plant miRNAs appear to have more limited target sets (Schwab et al., 2005), which are usually multiple members of the same gene family or even members of a single monophyletic clade of a larger family (Bartel and Bartel, 2003). These qualities can be used to facilitate the comparison of multiple mutant combinations with the effects of ectopic expression of the corresponding miRNA. In the absence of such a comparison, the prevailing model for high specificity and potency of plants miRNAs has yet to be verified. For example, in one case, ectopic

[1] To whom correspondence should be addressed. E-mail yuval.eshed@weizmann.ac.il; fax 972-8934-4181.
The author responsible for distribution of materials integral to the findings presented in this article in accordance with the policy described in the Instructions for Authors (www.plantcell.org) is: Yuval Eshed (yuval.eshed@weizmann.ac.il).
[W] Online version contains Web-only data.
Article, publication date, and citation information can be found at www.plantcell.org/cgi/doi/10.1105/tpc.105.040725.

miR164 induced cotyledon fusion and meristem arrest, mimicking the double mutant phenotype of two out of the five NAC domain genes targeted by this miRNA (Aida et al., 1997; Jones-Rhoades and Bartel, 2004; Laufs et al., 2004; Mallory et al., 2004b; Baker et al., 2005). However, overexpression of the miR165/6 failed to mimic the seedling arrest and production of a cylindrical monocot-like radial shoot observed in multiple mutants of the five miR165/6 *PHABULOSA* (*PHB*)-like targets (Emery et al., 2003; Li et al., 2005; Prigge et al., 2005; Williams et al., 2005a). The failure to recapitulate the phenotype in this latter case may reflect the inability of strong *35S:miR165/6* embryos to survive after transformation. Such a proposal could be confirmed by more precise viability-independent expression of the miR165/6.

Deciphering the role of TFs and their miRNA regulators in pattern formation can benefit greatly from spatial and temporal manipulation of their activities. This way, early deleterious effects can be bypassed and the autonomy of specific miRNA-induced perturbations examined. Such tissue-specific silencing using RNA interference (RNAi) has been successfully applied in plants (Watson et al., 2005), but RNAi has also been observed to induce systemic spread of gene silencing (reviewed in Voinnet, 2005). Notably, the common complexes involved in miRNA and short interfering RNA (siRNA) biogenesis and processing raises the possibility of a systemic component to miRNA-mediated regulation. In support of such a role, different miRNAs have been found in conducting phloem sap, a possible conduit for their systemic spread (Yoo et al., 2004). However, while unequivocal proof for long distance translocation of silencing signals was perceived through grafting experiments between silenced and nonsilenced transgenic tobacco (Palauqui et al., 1997), no such evidence has been provided for miRNA signals. Moreover, in mature *Arabidopsis thaliana* tissues, there is a strict overlap between *pre miR171* promoter and miR171 activity monitored by a sensor construct, suggesting that this miRNA maintains strict spatial autonomy (Parizotto et al., 2004).

Many plant miRNAs appear to have a long coevolutionary history with their targets, extending back to moss and lycopods (Floyd and Bowman, 2004; Axtell and Bartel, 2005). The pairing structure of the miRNA and nearly perfect complementary miRNA* can be highly conserved. Though sequence conservation also occurs outside the domain of the miRNA and its complement, it is the general predicted structure of the pre-miRNA foldback, rather than its sequence per se, that is conserved between the distantly related *Arabidopsis* and rice (*Oryza sativa*) (Reinhart et al., 2002). This raises the question whether pre-miRNAs retain functional conservation between distant species. Such conservation would involve efficient miRNA biogenesis, including correct spatial recognition and processing of the miRNA/miRNA* from the pre-miRNA foldback structure (reviewed in Chen, 2005). Likewise, the coevolutionary history of miRNA and their targets also raises the question of whether unique characteristics define particular mRNAs as targets. Evidence from metazoans suggests that this is not the case, as the miRNA sequence and its complement in the foldback structure can be substituted and target novel transcripts (Dickins et al., 2005). Similarly, analysis in *Arabidopsis* demonstrated that the miRNA and its complement miRNA* domains of the *pre miR171* backbone could be substituted to produce a novel miRNA that successfully targeted green fluorescent protein (GFP) (Parizotto et al., 2004). However, the capability and efficacy of the manipulated pre-miRNA in targeting multiple endogenous genes not normally targeted by miRNA regulation has yet to be examined.

In order to explore the extent and autonomy of downregulation that can be induced by miRNAs, we have chosen an experimental platform that uses sets of target genes for which complete conventional mutants are also available. Furthermore, miRNA ectopic expression has been brought under the control of in vivo constitutive or tissue-specific ectopic expression of pre-miRNAs guided by RNA Pol II promoters. This system enabled us to demonstrate that miRNAs have the potential to impose full or partial phenocopies of multiple mutants in several independent assays. These observations enabled us to expand the range of miRNA control by custom-designed pre-miRNAs that can stimulate phenocopy of mutations in genes not naturally regulated in this manner. Endogenous and synthetic *Arabidopsis* pre-miRNAs were functionally conserved in tomato (*Solanum lycopersicum*) and tobacco (*Nicotiana tabacum*), and tissue-specific miRNA misexpression produced phenotypes that are limited to the area of expression. Hence, these data suggest that miRNA activities are quantitative and, at least for distances greater than few cells, do not act outside of their domain of expression.

RESULTS

Precise Ectopic Expression of Endogenous miRNA Can Phenocopy Multiple Mutant Combinations

Plant miRNAs, such as miR164, have been ectopically expressed using the *35S* promoter directly or through chemical induction driving the stem foldback that constitutes the pre-miRNA with various 5′ and 3′ endogenous additions (Figure 1A; Guo et al., 2005). We wished to examine the ability of precise spatial expression of miRNA activity to effectively monitor miRNA potential. Transactivation of protein-encoding genes using the LhG4-OP system has been effective in driving strong, specific expression and obviating early deleterious effects of gene overexpression (Moore et al., 1998). To assay the capacity of this system to express pre-miRNAs, genomic fragments containing the pre-miRNA foldback flanked by short 5′ and 3′ pre-miRNA sequences were cloned behind an OP array followed by a TATA box (see Supplemental Table 1 online). In the case of *OP:miR164b*, the resulting T2 lines (see Methods for selection and scoring of transgenic lines; summarized in Table 1) were transactivated using the *PHB:LhG4* promoter, which is expressed in the developing cotyledon primordia and throughout the apical meristem (Figure 1C) to provide *PHB≫miR164b* F1s (Figure 1E; ≫ denotes transactivation). Expression of miR164 under this promoter mimicked the fused cotyledon and meristem arrest phenotype of the *cup-shaped cotyledon1* (*cuc1*) and *cuc2* double mutant, two of miR164's six targets (Figure 1D). These observations indicate that expression of *pre miR164b* using the transactivation system can efficiently deplete cells of target gene activities.

To extend these observations to other *Arabidopsis* miRNAs, we expressed *OP:miR165b* using the promoter of one of its

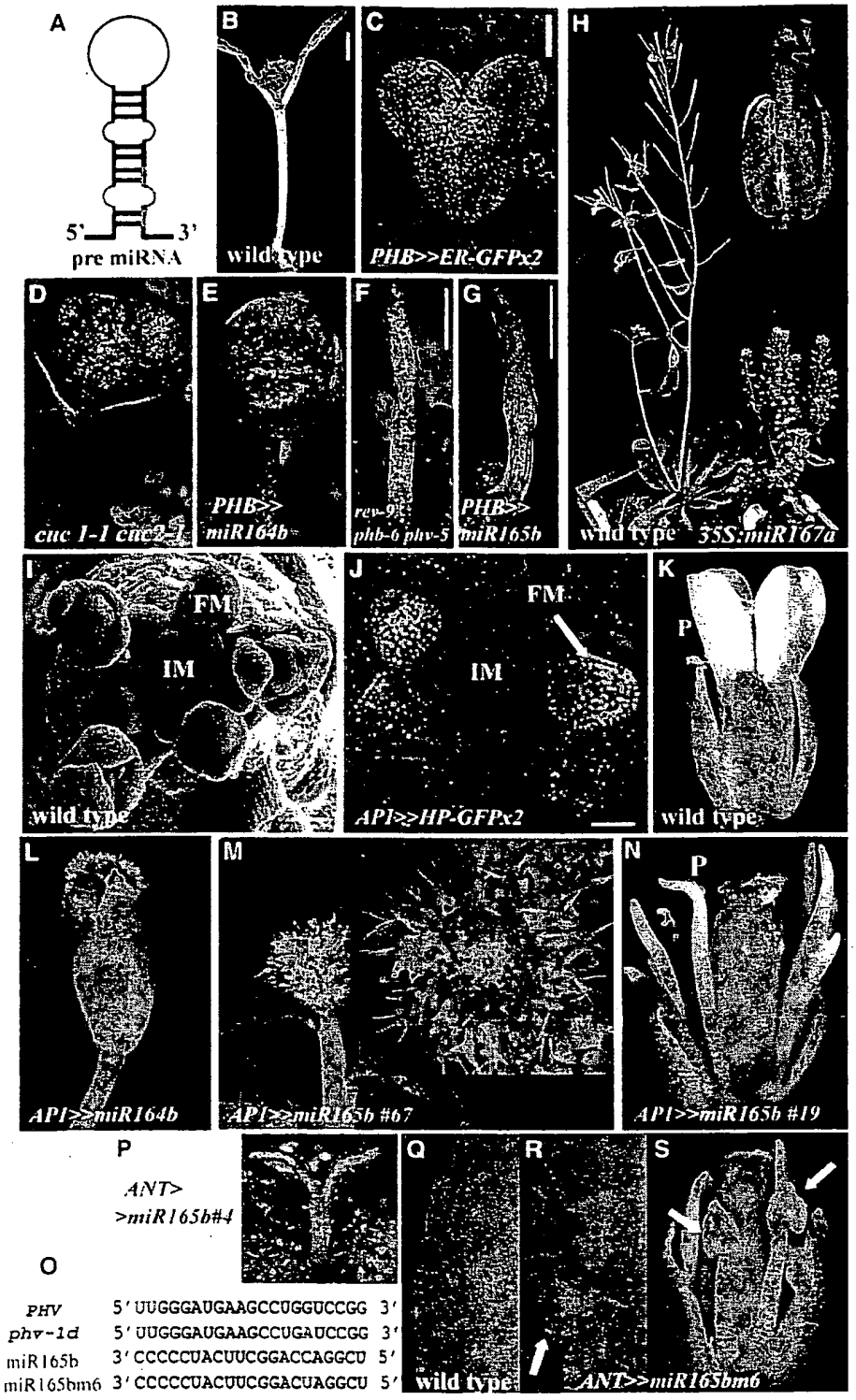

Figure 1. miRNAs Can Quantitatively Regulate Multiple Transcripts Simultaneously and Phenocopy Their Combined Loss of Function.

(A) A scheme of an endogenous pre-miRNA. The red and blue fragments will be cleaved by DICER-LIKE1 (DCL1) to generate the miRNA and miRNA*, respectively.

(B) A 10-d-old wild-type seedling.

(C) The promoter of *PHB* drives GFP expression throughout the shoot apex in wild-type heart-stage embryos.

target genes, the *PHB:LhG4* driver. miR165/6 target the five *PHB-like* genes that redundantly promote meristem establishment and maintenance as well as differentiation of lateral organs and the vasculature. *phb phavoluta* (*phv*) *revoluta* (*rev*) triple mutants or loss of all of the five *PHB-like* genes result in seedling arrest after the production of a cylindrical monocot-like radial shoot in which the apical meristem activity is abolished (Figure 1F; Emery et al., 2003; Prigge et al., 2005). However, previous overexpression studies with *35S:miR165* resulted in variable seedling phenotypes in which the most extreme plants had small leaves with some polarity defects (Li et al., 2005). By contrast, *PHB≫miR165b* plants gave rise to radial seedlings, phenocopying the multiple mutant combination (Figure 1G). These results illustrate that specific miRNA expression can abolish target gene activity and demonstrate the potential potency of precise pre-miRNA misexpression as a vehicle for simultaneous downregulation of multiple members of the same gene family.

35S-Driven miRNAs Can Faithfully Mimic Loss-of-Function Phenotypes

It is likely that the inefficiency of *35S:miR165a* in producing a phenocopy of the *PHB-like* genes reduction is due to their spatial expression in early stage embryos and their importance in embryogenesis. *Auxin Response Factor6* (*ARF6*) and *ARF8* are the only predicted targets of miR167, and *arf6 arf8* double mutants are viable, late flowering, have dark green leaves, and exhibit unexpanded 2nd and 3rd whorl floral organs (Nagpal et al., 2005). To assay whether the *35S* promoter can effectively drive a miRNA-mediated reduction in these genes, we assayed *35S:pre miR167a* transformants. Out of 20 independent T1 plants, eight had a similar phenotype to that reported for *arf6 arf8* double mutants both vegetatively and in flowers, while the remainder had a range of weaker phenotypes (Figure 1H, Table 1). No additional features than described for the double mutants were noticed. Thus, depending on the miRNA and its targets, elevated ectopic miRNA expression by the constitutive *35S* promoter can specifically reduce multiple target gene activities to levels that parallel that of multiple loss-of-function mutants.

Precise Expression of miRNAs Can Reveal Novel Mutation Patterns

Embryonic expression of either miR164 or miR165 resulted in a seedling phenocopy of multiple mutants in the corresponding target genes. While *cuc1 cuc2* seedlings can be rescued using tissue culture, *phb phv rev* or plants mutant for all five *PHB-like* mutant genes do not develop beyond the seedling stage. Because the *CUC-like* and *PHB-like* genes are active throughout plant development, the use of tissue-specific miRNA expression could reveal functions of these genes later in plant development. To examine the utility of this approach, transactivation of selected strong *OP:miR164b* and *OP:miR165b* lines was performed using the promoter of the flower meristem gene *APETALA1* (*AP1*).

As shown in Figures 1I and 1J, the expression mediated by *AP1* promoter initiates transcript accumulation throughout young floral meristems. In *AP1≫miR164b* plants, the sepals are completely fused, petals are absent, and stamens exhibit fusion to each other and the gynoecium (cf. Figures 1L and 1K). This phenotype is similar, albeit more severe than that observed in *cuc1 cuc2* flowers generated through tissue culture (Aida et al., 1997). In *AP1≫miR165b* plants, only radial filamentous structures were observed in the place of flowers, consistent with the miR165 effectively eliminating flower meristem function (Figure 1M). These findings are consistent with the observed seedling phenotypes, indicating that the *PHB-like* genes are essential for embryo and flower meristem maintenance. These observations demonstrate that the transactivation system can be effectively used in conjunction with miRNA-mediated loss of gene activity in specific cells at any stage of the plant's life cycle.

Low Levels of miRNA Expression or High Levels of Inefficient miRNA Suggest That Plant miRNAs Can Act in a Quantitative Fashion

Tissue-specific transactivation of pre-miRNAs identified lines producing a loss-of-function phenocopy but also uncovered OP:miRNA lines that induced mild phenotypes (Table 1). For

Figure 1. (continued).

(D) *Arabidopsis cuc1 cuc2* double mutant seedlings.
(E) F1 seedlings of *OP:miR164b* transactivated by *PHB:LhG4*.
(F) A monocot-like *phv phb rev* triple mutant seedling.
(G) A monocot-like *PHB≫miR165b* seedling of comparable age.
(H) Whole shoot and flower (inset) of *35S:miR167a* plant next to same age wild type display identical alterations found in *arf6 arf8* double mutants (cf. with Nagpal et al., 2005).
(I) Scanning electron micrograph of wild-type flowering apex.
(J) A cross section through *AP1≫HP-GFP* flowering apex with expression throughout emerging flower meristems.
(K) Wild-type flower.
(L) Fused sepals and absent petals in *AP1≫miR164b* flower.
(M) Flowering apex and filamentous flowers (inset) of strong *AP1≫miR165b* plant.
(N) Normal sepals, radial petals, distorted stamens, and multiple carpels in a weak *AP1≫miR165b* flower.
(O) Sequence alignment of the wild type and *phv-1d* mutant with corresponding miR165b and miR165bm6.
(P) Seedling expressing *ANT≫miR165b#4* results in radialized cotyledons and aborted meristem.
(Q) and **(R)** Adaxial surface of wild-type **(Q)** and *ANT≫miR165bm6* **(R)** leaves. Note the adaxial outgrowths of the transgenic leaf (arrow).
(S) Normal sepals, distorted stamens, and multiple carpels in a strong *ANT≫miR165bm6* flower.
FM, flower meristem; IM, inflorescence meristem; P, petal. Bars = 3 mm in **(B)**, **(F)**, and **(G)** and 20 μm in **(C)**, **(I)**, and **(J)**.

Table 1. Endogenous and Synthetic miRNAs Examined in This Study

miRNA and Its Pre-miRNA Backbone	Transgenes and Recipient Species[a]	Target Genes	Target Gene Function and Loss-of-Function Mutant Description	Frequency and Range of Phenotypic Responses in Independent Lines		
				Strong	Intermediate	Weak
miR164/pre miR164b	*Arabidopsis* *OP:miR164b*[b]	NAC domain TFs *CUC1*, *CUC2*, *NAC1*, At5g07680, At5g61430, At5g39610	Embryonic meristem establishment, organ separation, and lateral root outgrowth (Figure 1D)	10	0	0
	tomato *OP:miR164b*[c]	Tomato NACs		2	8	1
miR165/pre miR165b	*Arabidopsis* *OP:miR165b*[b]*	HD-ZIP TFs *PHV*, *CNA*, *REV*, *ATHB8*, *PHB*	Meristem establishment and maintenance, adaxial differentiation of lateral organs, and vasculature patterning (Figure 1F)	23	8	2
	tomato *OP:miR165b*[c]	Tomato PHB-like		1	3	0
miR165/pre miR165a	*Arabidopsis* *OP:miR165a*[b]*	As for miR165b	As for miR165b	17	2	2
miR166/pre miR166g	*Arabidopsis* *OP:miR166g*[b]*	As for miR165b	As for miR165b	16	3	3
miR165m6/pre miR165b	*Arabidopsis* *OP:miR165m6*[c]	As for miR165b but with reduced homology toits targets	As for miR165b	1	1	0
miR167/pre miR167a	*Arabidopsis* *35S:miR167a*[b]	ARF TFs *ARF6*, *ARF8*	Promotion of flowering and JA-mediated flower organ maturation (Nagpal et al., 2005)	8	10	2
miR-ARF/pre miR164b	*Arabidopsis* *35S:miR-ARF*[b]	ARF TFs *ARF2*, *ARF3/ETT*, *ARF4*	Abaxial differentiation of lateral organs, vascular development, flowering, and cell growth (Figure 2D)	9	8	3
	tomato *35S:miR-ARF*[c]			3	4	0
	tobacco *35S:miR-ARF*[c]			2	6	0
miR-NGA/pre miR164a	*Arabidopsis* *35S:miR-NGAa*[b]	B3 domain TFs *NGA1*, *NGA2*, *NGA3*, *NGA4*	Lateral organ growth (Figures 3E and 3H)	5	9	6
	OP:miR-NGAa[b]			2	6	2
	tomato *35S:miR-NGA*[c]	Weak homology with *NGA-like*/BI934304 and BI934637		0	5	4
miR-NGA/pre miR164b	*Arabidopsis* *35S:miR-NGAb*[b]	As for miR-NGAa	As for miR-NGAa	7	9	4

Frequent silencing was observed in subsequent generations for the lines marked with asterisks.

[a] The *10OP:miRNA* lines were examined upon transactivation with a promoter LhG4 driver. Combinations with specific promoters are described in the text. The *35S:miRNA* lines were scored directly as T1s and showed consistent phenotypes upon cross with the wild type.

[b] Phenotype relative to loss-of-function phenocopy (close resemblance is strong).

[c] Phenotype scoring is relative to other transgenic lines carrying the same construct because corresponding mutants are not available.

example, when a weak *OP:miR165b* line was transactivated with the *AP1:LhG4* promoter, the growth of the petals and stamens was markedly affected and additional carpels were formed (Figure 1N). Associations between phenotype strength and transcription levels have been shown previously for ectopic miR164 and miR166g expression (Laufs et al., 2004; Williams et al., 2005a). Likewise, assaying both the weak and strong *OP:miR165b* lines with the same promoters revealed consistent phenotype strengths restricted to the promoter's expression domain. These observations imply that when expressed in a discrete group of cells, miR165 can act in a quantitative fashion.

We hypothesized that quantitative action of miRNA may also be achieved by the generation of miRNA with lower homology. This was based on the observation that mRNA of the dominant *phv-1d* miRNA-resistant mutation was still cleaved (our unpublished data; Tang et al., 2003). The *phv-1d* molecular lesion is a G-to-A transition in the miR165/6 target region opposite position 6 from the 5′ end of the miR165/6 (Figure

1O). We created a theoretically less-efficient version of miR165b. Thus, miR165bm6 (C-to-U substitution in position 6 of the miR165b) mimics the corresponding position of the *phv-1d* mutation in the miRNA rather than in the target. The efficacy of the modified miRNA was demonstrated by its ability to restore wild-type morphology to the *phv-1d* mutant plants (see Supplemental Figure 1 online). The *AINTEGUMENTA:LhG4* (*ANT*) promoter is expressed in the primordia of all above-ground organs. *ANT≫miR165b* plants exhibited a strong phenotype of radialized cotyledons and an aborted apical meristem (Figure 1P). By contrast, *ANT≫miR165m6* plants had a weak; abaxialized phenotype, consistent with inefficient miR165bm6 action. The adaxial surface of the leaves developed localized outgrowths (no effect was observed on the abaxial leaf surface), while in the flowers, the stamens locules were reversed and the gynoecium, like that of weak *AP1≫miR165b* lines, had additional carpels (Figures 1Q to 1S). A similar floral phenotype was observed of *AP1≫ miR165m6* plants (see Supplemental Figure 1 online). The mild abaxialized phenotype of *OP:miR165bm6* plants and that of the weak *OP:miR165b* lines argues that miRNAs can act in a quantitative fashion depending on the pairing quality and quantity of the miRNA with respect to its target mRNAs.

General Strategy for Developing Synthetic miRNA on the Backbone of Native miRNA

Ectopic expression of endogenous pre-miRNAs allowed controlled downregulation of multiple coregulated miRNA targets. This prompted us to explore the possibility to design synthetic miRNA that will target genes not normally regulated by miRNA. We used the *pre miR164b* backbone as a template to approach these questions based on the consistency and efficacy of miR164b in the overexpression analysis. In addition, this backbone contains a bulge at position 4 of the conceptualized Dicer-generated miRNA/miRNA* duplex in the desired miRNA strand (marked red in Figure 2B). Asymmetric instability in this hybrid is believed to help differentiate between the miRNA and miRNA* in the RNA-induced silencing complex (RISC) (Schwarz et al., 2003), thus theoretically helping define the miRNA (upper strand in pre-miRNA, Figure 2B) irrespective of the sequence introduced. As initial gene targets for synthetic miRNA regulation, we selected the abaxial promoting *ARF3* and *ARF4* along with *ARF2*, for which respective mutations have been described (Li et al., 2004; Pekker et al., 2005; Okushima et al., 2005b; Schruff et al., 2006). Importantly, these *ARFs* contain common, conserved sequences, which are the basis for negative coregulation by evolutionary conserved transacting siRNAs (ta-siRNAs), siR2141 and siR2142 (Allen et al., 2005; Williams et al., 2005b). The target sequences of these ta-siRNAs (two sites in *ARF3/ETTIN* [*ETT*] and *ARF4* and one in *ARF2*) are conserved in *Arabidopsis*, tomato, and monocotyledonous plants and suggest that *ARF2* may have overlapping functions with *ARF3/ETT* and *ARF4* (Figure 2A; Pekker et al., 2005; Williams et al., 2005b). Exploiting this, we designed a miRNA that should directly target these three *ARFs* and ensured that it began with U, like most plant miRNAs. As shown in the bottom line of Figure 2B, mismatches were introduced into the miRNA complementary sequence to mimic the predicted stem of the miR164b precursor, assuming that bulges in the miR164 backbone contain essential recognition and processing information. The miR-ARF2/3/4 (hereafter referred to as miR-ARF) was integrated into the *pre miR164b* backbone by direct gene synthesis (Figure 2B, right panel), and the resulting *pre miR-ARF* was cloned behind the *35S* or *OP* promoter.

Synthetic miRNA Efficiently Regulates ARF2, 3, and 4, Which Are Naturally Regulated by Transacting siRNAs

Arabidopsis ett/arf3 plants are characterized by a loss of abaxial identity in the gynoecium, while in *ett/arf3 arf4* double mutants, all lateral organs exhibit reduced abaxial identity and outgrowths on the abaxial surface of their leaves (Figure 2C; Pekker et al., 2005). Triple *ett/arf3 arf4 arf2* mutants are unavailable due to the tight genetic linkage between *arf4* and *arf2* (Okushima et al., 2005a). Strikingly, all *35S:miR-ARF Arabidopsis* transformants exhibited phenotypes consistent with an effective targeting of the three *ARF* genes. Plants with a strong phenotype resembled *ett/arf3 arf4* double mutants but had more outgrowths on the abaxial leaf surface (Figures 2C to 2E, Table 1) as well as an increased floral organ number and frequently radialized stamens (Figures 2F to 2H). Similar to *arf2* single mutants, these *35S:miR-ARF* plants were also late flowering (Ellis et al., 2005; Okushima et al., 2005b).

A Synthetic miRNA Born on a Stem-Loop Precursor Efficiently Guides RISC Complexes

We isolated RNA from plants of a *35S:miR-ARF* line with a strong phenotype and verified by RNA gel blot analysis that miR-ARF was efficiently processed from its precursor by identifying its 21-nucleotide miRNA, which was comparable in size with the endogenous miR164 (Figure 2I). After processing, miRNAs enter the RISC complex and guide cleavage of their target transcripts, inducing their degradation and/or interference with translation (Llave et al., 2002b; Aukerman and Sakai, 2003; Chen, 2004). To examine the mode of action of the synthetic miRNA, we assayed the relative abundance of the full-length *ARF* transcripts using RNA gel blot analysis. For all three, a significant but incomplete reduction in RNA levels was observed in *35S:pre miR-ARF Arabidopsis* plants (Figure 2J).

Cleavage of the three *ARF* genes by the synthetic miR-ARF was investigated using 5′ RNA ligase-mediated rapid amplification of cDNA ends (RLM-RACE) analysis (Kasschau et al., 2003). Endogenous ta-siRNA–directed cleavage (siR2141 and siR2142) of *ARF* transcripts has been shown in *Arabidopsis* (Allen et al., 2005; Williams et al., 2005b). However, a much greater abundance of cleaved products of all three *ARF* genes was observed in *35S:miR-ARF* plants than in wild-type *Arabidopsis* (Figure 2K; see Supplemental Figure 2 online). In wild-type plants, we could detect products at relatively low amounts from the ta-siRNA–mediated cleavage at both *ARF3/ARF4* A and *ARF3/ARF4* B sites using primers downstream of the B site (primer b, Figure 2K). For *35S:miR-ARF* plants, we managed to detect only B-site cleavage products with primer B, but using a different primer (primer a between the A and B sites for *ARF4*), we amplified abundant products from cleavage at site A (Figure 2K). In the *35S:miR-ARF* plants, sequence analysis demonstrated that

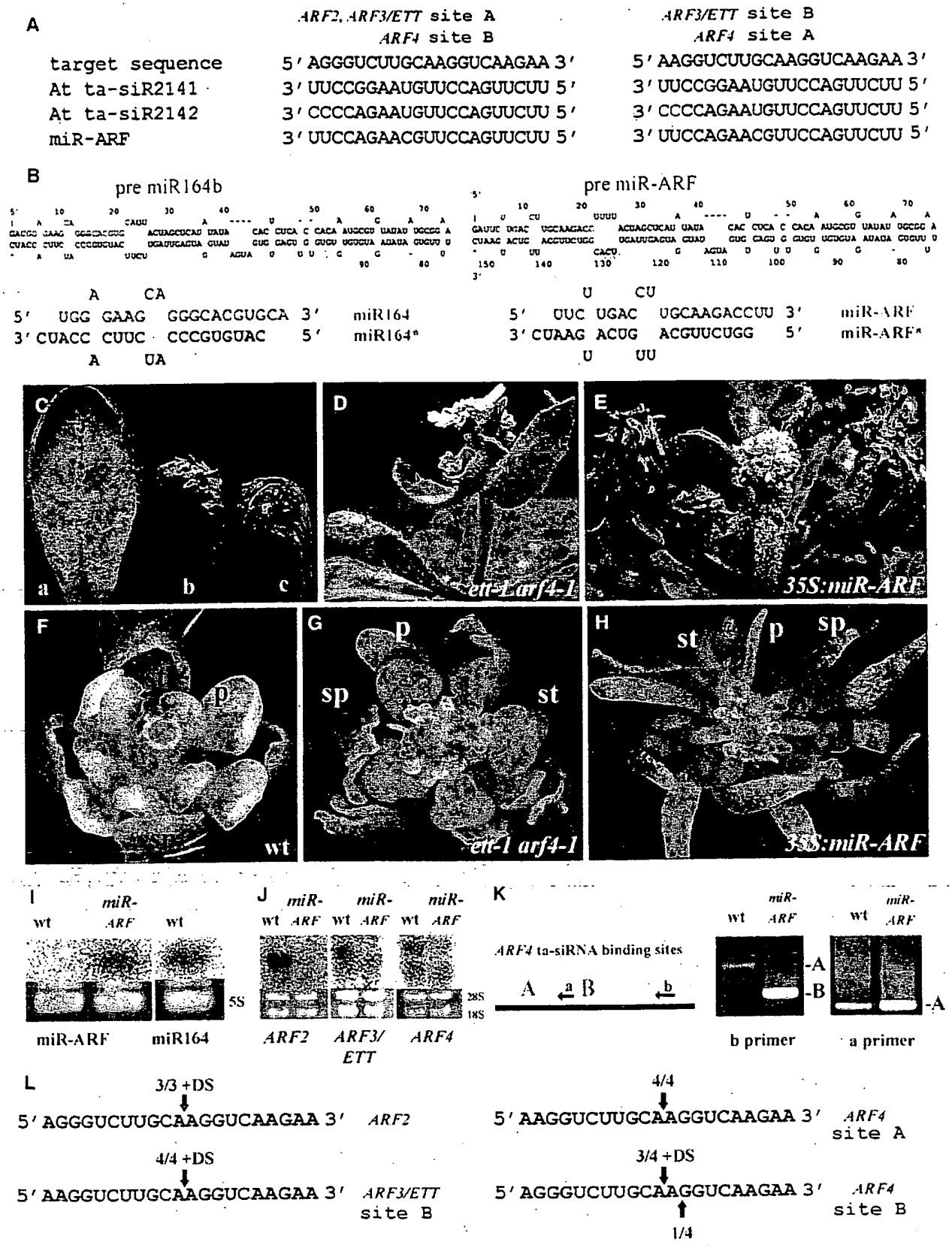

Figure 2. Custom-Designed Synthetic miRNAs Efficiently Regulate ta-siRNA Targets.

cleavage in the target mRNA occurred consistently between nucleotides 10 and 11 at miR-ARF complementary sites (marked in Figure 2L), while much more dispersed cleavage products were amplified from the wild type (see Supplemental Figure 2 online; Allen et al., 2005). We therefore conclude that miRNAs generated by a stem-loop precursor guide the RISC complexes more specifically than ta-siRNA–mediated cleavage.

Synthetic miRNA Efficiently Regulates the *NGATHA* Multigene Family Not Normally Associated with RISC-Mediated Control

To develop the use of synthetic miRNA beyond gene families that are normally regulated by various RISC-based small RNA regulation, we next targeted the *NGATHA* (*NGA*) genes for which there is no evidence of this form of regulation.

The *NGA* clade is composed of four genes (*NGA1-4*); all are closely related to the RAV-like proteins in the structure of the B3-DNA binding domain but do not have an AP2 domain (Figure 3A). Like *ett* mutations, mutants in *nga1* phenotypically enhance the *kanadi1* mutant phenotype in the gynoecium (Bowman et al., 2002; *nga1* was renamed from *howard*). We identified *NGA1* and found that all four *NGA* genes redundantly regulate lateral organ growth (as will be described elsewhere). However, only minor morphological alterations are apparent in any of the single gene mutants. A single consensus stretch of 21 nucleotides within the B3 domain was identified that could constitute a common synthetic miRNA target site in the four *NGA-like* genes of *Arabidopsis* (Figure 3B). This 21-nucleotide sequence fulfilled the available criteria of allowable mismatches in number and position as well as low free energy characterizing endogenous plant miRNAs (Figure 3B; Allen et al., 2005; Schwab et al., 2005). The 21-nucleotide specificity was confirmed in the genome via BLAST search and was modified to begin with a U like most plant miRNAs. The designed 21 nucleotides were introduced into the miR164a and miR164b backbones to generate miR-NGAa and miR-NGAb, respectively (Figure 3C).

nga1 nga2 nga3 nga4 quadruple mutant plants have shorter and wider leaves than the wild type, sepals and petals are broad, and petals are slightly green-yellow. Style development is severely impaired, with disruptions in the coordinated growth that normally seal the two-carpel gynoecium. Consequently, the gynoecium remains distally unfused, with distinctive projections emanating from the top of the valves (cf. Figures 3E and 3H with 3D and 3G). Remarkably, plants of *35S:miR-NGAa* and *35S:miR-NGAb* showed phenotypic alterations approaching that of the *nga1 nga2 nga3 nga4* quadruple mutant plants (Figures 3F to 3I, Table 1). These results show that miRNA-dependent control can be extended to other multigene families.

NGA RNA Analysis Detects Cleavage Products and Differential Reduction of NGA RNA

We asked whether the molecular processing of NGA RNA by miR-NGA is similar to RISC-mediated processes. An RNA gel blot from RNA extracted from plants of a line with a strong phenotype confirmed the presence of the 21-nucleotide synthetic miR-NGA, and RLM-RACE analysis identified miRNA-directed cleavage products (Figures 3K and 3L). No evidence of *NGA-like* cleavage products was observed in RNA from wild-type inflorescences. Notably, the predominant cleavage position as determined by direct sequencing of the RLM-RACE products was identical in all four *NGA* genes and was comparable to a common cleavage site for endogenous miRNAs (including that of miR-164b) occurring between positions opposing 10 and 11 5′ of the miR-NGA (as marked in Figure 3B). However, though RNA levels of *NGA1* were reduced in *35S:miR-NGAa* plant inflorescences, very mild reduction in the levels of *NGA3* was detected (Figure 3M). This could be due to attenuation of protein translation or a transcriptional autofeedback loop.

We next asked whether miR-NGA could ameliorate the phenotype produced by overexpression of the *NGA1* gene. The *CAB3:LhG4* (chlorophyll *a/b* binding promoter) line drives expression throughout photosynthetic tissues, and *CAB3≫NGA1*

Figure 2. (continued).

(A) Sequence alignment of the ta-siRNA binding sites in *Arabidopsis ARF2*, *ARF3*, and *ARF4*, the endogenous ta-siRNAs, and a designed miR-ARF sequence with better homology to all target sites. The A and B sites are designated according to Allen et al. (2005). Mismatches are marked red and G-U wobbles cyan.

(B) Predicted folding and dicing of the pre miR164b backbone before (left) and after (right) replacement of miR164 with the miR-ARF sequence.

(C) Abaxial side of wild-type (a), *ett-1 arf4-1* (b), and *35S:miR-ARF* (c) leaves.

(D) Bolting shoot of *ett-1 arf4-1* plant.

(E) Bolting shoot of *35S:miR-ARF* plant.

(F) to **(H)** Flowers of wild-type **(F)**, *ett-1 arf4-1* **(G)**, and *35S:miR-ARF* plants **(H)**. Note the gradual increase in the number of sepals, stamen radialization, and decrease in petal width. sp, sepal; p, petal; st, stamen.

(I) Detection of miR-ARF and miR164 in wild-type and *35S:miR-ARF* plants by RNA gel blot analysis. Both miRNAs are the same ~21 nucleotides.

(J) Reduced levels of full-length transcripts of the three *ARF* genes in *35S:miR-ARF* plants.

(K) A scheme of *ARF4* cDNA with primers used for RLM-RACE detection. Gel images showing RLM-RACE–detected wild-type and *35S:miR-ARF* (*miR-ARF*) cleavage products at sites A and B detected using either primer a or b, where A is the expected gel position for a product cleaved at site A, and B is the expected gel position of product cleaved at site B. In *35S:miR-ARF*, amplification products are more prevalent relative to the wild type. In addition, amplification of a product cleaved at site A could only be obtained with the a primer (gels for PCR products of *ARF2* and *ARF3* cleavage analysis are shown in Supplemental Figure 2 online).

(L) Summary of cleavage analysis by direct sequencing of RLM-RACE products (see Supplemental Figure 2 for details) and product cloning of the three *ARF* genes. Cleavage analysis for *35S:miR-ARF* plants is shown, and the dispersed cleavage products of the wild type are shown in Supplemental Figure 2 online and in Allen et al. (2005). DS, direct sequencing.

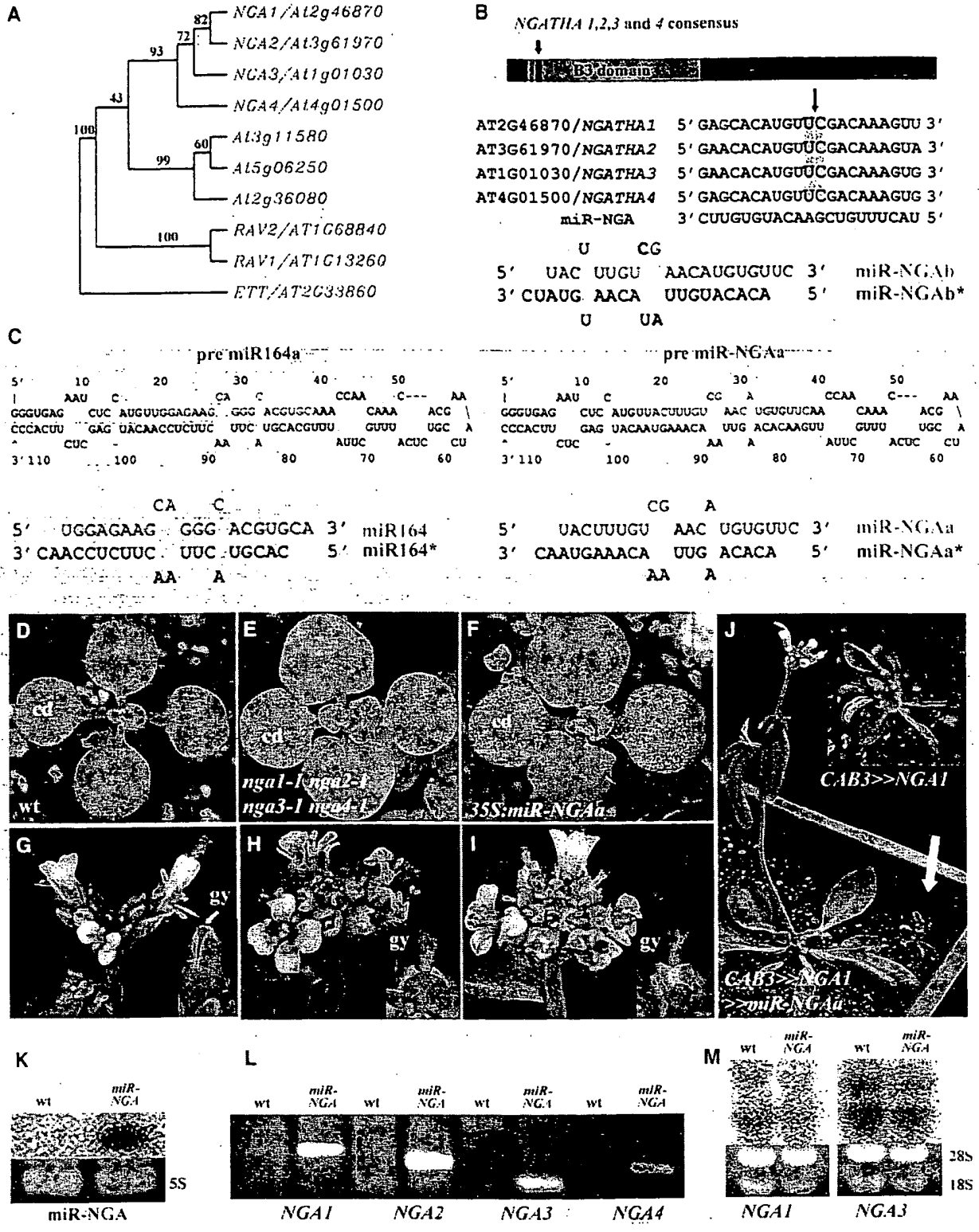

Figure 3. Custom-Designed Synthetic miRNA Efficiently and Specifically Codownregulate Non-Native Small RNA Targets.

plants are dwarfed with small leaves (Figure 3J). However, in plants where both *NGA1* and *miR-NGA* were cotransactivated by *CAB3:LhG4* (*CAB3≫NGA1* and *miR-NGAa*, Figure 3J), plant stature and leaf growth resembled that of *CAB3≫miR-NGAa* plants (a near wild-type phenotype; data not shown), indicating that the levels of NGA protein from *NGA* gene overexpression were efficiently reduced by miR-NGA.

Thus, custom-designed miRNAs that follow a few basic rules of pairing are capable of simultaneously and efficiently downregulating multiple transcripts that are not naturally regulated by small RNAs and induce morphological changes that match computer predictions for target specificity.

Arabidopsis Pre-miRNAs Can Effectively Regulate Cross-Species Targets

To investigate the functional conservation of *Arabidopsis* pre-miRNA processing in distantly related species, we first introduced *OP:miR164b* into tomato, a distantly related plant species that shows conserved miR164 targets (N. Ori, personal communication). The progenies of two selected *35S≫miR164b* lines had fused cotyledons (Figure 4A), a similar phenotype to the petunia (*Petunia hybrida*) *no apical meristem* mutant (Souer et al., 1996). Thus, misexpression of *pre miR164b* resulted in uniform, heritable, and stable lines capable of simultaneous downregulation of multiple members of the same gene family both in *Arabidopsis* and in tomato. We also expressed the *OP:miR165b* in tomato plants whose homologous target genes are also conserved (our analysis) to explore whether this functional conservation of pre-miRNAs in other species is a general phenomenon. The At *FILAMENTOUS FLOWER* (*FIL*) promoter drives expression throughout tomato leaf primordia before becoming abaxially restricted (Lifschitz et al., 2006). *FIL≫miR165b* plants had abaxialized, filamentous leaves consistent with miR165b function in downregulating the adaxial-promoting *PHB-like* genes in tomato (Figures 4B and 4C). The abaxial nature of the filamentous leaves was evident by the prevalence of long linear trichomes and the absence of short globular ones, a typical composition of abaxial leaf epidermis (Reinhardt et al., 2005).

Subsequently, we tested whether the synthetic *pre miR-ARF* would also function in other species. *35S:miR-ARF* tobacco and tomato transformants exhibited phenotypes consistent with the specific transformations of abaxial cell types into adaxial ones observed in *35S:miR-ARF Arabidopsis* plants. The leaves of *35S:miR-ARF* tomato plants had small, misshapen, up-curled leaflets that were darker green and developed outgrowths on their abaxial surface (Figure 4D). The inflorescence structure approximated that of the wild type, but in the flowers, the number of sepals was increased, sepals and petals were narrower and shorter, and white rather than green carpels were topped by thick, green style/stigmatic tissue (Figures 4E to 4H). Such redistribution of gynoecium cell types is similar to single mutations in *ett/arf3* in *Arabidopsis*, where style tissues are expanded basally (Figures 4L and 4M).

Similarly, *35S:miR-ARF* tobacco lines had small, up-curling leaves that, in more severe lines, developed outgrowths on the abaxial leaf surface (Figure 4I). Flowering was delayed, and when it finally occurred in severe lines, the corolla remained largely green. Strikingly, very pronounced abaxial outgrowths developed around the entire corolla circumference, mostly in its distal third (Figure 4J). However, even in the most severe lines, the adaxial (inner) side of the corolla surface was unchanged. As in tomato, the gynoecia had basally expanded green stigma (Figure 4K). These results confirm and extend previous suggestions on the central role of the three *ARFs* in promotion of abaxial identity in all lateral organs in *Arabidopsis* and allow expansion of this role to the remotely related Solanaceae.

To associate the *35S:miR-ARF* phenotype of tomato and tobacco with miR-ARF activity, 5′ RLM-RACE was used. As with *Arabidopsis*, tomato *ARF3/ETT* has two presumptive tasiRNA target sites and, thus, two miR-ARF target sites (Figure 5A). In *35S:miR-ARF* tomato plants, we detected much higher levels of cleavage at both A and B sites than in wild-type tomato plants (Figure 5B). Notably, the predominant cleavage position within the target site was shifted one nucleotide 3′ relative to that observed in *Arabidopsis* (Figure 5C). These observations suggest that the *pre miR-ARF* is functionally conserved in tomato. In tobacco, we only tested miR-ARF activity at the A site of the ARF3/ETT homolog by cleavage analysis. However, the level of cleaved transcript detected was again greater than that observed in wild-type tobacco plants and occurred predominantly at the same position within the target domain that was observed in tomato (Figures 5B and 5C).

Figure 3. (continued).

(A) A phylogenetic tree of the NGA-like proteins and their closest *Arabidopsis* homologs. Tree was constructed with the ~120 amino acids that constitute the B3 domain as shown in Supplemental Figure 3 online. ETT was included as an outgroup, and numbers represent bootstrap percentage from 1000 trials.

(B) A general scheme of *NGA1/2/3/4* transcripts, outlining the position of a consensus sequence aligned. A synthetic miRNA has 0 to 2 mismatches with all four, and its conceptual dicing from pre miR164b backbone is illustrated. The arrow above pileup denotes cleavage point as described below.

(C) Predicted folding and dicing of the pre miR164a backbone before (left) and after (right) replacement of miR164 with the miR-NGA sequence.

(D) to **(F)** Young seedling of wild-type **(D)**, *nga1-1 nga2-1 nga3-1 nga4-1* quadruple mutant **(E)**, and *35S:miR-NGAa* **(F)** plants. Note the angular leaf blade of the mutants compared with the round leaf blade of the wild type. cd, cotyledons.

(G) to **(I)** Inflorescence and pre-anthesis flower (insets) of wild-type **(G)**, *nga1-1 nga2-1 nga3-1 nga4-1* quadruple mutant **(H)**, and *35S:miR-NGAa* **(I)** plants. Note the broad yellowish petals and the protruding distal portion of the unfused gynoecium (gy).

(J) Cotransactivation of *NGA1* and miR-NGAa by *CAB3* promoter eliminates dwarfism induced by ectopic *NGA1* with the same promoter line (inset).

(K) Detection of miR-NGA in wild-type and *35S:miR-NGAa* plants by RNA gel blot analysis.

(L) RLM-RACE detection of cleaved products of the four *NGA-like* transcripts in *35S:miR-NGAa* (*miR-NGA*) plants but not wild-type plants.

(M) RNA gel blot analysis reveals differential reduction in RNA levels of *NGA1* and *NGA3* in wild-type and *35S:miR-NGAa* plants.

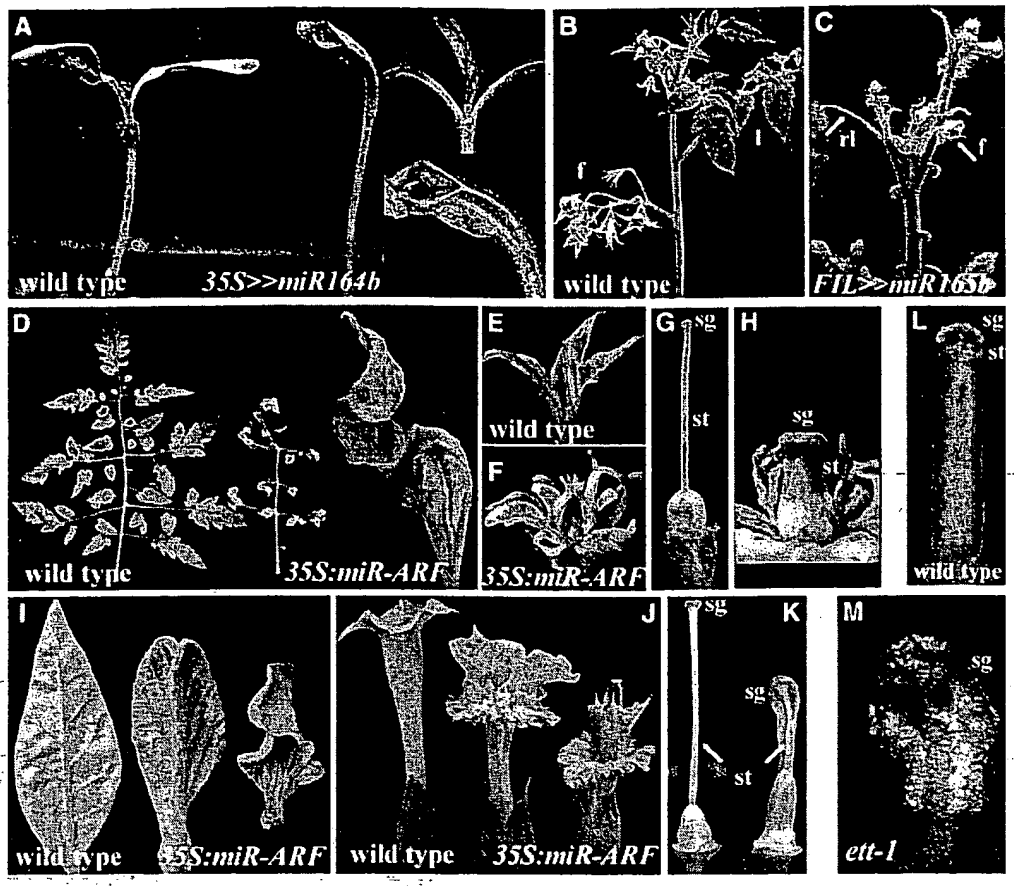

Figure 4. *Arabidopsis* Pre-miRNA Backbones Induce Homologous Mutant Phenotypes Heterologously.

(A) Wild-type and F1 tomato seedlings of *OP:miR164b* transactivated by *35S:LhG4*. The top and bottom insets are close-ups of the upper portion of the seedling.

(B) and **(C)** Upper part of wild-type **(B)** and *FIL≫miR165b* **(C)** tomato shoots. Leaves in **(C)** are short and radial, and floral organs are narrow. l, leaf; f, flower; rl, radialized leaf.

(D) Abaxial side of wild-type and *35S:miR-ARF* leaves. A close-up of *35S:miR-ARF* leaf at the right illustrates the abaxial-specific outgrowths found along the veins.

(E) to **(H)** Flowers (**[E]** and **[F]**) and carpels (**[G]** and **[H]**) of wild-type (**[E]** and **[G]**) and *35S:miR-ARF* (**[F]** and **[H]**) tomato plants. Note the thin sepals and petals, the short style, and the thickened green stigma of the transformant. st, style; sg, stigma.

(I) to **(K)** Comparison of leaves **(I)**, flowers **(J)**, and carpels **(K)** of wild-type (left) and *35S:miR-ARF* tobacco plants. Gradual effects from weak to strong (right) are notable in independent T1 plants. As in tomato, abaxial leaf outgrowths are evident along the veins. Corolla outgrowths are external (abaxial) only.

(L) and **(M)** Gynoecium of wild-type **(L)** and *ett-1* **(M)** *Arabidopsis* plants. As in tomato and tobacco, stigmatic tissue in the mutant is expanded basally while style length is reduced.

Use of the *35S:miR-NGAa* construct in tomato resulted in a fruit phenotype, and miR-NGA–mediated cleavage in the tomato *NGA-like* transcripts (*NGA-like*/BI934304 and BI934637) was detected, albeit at low levels (see Supplemental Figure 3 online). In this case, it is likely that mismatches in the critical 5′ region of the miR-NGA relative to the target mRNAs obviate efficient miRNA regulation.

Cell-Autonomous Effects of miRNA Expression

It has been suggested that miRNA activities might not be cell-autonomous (e.g., short-range movement of miR166 was suggested to account for restriction of the *PHB-like* activities from the abaxial side of emerging organ primordial) (Juarez et al., 2004; Kidner and Martienssen, 2004). The potency of miRNA target regulation and its efficacy across species allowed examination of cell autonomy by the different criteria of tissue specificity and gross systemic spread. To examine the autonomy of miRNA action, we specifically expressed *pre miR166g*, *pre miR165a*, or *pre miR165b* in the 2nd and 3rd whorl floral organ primordia of *Arabidopsis* using an *AP3* driver line (*AP3:LhG4*; Figure 6A, Table 1). As expected, in *AP3≫miR165/6* plants, petals and stamens became completely radialized, a typical morphology for organs lacking abaxial/adaxial asymmetry (Figure 6C).

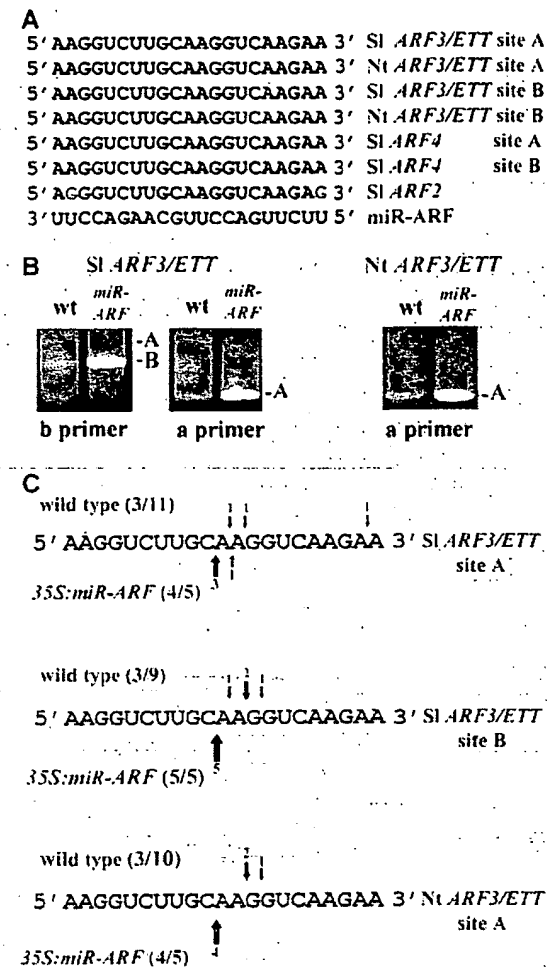

Figure 5. Induction of Solanaceae Target Cleavage by *Arabidopsis*-Based Synthetic Pre-miRNAs.

(A) Sequence alignment of tomato *ARF2/3/4*, tobacco *ETT/ARF3*, and miR-ARF. The nucleotides not in gray are predicted wobbles.

(B) Gel images showing RLM-RACE detection of tomato and tobacco *ARF3* cleavage products from wild-type and *35S:miR-ARF* (*miR-ARF*) plants. Primer position follows the *ARF4* design in Figure 2K. Cleavage products at sites A and B were detected using either primer a or b, where A is the expected gel position for a product cleaved at site A, and B is the expected gel position of product cleaved at site B.

(C) Cleavage point mapping of tomato and tobacco *ARF3*. Arrows mark cleavage sites in sequenced, cloned products, where arrow size corresponds with frequency of clones obtained (also given). Arrows above each sequence are for clones obtained from the wild type, and those below are from *35S:miR-ARF* plants. The number of clones matching the predicted target region out of total number of sequenced clones is shown in parentheses.

In the upper part of the stamens, guard cells that are typically restricted to the abaxial connective tissue were present all around (Figure 6D). In contrast with the 2nd and 3rd whorl organs, normal gynoecia were formed (Figure 6C), suggesting autonomous restriction imposed on miR165/6 activity or, alternatively, insensitivity of the gynoecium. Thus, we expressed *pre miR165b* by the gynoecium-specific promoter of *CRABS CLAW* (*CRC*) that drives expression throughout the gynoecium valve anlagen before becoming abaxially restricted (Figure 6B). In *CRC≫miR165b* plants, a thin gynoecium was formed, without adaxial placenta and ovules, while the stamens and petals were unaffected (Figure 6E). Thus, expression of *pre miR165/6* in cells of organ primordia bordering other primordia provided no evidence for expanded miRNA activity.

The striking phenotype of tomato and tobacco plants expressing *35S:pre miR-ARF* provided an opportunity to phenotypically assay for systemic translocation of this miRNA. In six out of six reciprocal grafts between strong *35S:miR-ARF* and wild-type tomato, both rootstock and scion maintained autonomous morphology over 6 months (Figure 6F). Likewise, the dramatic morphological effects of ectopic miR-ARF expression did not cross graft barriers in two out of two reciprocal tobacco grafts between *35S:miR-ARF* and the wild type, even though graft union supported viable scions for over 6 months (Figures 6G to 6I). As long-range movement often follows source to sink flow, we repeatedly defoliated the wild-type shoots after complete graft union was obtained in both tomato and tobacco (arrows in Figures 6F and 6G). After 2 months of such repeated defoliation, all new emerging leaves and subsequently floral primordia had a wild-type appearance. Thus, using morphological criteria, no support for short or long-range translocation of miRNA-induced alterations was observed.

DISCUSSION

Pattern formation of plant organs often involves regulation of TF families by miRNAs. In this study, we have systematically demonstrated that miRNA can simultaneously quench the activity of their multiple predicted TF targets to levels matched by conventional loss-of-function mutations. However, no morphological alterations beyond the computational predictions for target specificity were encountered, suggesting very limited and precise targeting. The efficient silencing potential was not restricted to genes naturally regulated by small RNAs, and *Arabidopsis* pre-miRNA backbones were efficiently processed to induce homologous loss-of-function phenotypes in distantly related tomato and tobacco. Finally, we have demonstrated that miRNA activities can be quantitative, do not cross graft barriers, and at least for short distances, exert autonomous effects.

Gene Silencing with miRNAs

Functional overlap (redundancy) presents a difficult logistic obstacle for in vivo characterization of gene function in general and more so in plants that in many cases have undergone multiple cycles of polyploidization and subsequent selective gene loss (Moore and Purugganan, 2005). Here, we show that miRNAs can potentially abolish simultaneously the activities of all of their targets to levels matched by conventional loss-of-function mutations. Endogenous pre-miRNA–encoding genes of *Arabidopsis* could be modified to specifically target (sequence allowing) selected gene families. The range of phenotypic perturbations, even at the high levels of ectopic expression, did not exceed that of corresponding multiple mutant combinations in

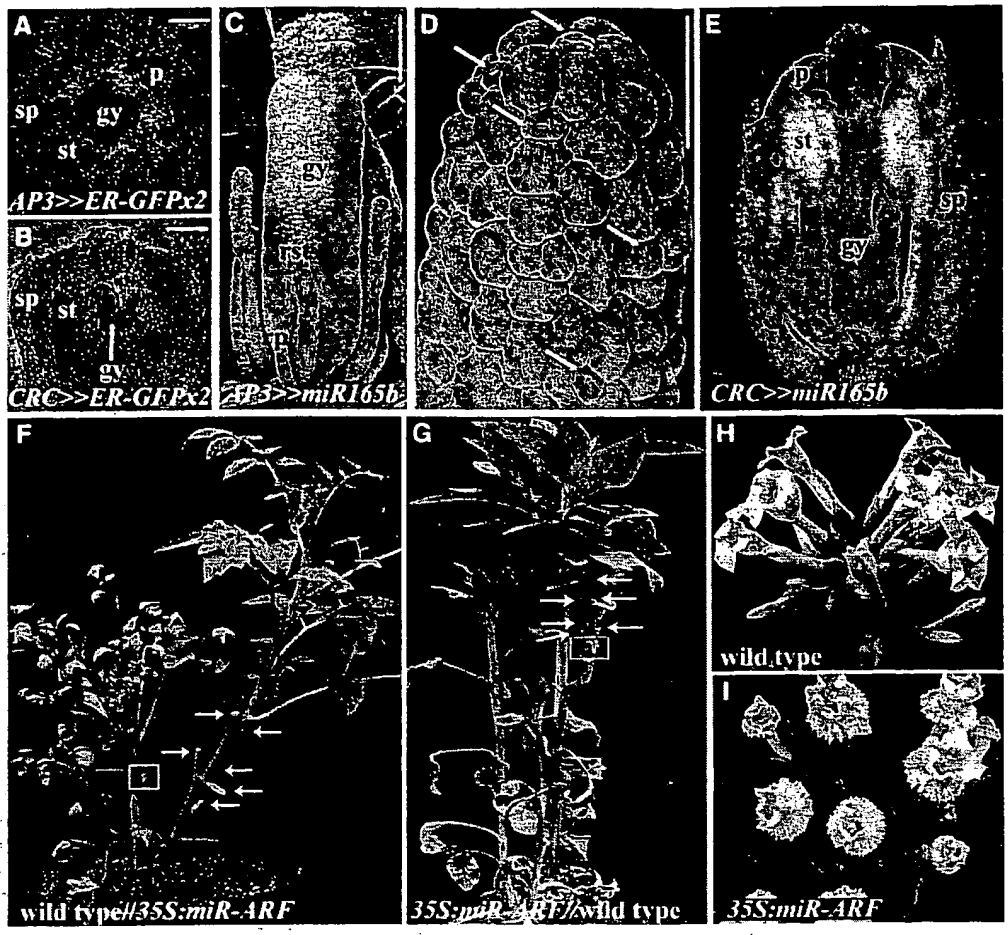

Figure 6. miRNA Activities Are Spatially Restricted and Do Not Cross Graft Joints.

(A) Transverse section of an *Arabidopsis* flower showing promoter *AP3*-mediated expression of GFP limited to petals and stamen.

(B) Longitudinal section of same age *Arabidopsis* flower showing that promoter *CRC*-mediated expression of GFP is limited to carpels.

(C) Flower of *AP3≫miR165b* plant with radial petals and stamens but normal gynoecium.

(D) Close-up of radial stamens with normally abaxial-restricted guard cells scattered all around (arrows).

(E) Flower of *CRC≫miR165b* plant with thin gynoecium and normal stamens.

(F) A graft of *35S:miR-ARF* on wild-type tomato. Picture was taken 4 months after grafting and after two rounds of defoliation (arrows) of wild-type leaves. Newly initiating shoots remain normal. White box shows graft union.

(G) to **(I)** A graft of the wild type on *35S:miR-ARF* tobacco **(G)**. Here, too, defoliation (arrows) of wild-type leaves did not stimulate miRNA-derived phenotype on wild-type shoot. The white box shows the graft union. Upon flowering, wild-type acceptor shoots were normal **(H)** even though *35S:miR-ARF* donor flowers are highly distinct **(I)**.

sp, sepal; p, petal; st, stamen; gy, gynoecium; rp, radial petal; rst, radial stamen. Bars = 50 μm in **(A)** and **(B)** and 100 μm in **(C)** and **(D)**.

the predicted target genes, suggesting that off-targets are not significantly affected. It was also possible to reduce the complementarity of the miRNA to its targets and to produce weaker phenotypes. The specific sequence requirements for recognition of targets by their corresponding miRNA were formulated earlier (Allen et al., 2005; Schwab et al., 2005). Following these basic rules, we could custom design synthetic miRNAs that were as efficient as endogenous ones in simultaneous downregulation of multiple targets, and all are members of the same gene family. Using such sequence-specific design, it should be possible to specifically target unique isoforms generated via alternative splicing or target multiple homologs ordered in tandem. Such application might be highly significant for plant genomes; it is estimated that 29% of the rice genes are organized in clusters of gene families (International Rice Genome Sequencing Project, 2005) and are not amenable for functional analysis via classical genetic tools.

Most of the miRNAs and gene family targets found in plants have a long coevolutionary history. Nearly all highly conserved miRNAs and corresponding gene target sites are identical in *Arabidopsis* and rice, and some are also shared with nonvascular plants (Floyd and Bowman, 2004; Axtell and Bartel, 2005). Comparison of the pre-miRNA genes between *Arabidopsis* and other species shows some conservation beyond the miRNA and

its complement to provide similarity in predicted folding (Reinhart et al., 2002; Floyd and Bowman, 2004). Using phenotypic and molecular assays, we found that pre-miRNAs were processed efficiently when the miRNA sequence and its complement were substituted in *Arabidopsis* and that these synthetic *Arabidopsis* miRNAs and their native counterparts functioned in distantly related Solanaceae species. Recent work in mammal cells suggests that the miRNA RISC loading complex processes the pre-miRNA directly, unwinding and loading the mature miRNA to Argonaute2 of the RISC (Maniataki and Morelatos, 2005). Thus, basic, conserved structural elements of the pre-miRNA secondary structure may be sufficient for miRNA RISC loading complex recognition and processing, and these are maintained in the manipulations we performed.

Endogenous plant miRNAs and the synthetic miRNAs we tested have a high degree of homology to their targets and mediated gene suppression primarily through cleavage. In metazoans, miRNA-mediated cleavage also occurs where the miRNA has a high degree of homology with the coding region of its target (Yekta et al., 2004). Using appropriate computational analyses, this effective and stable mechanism for gene targeting can be broadly applied in all organisms with miRNA machinery.

RNAi versus miRNA Silencing

Long hairpin RNAi constructs provide perfectly matched double-stranded RNA strands cleaved to short siRNAs, while miRNAs are processed from precursors containing mismatches and bulges. We assume that it is those mismatches that provide structural information for Dicer activities guiding precise cleavage of the same 21 nucleotides. As such information is missing in the perfect match stems, a mixture of mers is produced unless phased first by precise guiding cleavage (Allen et al., 2005). Moreover, even though a single miRNA molecule is generated per one pre-miRNA, efficient downregulation of multiple targets with matching sequence homology can be achieved. This result is in contrast with the long stem-loop RNAi vectors or cosuppression lines where downregulation of a specific transcript only is commonly evident. For example, Chuang and Meyerowitz (2000) demonstrated specific downregulation of *AP1* using RNAi. However, despite the sequence being used having long stretches of perfect homologies with the homologous *CAULIFLOWER* (*CAL*) gene, no *ap1 cal-like* plants were observed. Likewise, RNAi-targeted suppression of *ARF2* in *Arabidopsis* (Li et al., 2004) and *ARF4* in tomato (Jones et al., 2002) resulted in a specific single mutant phenotype, in contrast with our results. Keeping in mind that double-stranded RNA is also amplified and dependent on the activities of RNA-dependent RNA polymerase (RdRp), stoichiometric effects of miRNAs appear to be much more potent (Sijen et al., 2001).

Quantitative versus Qualitative Regulation by miRNAs

Most plant miRNAs target TFs that play critical roles in morphogenesis. In animals, recent studies suggest that miRNAs and their targets are expressed in adjacent, largely nonoverlapping domains through transcriptional control (Stark et al., 2005). Under this scenario, miRNAs function to confer robustness on gene expression boundaries. In plants, the evidence of miRNA function paints a more complex picture. It has been proposed that miRNAs act to clear cells of their target gene activities as supported by the strong developmental phenotypes of dominant miRNA-resistant mutations (Rhoades et al., 2002). Such a mode of action is attractive for modeling formation and stabilization of sharp boundaries between adjacent expression domains. However, observations of miR165/6 and miR164 expression and action relative to their respective *PHB-like* and *CUC-like* targets suggest a more quantitative role for the miRNA through dampening down target gene expression levels in cells coexpressing both (McConnell et al., 2001; Bao et al., 2004; Baker et al., 2005; Li et al., 2005; Williams et al., 2005a). In both cases of miRNA/target pairs, increased target levels were observed when either the target was resistant to its miRNA or when endogenous miRNAs were reduced by mutation. Since zonation of the plant apical meristem into central and peripheral domains is an ongoing, dynamic process, the slow gradual restrictions of expression domains of both *CUC-like* and *PHB-like* multiple-family members likely reflects a more fluid regulation of these genes by their corresponding miRNAs. Similarly, during leaf morphogenesis, cell position rather than lineage is important until relatively late in leaf development (reviewed in Scheres, 2001). Therefore, proper leaf morphogenesis involves a continual interplay between adaxial-promoting *PHB-like* and abaxial-promoting *ARF2/3/4* TFs, each class with supporting small RNA regulation (miR165/6 and siR2141/2, respectively) to reinforce cell identity. In such a scenario, the ta-siRNAs and miR165/6 may be coexpressed with, and fine-tune, target gene expression as part of the ongoing process of acquiring and translating positional information.

Our experiments with endogenous *pre miR165b*, *pre miR164b*, and *pre miR167a* overexpression indicate that plant miRNAs have the potential to act in a quantitative fashion. High and/or precise pre-miRNA expression of these miRNAs mimicked multiple mutants of the target genes, demonstrating that these plant miRNAs have the potential to clear cells of their target gene activities. However, weak overexpression elicited mild phenotypes only, presumably by reducing and not eliminating target gene function. Thus, it appears that a broad range of plant miRNAs can act quantitatively, depending on expression levels. The weak abaxialized phenotype obtained from strong specific overexpression of the miR165bm6 with reduced homology to its *PHB-like* gene transcripts (Figure 1; see Supplemental Figure 1 online) also suggests that miRNA target mismatches are a potential source for inefficiency in miRNA action. A striking feature of endogenous plant miRNAs is the evolutionary conservation of miRNA target mismatches, even between the critical 5′ region of the miRNA and its target (Axtell and Bartel, 2005). The synthetic miR-ARF and miR-NGA we assayed had perfect homology to target regions in *ETT/ARF4* and *NGA2*, respectively. From the simple perspective of thermodynamic rules of pairing, this should maximize the miR-ARF and miR-NGA in terms of negative regulation of these targets. While we cannot say whether perfect miRNA target homology is the most efficient form of these or any other miRNAs, our results suggest that perfect-match miRNAs are as efficient as native ones. If a perfect target match is the most efficient form of a miRNA, the evolutionary conservation of mismatches suggests a selection for miRNA inefficiency. One

possibility is that an inefficient miRNA, combined with variable levels of pre-miRNA transcription, contributes to a wider range of target gene outputs, which can be translated into a morphogenetic gradient. Thus, it can be speculated that while plant miRNAs have the capacity to clear cells of target gene activities, they act endogenously to both clear cells of their targets and to dampen their expression, depending on the miRNA and developmental context.

Local versus Systemic Regulation by miRNA

The quantitative nature of miRNA regulation and the transient nature of the pattern formation process do not support a role for long-distance miRNA transport. In agreement, we could not find any evidence for translocation of miR-ARF effects across graft barriers in tomato and tobacco. In *Arabidopsis*, we also failed to find phenotypic evidence of miR165a/b or miR166g moving small cellular distances in the developing flower. Still, a context-dependent short-range movement (one to two cells) of selected miRNAs in particular domains cannot be ruled out, a feature common to other macromolecules shown to traffic from cell to cell (Gallagher et al., 2004; Kurata et al., 2005). DCL4 activities are required for cell-to-cell spread of transgene-born silencing signals (Dunoyer et al., 2005), suggesting that siRNAs do provide the spreading sequence-based information agent. Significantly, mutations in *DCL4* or in components of the RdRP machinery that abolish systemic silencing spread do not affect patterning. Thus, miRNAs and siRNAs might not serve as equal substrates for trafficking. siRNAs contrast with miRNAs in having a perfect match with their target mRNA. In this respect, one possible role for mismatches between miRNAs and their targets is that they act as a means to avoid the miRNA acting as a template for the RdRP silencing machinery. The miR-ARF, which has a perfect match to *ARF3/ETT* and *ARF4* of tomato and *ARF3/ETT* of tobacco, failed to elicit a systemic silencing response, suggesting that the miRNA/target mismatches may not function in this process. Thus, regulated expression of synthetic miRNA can allow for targeting of multiple transcripts for simultaneous sector analysis and for bypassing early lethality associated with multiple mutant combinations.

METHODS

Plant Material

The *Arabidopsis thaliana* plants described are all in the Landsberg *erecta* background. Plants were grown under 18 h of cool white fluorescent light at 20°C. M82 tomato (*Solanum lycopersicum*) and Samsun tobacco (*Nicotiana tabacum*) plants were grown in greenhouse conditions with temperatures ranging between 18 and 25°C. The *nga1* mutation was identified in a *gymnos kanadi* background (Bowman et al., 2002). Map-based identification of At2g46870 as the gene mutant in *nga1* will be described elsewhere. *nga1* has a premature stop codon at Gln-203. *nga2-1* (At3g61970) (a kind gift from Venkatesan Sundaresan) contains a Ds insertion at +142 from the first Met codon within the B3 domain-encoding region. *nga3-1* (At1g01030) has a T-DNA insertion (Garlic/Sail_232_E10) at position +238 from the first Met codon, likewise within the B3-encoding domain, and *nga4-1* (At4g01500) (also a kind gift from Venkatesan Sundaresan) has a DS insertion +112 from the first Met codon, again within the B3 domain. *nga1-1 nga2-1 nga3-1 nga4-1* quadruple mutant plants were produced by conventional breeding. In the F2, presumptive quadruple mutant plants with a distinct phenotype appeared at an approximate ratio of 1:256, and their genotype was verified using PCR (see Supplemental Table 3 online for primer details).

Grafting

We used a classic wedge-shaped/slit grafting technique with the site of union wrapped by Parafilm. Plants were kept for 2 to 3 d in the shade and for 7 d in 80% humidity provided by plastic bags. Success exceeds 90%.

Pre-miRNA Clones and Plant Transformation

For isolation of pre-miRNA–containing sequences, the genomic DNA flanking the predicted stem-loop of different, annotated pre-miRNAs was amplified using PCR (see supplemental tables online for primers and details). Details on the stem-loop and short 5′ and 3′ ends are summarized in Supplemental Table 1 online. The *pre miR165bm6* and *pre miR-NGAa* synthetic genes were generated by assembly PCR, as detailed in the legend of Supplemental Table 2 online. The *pre miR-ARF* and *pre miR-NGAb* synthetic genes were synthesized by Epoch Biolabs and DNA 2.0, respectively. To produce pre-miRNA stem-loop representations, we used the Web-based mfold program (Zuker, 2003). After sequence verification, the pre-miRNA clones were cloned behind an *OP* array (10OP-TATA-BJ36) or *35S* promoter (ART7) and transferred into the binary pMLBART (for *Arabidopsis*) or pART27 (for tomato and tobacco) vectors (Eshed et al., 2001). A 6-kb *PHB* promoter and a 6.1-kb At *FIL* promoter were PCR amplified with the primers in Supplemental Table 2 online. *FIL*, *PHB*, and *35S* promoters were subcloned in front of LhG4 (Moore et al., 1998) and subsequently cloned into the pART27 or pMLBART binary vector. Other transactivation driver lines were described earlier (Pekker et al., 2005). Cotyledon transformation in tomato and leaf disc transformation in tobacco were performed according to McCormick (1991) and Horsch et al. (1985), respectively. *Arabidopsis* transgenic lines were generated by the floral dip method, and BASTA-resistant transformants were selected on soil.

Evaluation of Transgenic Lines

Two types of evaluation of transgenic lines were performed. Primary *35S:miRNA* T1 lines were scored directly as having a strong, intermediate, or weak phenotype. Selected 2 to 10 lines (fertility allowing) were backcrossed (BC) with the wild type, and a minimum of 30 BC1 progeny were scored to assay phenotype severity and heritability. Unless otherwise mentioned, original phenotypes were faithfully transmitted, and only lines with a single T-DNA insert locus were used for molecular analyses. Alternatively, in order to screen for independent, primary 10OP:pre-miRNA transformants, 10 to 30 T1 plants were crossed to homozygous promoter:LhG4 lines, and a minimum of 30 promoter≫miRNA F1 plants per cross were scored. Each primary line was designated as strong, intermediate, or weak on the basis of the morphology of the F1 progenies. Only 10OP:pre-miRNA lines with single, unlinked T-DNA insert loci were used for further experiments. In all cases, unless otherwise mentioned, strong lines were used for morphological and molecular characterizations.

RNA Isolation and Analysis

Total RNA was extracted using TRI Reagent (Sigma-Aldrich) according to the manufacturer's instructions. High molecular weight RNA was normalized by spectrophotometry to 20 μg/lane. Radiolabeled probes for RNA gel blot analysis of mRNAs were made by random priming reactions. Probes consisted of the 3′ (to the stop codon) 1049 bp (*ETT*), 1497 bp (*ARF4*), 1459 bp (*ARF2*), 617 bp (*NGA1*), and 828 bp (*NGA3*) of these

genes annotated cDNAs. Equivalent loading of samples was monitored by detection of 28S and 18S RNA in all gels prior to blot transfer.

Low molecular weight RNA was purified with an RNeasy plant mini kit (Qiagen), resolved on a 17% polyacrylamide-urea gel, transferred to a Zeta-Probe GT membrane (Bio-Rad), and probed with a ^{32}P end-labeled oligonucleotide, complementary to the mature miRNAs (see Supplemental Table 4 online). Equivalent loading of samples was shown by detection of 5S RNA in all gels prior to blot transfer.

Isolation of Tomato and Tobacco cDNAs

The complete coding sequences of the *ARF2*, *ARF3/ETT*, and *ARF4* genes of tomato were cloned using primers designed from the alignment of different tomato EST sequences in GenBank. A partial *ARF3/ETT* gene of *N. tabacum* was isolated using homology with the tomato *ARF3/ETT* gene (see supplemental tables online for primer details). Young leaves, apices, and flowers were harvested, and total mRNA was extracted from vegetative and reproductive shoot tips using Trizol reagent. cDNA template was synthesized from 1 μg of total RNA using Superscript II reverse transcriptase (Invitrogen) or PowerScript RT enzyme (Clontech).

RACE Analysis of Cleaved miRNA Target Genes

Cleavage sites in the miRNA target genes were mapped using RLM-RACE, a modified 5′ RACE procedure as described by Kasschau et al. (2003), using the GeneRacer (Invitrogen) protocol coupled with nested gene-specific primers ~200 to 400 nucleotides downstream of the predicted miRNA target site (see Supplemental Table 5 online). The PCR products were purified and directly sequenced or cloned into pDrive (Qiagen) or pCRII (Sigma-Aldrich) and sequenced.

Microscopy and Confocal Imaging

Tissue preparation and histological analyses were performed according to Pekker et al. (2005). Scanning electron microscopy was performed using an XL30 ESEM FEG microscope (FEI). For confocal imaging, tissue was fixed in 2.5% paraformaldehyde overnight, osmotically adjusted, and frozen, and 20- to 45-μm sections were made with a Leica 2000 microtome. Fluorescence was observed by an Olympus CLSM500 microscope with an argon laser at 488 nm for excitation and 505 to 525 nm for GFP emission.

Accession Numbers

Tomato *ARF* sequence data from this article can be found in the GenBank/EMBL data libraries under accession numbers DQ340254 (Sl *ETT*), DQ340259 (Sl *ARF4*), and DQ340255 (Sl *ARF2*). Accession numbers for tobacco are DQ340258 (Nt *ARF2*), and DQ340256 and DQ340257 (Nt *ARF3/ETT*).

Supplemental Data

The following materials are available in the online version of this article.

Supplemental Table 1. Sequence Parameters of Pre-miRNA.

Supplemental Table 2. Primers for PCR-Mediated Cloning.

Supplemental Table 3. Primers for PCR-Mediated Genotyping of *NGATHA2-4* Insertion Alleles.

Supplemental Table 4. Oligonucleotides for miRNA Detection by RNA Gel Blot Analysis and Primers for RLM-RACE.

Supplemental Table 5. Gene-Specific Primers for RLM-RACE.

Supplemental Figure 1. Design of and Additional Phenotypes Induced by miR165bm6.

Supplemental Figure 2. Analysis of Cleavage Products of *Arabidopsis ARF* Genes.

Supplemental Figure 3. *NGA-Like* Gene Alignment and Cleavage Analysis in Tomato.

ACKNOWLEDGMENTS

We thank Eugenia Klein and the electron microscopy facility for help with scanning electron microscopy, Raya Eilam for help with tissue preparation techniques, and Vladimir Kiss for assistance with confocal laser scanning microscopy. We also thank Venkatesan Sundaresan, Michael Lenhard, the SIGNAL collection of Syngenta Seeds, and the ABRC stock center for providing plasmids and plant material. We thank John Bowman, Robert Fluhr, Naomi Ori, and members of Y.E.'s lab for comments and discussions and Detlef Weigel for sharing unpublished results. This work was made possible with funding from Grants 3328-02 from the U.S.–Israel Binational Agricultural Research and Development Fund and 386-02 from the Israel Science Foundation. J.P.A. is an honorary research fellow of the School of Biological Sciences (Monash University). Y.E. is an incumbent of the Judith and Martin Freedman Career Development Chair.

Received December 25, 2005; revised March 10, 2006; accepted March 20, 2006; published April 7, 2006.

REFERENCES

Achard, P., Herr, A., Baulcombe, D.C., and Harberd, N.P. (2004). Modulation of floral development by a gibberellin-regulated microRNA. Development **131,** 3357–3365.

Aida, M., Ishida, T., Fukaki, H., Fujisawa, H., and Tasaka, M. (1997). Genes involved in organ separation in *Arabidopsis*: An analysis of the cup-shaped cotyledon mutant. Plant Cell **9,** 841–857.

Allen, E., Xie, Z., Gustafson, A.M., and Carrington, J.C. (2005). microRNA-directed phasing during trans-acting siRNA biogenesis in plants. Cell **121,** 207–221.

Aukerman, M.J., and Sakai, H. (2003). Regulation of flowering time and floral organ identity by a microRNA and its *APETALA2*-like target genes. Plant Cell **15,** 2730–2741.

Axtell, M.J., and Bartel, D.P. (2005). Antiquity of microRNAs and their targets in land plants. Plant Cell **17,** 1658–1673.

Baker, C.C., Sieber, P., Wellmer, F., and Meyerowitz, E.M. (2005). The *early extra petals1* mutant uncovers a role for microRNA miR164c in regulating petal number in *Arabidopsis*. Curr. Biol. **15,** 303–315.

Bao, N., Lye, K.W., and Barton, M.K. (2004). MicroRNA binding sites in *Arabidopsis* class III HD-ZIP mRNAs are required for methylation of the template chromosome. Dev. Cell **7,** 653–662.

Bartel, B., and Bartel, D.P. (2003). MicroRNAs: At the root of plant development? Plant Physiol. **132,** 709–717.

Bartel, D.P. (2004). MicroRNAs: Genomics, biogenesis, mechanism, and function. Cell **116,** 281–297.

Bowman, J.L., Eshed, Y., Baum, S., Emery, J.F., Floyd, S.K., Alvarez, J., Hawker, N.P., Lee, J.Y., Siegfried, K.R., Khodosh, R., Tatom-Jaurez, M., and Perea, J.V. (2002). The story of *CRABS CLAW* (or How we learned to love the mutagen). Flowering Newsletter **31,** 3–11.

Chen, X. (2004). A microRNA as a translational repressor of *APETALA2* in *Arabidopsis* flower development. Science **303,** 2022–2025.

Chen, X. (2005). MicroRNA biogenesis and function in plants. FEBS Lett. **579,** 5923–5931.

Chuang, C.F., and Meyerowitz, E.M. (2000). Specific and heritable genetic interference by double-stranded RNA in *Arabidopsis thaliana*. Proc. Natl. Acad. Sci. USA **97,** 4985–4990.

Dickins, R.A., Hemann, M.T., Zilfou, J.T., Simpson, D.R., Ibarra, I., Hannon, G.J., and Lowe, S.W. (2005). Probing tumor phenotypes using stable and regulated synthetic microRNA precursors. Nat. Genet. **37,** 1289–1295.

Dunoyer, P., Himber, C., and Voinnet, O. (2005). DICER-LIKE 4 is required for RNA interference and produces the 21-nucleotide small interfering RNA component of the plant cell-to-cell silencing signal. Nat. Genet. **37,** 1356–1360.

Ellis, C.M., Nagpal, P., Young, J.C., Hagen, G., Guilfoyle, T.J., and Reed, J.W. (2005). *AUXIN RESPONSE FACTOR1* and *AUXIN RESPONSE FACTOR2* regulate senescence and floral organ abscission in *Arabidopsis thaliana*. Development **132,** 4563–4574.

Emery, J.F., Floyd, S.K., Alvarez, J., Eshed, Y., Hawker, N.P., Izhaki, A., Baum, S.F., and Bowman, J.L. (2003). Radial patterning of *Arabidopsis* shoots by class III HD-ZIP and *KANADI* genes. Curr. Biol. **13,** 1768–1774.

Eshed, Y., Baum, S.F., Perea, J.V., and Bowman, J.L. (2001). Establishment of polarity in lateral organs of plants. Curr. Biol. **11,** 1251–1260.

Floyd, S.K., and Bowman, J.L. (2004). Gene regulation: Ancient microRNA target sequences in plants. Nature **428,** 485–486.

Gallagher, K.L., Paquette, A.J., Nakajima, K., and Benfey, P.N. (2004). Mechanisms regulating SHORT-ROOT intercellular movement. Curr. Biol. **14,** 1847–1851.

Guo, H.S., Xie, Q., Fei, J.F., and Chua, N.H. (2005). MicroRNA directs mRNA cleavage of the transcription factor *NAC1* to downregulate auxin signals for *Arabidopsis* lateral root development. Plant Cell **17,** 1376–1386.

Horsch, R.B., Fry, J.E., Hoffmann, N.L., Eichholtz, D., Rogers, S.G., and Fraley, R.T. (1985). A simple and general method for transferring genes into plants. Science **227,** 1229–1231.

International Rice Genome Sequencing Project (2005). The map-based sequence of the rice genome. Nature **436,** 793–800.

Jones, B., Frasse, P., Olmos, E., Zegzouti, H., Li, Z.G., Latche, A., Pech, J.C., and Bouzayen, M. (2002). Down-regulation of *DR12*, an auxin-response-factor homolog, in the tomato results in a pleiotropic phenotype including dark green and blotchy ripening fruit. Plant J. **32,** 603–613.

Jones-Rhoades, M.W., and Bartel, D.P. (2004). Computational identification of plant microRNAs and their targets, including a stress-induced miRNA. Mol. Cell **14,** 787–799.

Juarez, M.T., Kui, J.S., Thomas, J., Heller, B.A., and Timmermans, M.C. (2004). MicroRNA-mediated repression of *rolled leaf1* specifies maize leaf polarity. Nature **428,** 84–88.

Kasschau, K.D., Xie, Z., Allen, E., Llave, C., Chapman, E.J., Krizan, K.A., and Carrington, J.C. (2003). P1/HC-Pro, a viral suppressor of RNA silencing, interferes with *Arabidopsis* development and miRNA unction. Dev. Cell **4,** 205–217.

Kidner, C.A., and Martienssen, R.A. (2004). Spatially restricted microRNA directs leaf polarity through *ARGONAUTE1*. Nature **428,** 81–84.

Kurata, T., et al. (2005). Cell-to-cell movement of the CAPRICE protein in *Arabidopsis* root epidermal cell differentiation. Development **132,** 5387–5398.

Laufs, P., Peaucelle, A., Morin, H., and Traas, J. (2004). MicroRNA regulation of the CUC genes is required for boundary size control in *Arabidopsis* meristems. Development **131,** 4311–4322.

Li, H., Johnson, P., Stepanova, A., Alonso, J.M., and Ecker, J.R. (2004). Convergence of signaling pathways in the control of differential cell growth in *Arabidopsis*. Dev. Cell **7,** 193–204.

Li, H., Xu, L., Wang, H., Yuan, Z., Cao, X., Yang, Z., Zhang, D., Xu, Y., and Huang, H. (2005). The putative RNA-dependent RNA polymerase RDR6 acts synergistically with ASYMMETRIC LEAVES1 and 2 to repress BREVIPEDICELLUS and microRNA165/166 in *Arabidopsis* leaf development. Plant Cell **17,** 2157–2171.

Lifschitz, E., Eviatar, T., Rozman, A., Shalit, A., Goldshmidt, A., Amsellem, Z., Alvarez, J.P., and Eshed, Y. (2006). The tomato FT ortholog triggers systemic signals that regulate growth and flowering and substitute for diverse environmental stimuli. Proc. Natl. Acad. Sci. USA, in press.

Lim, L.P., Lau, N.C., Garrett-Engele, P., Grimson, A., Schelter, J.M., Castle, J., Bartel, D.P., Linsley, P.S., and Johnson, J.M. (2005). Microarray analysis shows that some microRNAs down regulate large numbers of target mRNAs. Nature **433,** 769–773.

Llave, C., Kasschau, K.D., Rector, M.A., and Carrington, J.C. (2002a). Endogenous and silencing-associated small RNAs in plants. Plant Cell **14,** 1605–1619.

Llave, C., Xie, Z., Kasschau, K.D., and Carrington, J.C. (2002b). Cleavage of *Scarecrow-like* mRNA targets directed by a class of *Arabidopsis* miRNA. Science **297,** 2053–2056.

Mallory, A.C., Dugas, D.V., Bartel, D.P., and Bartel, B. (2004b). MicroRNA regulation of NAC-domain targets is required for proper formation and separation of adjacent embryonic, vegetative, and floral organs. Curr. Biol. **14,** 1035–1046.

Mallory, A.C., Reinhart, B.J., Jones-Rhoades, M.W., Tang, G., Zamore, P.D., Barton, M.K., and Bartel, D.P. (2004a). MicroRNA control of *PHABULOSA* in leaf development: Importance of pairing to the microRNA 5′ region. EMBO J. **23,** 3356–3364.

Maniataki, E., and Morelatos, Z. (2005). A human, ATP-independent, RISC assembly machine fueled by pre-miRNA. Genes Dev. **19,** 2979–2990.

McConnell, J.R., Emery, J., Eshed, Y., Bao, N., Bowman, J., and Barton, M.K. (2001). Role of *PHABULOSA* and *PHAVOLUTA* in determining radial patterning in shoots. Nature **411,** 709–713.

McCormick, S. (1991). Transformation of tomato with *Agrobacterium tumifaciens*. In Plant Tissue Culture Manual, Vol. B6, K. Lindsey, ed (Dordrecht, The Netherlands: Kluwer Academic Publishers), pp. 1–9.

Moore, I., Galweiler, L., Grosskopf, D., Schell, J., and Klaus, P.A. (1998). Transcription activation system for regulated gene expression in transgenic plants. Proc. Natl. Acad. Sci. USA **95,** 376–381.

Moore, R.C., and Purugganan, M.D. (2005). The evolutionary dynamics of plant duplicate genes. Curr. Opin. Plant Biol. **8,** 122–128.

Nagpal, P., Ellis, C.M., Weber, H., Ploense, S.E., Barkawi, L.S., Guilfoyle, T.J., Hagen, G., Alonso, J.M., Cohen, J.D., Farmer, E.E., Ecker, J.R., and Reed, J.W. (2005). Auxin response factors ARF6 and ARF8 promote jasmonic acid production and flower maturation. Development **132,** 4107–4118.

Okushima, Y., Mitina, I., Quach, H.L., and Theologis, A. (2005b). AUXIN RESPONSE FACTOR 2 (ARF2): A pleiotropic developmental regulator. Plant J. **43,** 29–46.

Okushima, Y., et al. (2005a). Functional genomic analysis of the *AUXIN RESPONSE FACTOR* gene family members in *Arabidopsis thaliana*: Unique and overlapping functions of ARF7 and ARF19. Plant Cell **17,** 444–463.

Palatnik, J.F., Allen, E., Wu, X., Schommer, C., Schwab, R., Carrington, J.C., and Weigel, D. (2003). Control of leaf morphogenesis by microRNAs. Nature **425,** 257–263.

Palauqui, J.C., Elmayan, T., Pollien, J.M., and Vaucheret, H. (1997). Systemic acquired silencing: Transgene-specific post-transcriptional silencing is transmitted by grafting from silenced stocks to non-silenced scions. EMBO J. **16,** 4738–4745.

Parizotto, E.A., Dunoyer, P., Rahm, N., Himber, C., and Voinnet, O. (2004). In vivo investigation of the transcription, processing,

endonucleolytic activity, and functional relevance of the spatial distribution of a plant miRNA. Genes Dev. **18,** 2237–2242.

Pekker, I., Alvarez, J.P., and Eshed, Y. (2005). Auxin response factors mediate *Arabidopsis* organ asymmetry via modulation of KANADI activity. Plant Cell **17,** 2899–2910.

Prigge, M.J., Otsuga, D., Alonso, J.M., Ecker, J.R., Drews, G.N., and Clark, S.E. (2005). Class III homeodomain-leucine zipper gene family members have overlapping, antagonistic, and distinct roles in *Arabidopsis* development. Plant Cell **17,** 61–76.

Reinhart, B.J., Weinstein, E.G., Rhoades, M.W., Bartel, B., and Bartel, D.P. (2002). MicroRNAs in plants. Genes Dev. **16,** 1616–1626.

Reinhardt, D., Frenz, M., Mandel, T., and Kuhlemeier, C. (2005). Microsurgical and laser ablation analysis of leaf positioning and dorsoventral patterning in tomato. Development **132,** 15–26.

Rhoades, M.W., Reinhart, B.J., Lim, L.P., Burge, C.B., Bartel, B., and Bartel, D.P. (2002). Prediction of plant microRNA targets. Cell **110,** 513–520.

Riechmann, J.L., et al. (2000). *Arabidopsis* transcription factors: Genome-wide comparative analysis among eukaryotes. Science **290,** 2105–2110.

Scheres, B. (2001). Plant cell identity. The role of position and lineage. Plant Physiol. **125,** 112–114.

Schruff, M.C., Spielman, M., Tiwari, S., Adams, S., Fenby, N., and Scott, R.J. (2006). The *AUXIN RESPONSE FACTOR 2* gene of *Arabidopsis* links auxin signalling, cell division, and the size of seeds and other organs. Development **133,** 251–261.

Schwab, R., Palatnik, J.F., Riester, M., Schommer, C., Schmid, M., and Weigel, D. (2005). Specific effects of microRNAs on the plant transcriptome. Dev. Cell **8,** 517–527.

Schwarz, D.S., Hutvagner, G., Du, T., Xu, Z., Aronin, N., and Zamore, P.D. (2003). Asymmetry in the assembly of the RNAi enzyme complex. Cell **115,** 199–208.

Sijen, T., Fleenor, J., Simmer, F., Thijssen, K.L., Parrish, S., Timmons, L., Plasterk, R.H.A., and Fire, A. (2001). On the role of RNA amplification in dsRNA-triggered gene silencing. Cell **107,** 465–476.

Souer, E., van Houwelingen, A., Kloos, D., Mol, J., and Koes, R. (1996). The *no apical meristem* gene of Petunia is required for pattern formation in embryos and flowers and is expressed at meristem and primordia boundaries. Cell **85,** 159–170.

Stark, A., Brennecke, J., Bushati, N., Russell, R.B., and Cohen, S.M. (2005). Animal microRNAs confer robustness to gene expression and have a significant impact on 3′UTR evolution. Cell **123,** 1133–1146.

Tang, G., Reinhart, B.J., Bartel, D.P., and Zamore, P.D. (2003). A biochemical framework for RNA silencing in plants. Genes Dev. **17,** 49–63.

Voinnet, O. (2005). Non-cell autonomous RNA silencing. FEBS Lett. **579,** 5858–5871.

Watson, J.M., Fusaro, A.F., Wang, M., and Waterhouse, P.M. (2005). RNA silencing platforms in plants. FEBS Lett. **579,** 5982–5987.

Williams, L., Carles, C.C., Osmont, K.S., and Fletcher, J.C. (2005b). A database analysis method identifies an endogenous trans-acting short-interfering RNA that targets the *Arabidopsis ARF2*, *ARF3*, and *ARF4* genes. Proc. Natl. Acad. Sci. USA **102,** 9703–9708.

Williams, L., Grigg, S.P., Xie, M., Christensen, S., and Fletcher, J.C. (2005a). Regulation of *Arabidopsis* shoot apical meristem and lateral organ formation by microRNA miR166g and its AtHD-ZIP target genes. Development **132,** 3657–3668.

Yekta, S., Shih, I.H., and Bartel, D.P. (2004). MicroRNA-directed cleavage of HOXB8 mRNA. Science **304,** 594–596.

Yoo, B.C., Kragler, F., Varkonyi-Gasic, E., Haywood, V., Archer-Evans, S., Lee, Y.M., Lough, T.J., and Lucas, W.J. (2004). A systemic small RNA signaling system in plants. Plant Cell **16,** 1979–2000.

Zuker, M. (2003). Mfold web server for nucleic acid folding and hybridization prediction. Nucleic Acids Res. **31,** 3406–3415.

nature biotechnology

Expression of artificial microRNAs in transgenic *Arabidopsis thaliana* confers virus resistance

Qi-Wen Niu[1,4], Shih-Shun Lin[1,4], Jose Luis Reyes[1,3], Kuan-Chun Chen[1,3], Hui-Wen Wu[1], Shyi-Dong Yeh[2] & Nam-Hai Chua[1]

Plant microRNAs (miRNAs) regulate the abundance of target mRNAs by guiding their cleavage at the sequence complementary region. We have modified an *Arabidopsis thaliana* miR159 precursor to express artificial miRNAs (amiRNAs) targeting viral mRNA sequences encoding two gene silencing suppressors, P69 of turnip yellow mosaic virus (TYMV) and HC-Pro of turnip mosaic virus (TuMV). Production of these amiRNAs requires *A. thaliana* DICER-like protein 1. Transgenic *A. thaliana* plants expressing amiR-P69^{159} and amiR-HC-Pro^{159} are specifically resistant to TYMV and TuMV, respectively. Expression of amiR-TuCP^{159} targeting TuMV coat protein sequences also confers specific TuMV resistance. However, transgenic plants that express both amiR-P69^{159} and amiR-HC-Pro^{159} from a dimeric pre-amiR-P69^{159}/amiR-HC-Pro^{159} transgene are resistant to both viruses. The virus resistance trait is displayed at the cell level and is hereditable. More important, the resistance trait is maintained at 15 °C, a temperature that compromises small interfering RNA–mediated gene silencing. The amiRNA-mediated approach should have broad applicability for engineering multiple virus resistance in crop plants.

Plants possess several innate mechanisms to resist viruses, one of which entails the production of dominant resistance gene products that can trigger hypersensitive response and systemic acquired resistance[1,2]. However, transgenic technology offers the possibility to genetically modify plants with genes encoding virus tolerance/resistance. Over the last two decades, several strategies have been developed mostly based on the concept of pathogen-derived resistance[3].

The coat protein gene of the tobacco mosaic virus (TMV) was used in the first demonstration of virus-derived, protein-mediated resistance in transgenic plants[4]. Transgenic tobacco plants expressing high TMV coat protein levels were resistant to TMV virions but less so to TMV RNA. This pioneering observation was quickly confirmed by similar results with other viral coat protein genes[5]. In addition, dominant-negative mutant forms of viral proteins, for example, replicase[6] and movement proteins[7], also confer virus resistance in transgenic plants.

RNA-mediated virus resistance can be brought about by expression of satellite RNA, defective interfering RNA or the noncoding region of viral genome RNAs, which interfere competitively with virus replication[7]. This type of resistance can also be accomplished by expression of viral sequences in the sense or antisense orientation[8,9] or in double-stranded forms[10]. In these cases, expression triggers degradation of both the transgene RNA and the corresponding viral RNA via post-transcriptional gene silencing.

The post-transcriptional gene silencing pathway targets double-stranded (ds)RNA for degradation by DICER-like (DCL) proteins in a sequence-specific manner through the production of small interfering (si)RNA. Whereas DCL2 cleaves dsRNAs from replicating virus[11], DCL3 cleaves dsRNAs derived from endogenous transcripts through the activity of RNA-dependent RNA polymerases 2 and 6 (refs. 12,13). The siRNAs produced are incorporated into RNA-induced silencing complexes (RISC), which guide cleavage of target RNAs. Because post-transcriptional gene silencing is a host antiviral defense mechanism, it is not surprising that viruses encode suppressor proteins that can block this function[2,14–16].

Recently, miRNAs have been identified as important regulators of gene expression in both plants and animals. miRNAs are single-stranded RNAs, 20–24 nucleotides (nt) in length, generated from processing of longer pre-miRNA precursors[17] by DCL1 in *A. thaliana*[11]. These miRNAs are recruited to the RISC complex. Using RNA:RNA base-pairing, miRNAs direct RISC in a sequence-specific manner to downregulate target mRNAs in one of two ways. Limited miRNA:mRNA base-pairing results in translational repression, which is the case with the majority of the animal miRNAs studied so far. By contrast, most plant miRNAs show extensive base-pairing to, and guide cleavage of, their target mRNAs[18]. In *A. thaliana*, miRNAs are known to be important regulators of plant developmental processes.

Previous reports have shown that alteration of several nucleotides within an miRNA 21-nt sequence does not affect its biogenesis[19]. Therefore, it may be possible to modify plant miRNA sequence to target specific transcripts, originally not under miRNA control. To explore this possibility we used the 273-bp backbone of pre-miRNA^{159a} to generate artificial pre-miRNAs^{159} (pre-amiRNAs^{159}) containing sequences complementary to two plant viruses TYMV and TuMV.

[1]Laboratory of Plant Molecular Biology, Rockefeller University, 1230 York Avenue, New York, New York 10021, USA. [2]Department of Plant Pathology, National Chung Hsing University, 250 Kao Kung Road, Taichung, Taiwan 402. [3]Present addresses: Instituto de Biotecnologia-UNAM. Ave. Universidad 2001, Cuernavaca, Morelos 62215, Mexico (J.L.R.), Department of Plant Pathology, National Chung Hsing University, 250 Kao Kung Road, Taichung, Taiwan 402 (K.-C.C.). [4]These authors contributed equally to this work. Correspondence should be addressed to N.-H.C. (chua@mail.rockefeller.edu).

Received 12 June; accepted 25 September; published online 22 October 2006; doi:10.1038/nbt1255

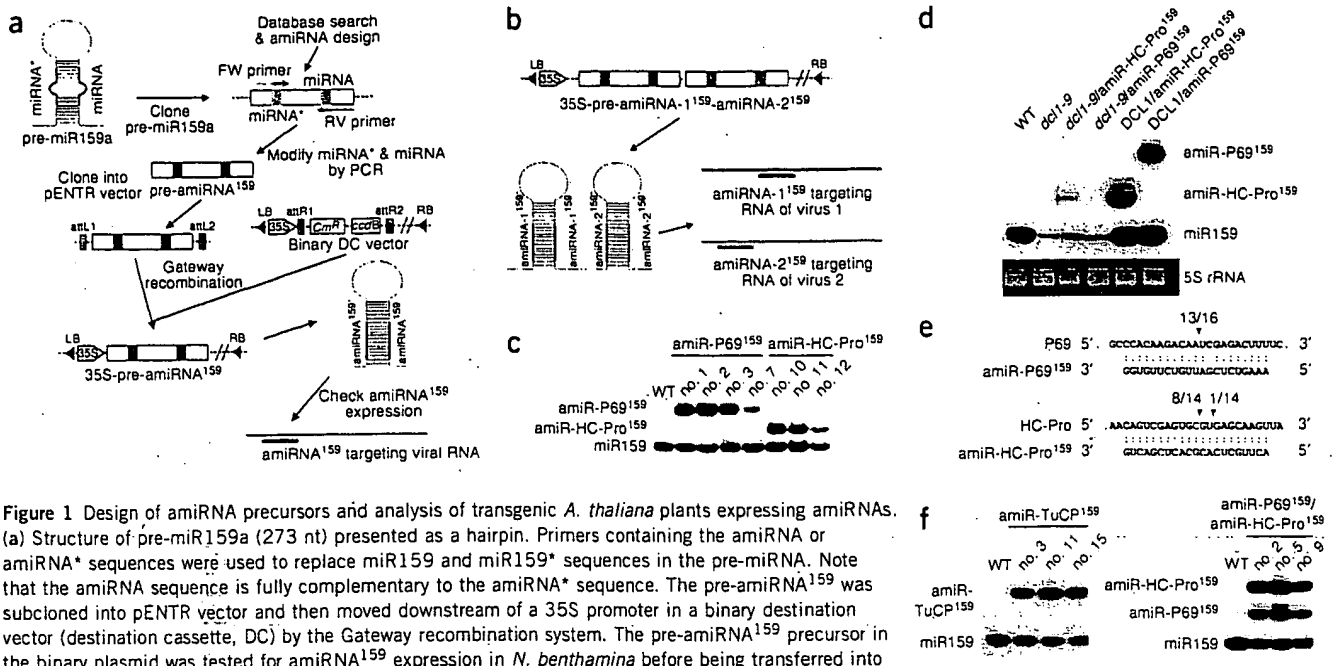

Figure 1 Design of amiRNA precursors and analysis of transgenic *A. thaliana* plants expressing amiRNAs. (a) Structure of pre-miR159a (273 nt) presented as a hairpin. Primers containing the amiRNA or amiRNA* sequences were used to replace miR159 and miR159* sequences in the pre-miRNA. Note that the amiRNA sequence is fully complementary to the amiRNA* sequence. The pre-amiRNA^{159} was subcloned into pENTR vector and then moved downstream of a 35S promoter in a binary destination vector (destination cassette, DC) by the Gateway recombination system. The pre-amiRNA^{159} precursor in the binary plasmid was tested for amiRNA^{159} expression in *N. benthamina* before being transferred into *A. thaliana*. (b) A binary vector carrying 35S-pre-amiR-P69^{159}/amiR-HC-Pro^{159}. In transgenic plants, this transgene can produce two different amiRNAs directed against two different viruses. (c) Transgenic plants carrying 35S-pre-amiR-P69^{159} or 35S-pre-amiR-HC-Pro^{159}. Four lines expressing amiR-P69^{159} (lines nos. 1, 2, 3 and 7) and three lines expressing amiR-HC-Pro^{159} (lines nos. 10, 11 and 12) were analyzed. The endogenous miR159 was used as a loading control. Each lane contained 10 μg total RNA. (d) Expression of amiRNAs requires DCL1. amiRNA transgenic plants were crossed with *dcl1-9* mutant and *dcl1-9* homozygous seedlings carrying 35S-pre-amiRNA transgenes were analyzed. Each lane contained 10 μg RNA. 5S rRNA and tRNAs were used as loading controls. (e) Mapping of cleavage site of P69 and HC-Pro mRNA by 5′RACE. The arrows indicate that 13/16 clones of P69 and 8/14 clones of HC-Pro were derived from products cleaved at the expected site. This cleavage site is located between nucleotides complementary to nucleotide 10 and 11 of the amiRNA. (f) Transgenic plants expressing amiR-TuCP^{159} or amiR-P69^{159}/amiR-HC-Pro^{159}. Three lines expressing amiR-TuCP^{159} lines (nos. 3, 11 and 15) and three lines expressing amiR-P69^{159}/amiR-HC-Pro^{159} lines (nos. 2, 5 and 9) were analyzed. The endogenous miR159 was used as a loading control. Each lane contained 10 μg total RNA.

Both TYMV and TuMV can infect Brassica and non-Brassica hosts inflicting significant economic damages worldwide[20–23]. TYMV is a tymovirus with an RNA genome that encodes three proteins, one of which is a 69-kDa movement protein with silencing suppressor function[24]. TuMV, a potyvirus, encodes a large polyprotein, which is post-translationally processed into several smaller proteins[25]. HC-Pro, a viral proteinase with multiple functions, acts as a silencing suppressor. Because viral suppressors play an important role in counteracting host defense, we chose to design amiRNAs to target these sequences. In addition, we have also designed amiRNAs to target the coat protein sequences of TuMV.

In this study, we demonstrate that transgenic plants can generate two amiRNAs from pre-amiRNAs—amiR-P69^{159} and amiR-HC-Pro^{159} with sequences complementary to P69 and HC-Pro coding sequence, respectively. Furthermore, when inoculated with the specific virus, these plants displayed specific resistance even at low temperatures that inhibit post-transcriptional gene silencing. In addition, expression of a dimeric amiRNA precursor, which can generate both amiR-P69^{159} and amiR-HC-Pro^{159}, conferred resistance to both viruses. During the preparation of this manuscript, Schwab *et al.*[26] and Alvarez *et al.*[27] reported the successful downregulation of plant genes by amiRNAs targeting individual genes or groups of endogenous genes. These amiRNAs were constructed using precursors of miR164b, miR172a and miR319a as backbones. Furthermore, plum pox virus chimeras bearing endogenous miRNA target sequences displayed reduced infectivity in plants[28]. The use of synthetic miRNAs and multiple miRNA genes to downregulate gene expression has also been reported in animal and human cells[29–33].

RESULTS

Expression of amiRNAs in transgenic *A. thaliana*

Preliminary analysis showed that miRNA159 was expressed at high levels in all *A. thaliana* organs (data not shown). We therefore chose the 273-nt pre-miR159a hairpin structure (**Fig. 1a**) as a backbone for the construction and expression of amiRNAs termed amiRNA^{159}. The designs of pre-amiRNAs and expression of amiRNAs in transgenic plants are shown (**Fig. 1**).

Using oligonucleotide-directed mutagenesis, we replaced the 21-nt sequence of miR159 with the synthetic sequence 5′-AAAGUCUCG AUUGUCUUGUGG-3′ (amiR-P69^{159}) or 5′-ACUUGCUCACGCAC UCGACUG-3′ (amiR-HC-Pro^{159}) directed against a region of the mRNA encoding the suppressor P69 or HC-Pro, respectively. We obtained expression of amiR-HC-Pro^{159} and amiR-P69^{159} in wild-type transgenic lines (**Fig. 1a,c**) but their expression, like that of the endogenous miR159, was much reduced in *dcl1-9*, implicating DCL1 in their biogenesis (**Fig. 1d**). Four amiR-P69^{159} (nos. 1, 2, 3 and 7) and three amiR-HC-Pro^{159} (nos. 10, 11 and 12) independent transgenic lines were chosen for further experimentation.

Cleavage of P69 and HC-Pro mRNA

To see if the amiRNAs can mediate cleavage of target RNAs, we infiltrated *Nicotiana benthamiana* leaves with Agrobacterial cells carrying plasmids containing the constructs pBA-amiR-P69^{159}/pBA-P69-HA, pBA-amiR-HC-Pro^{159}/pBA-HC-Pro-HA, pBA002/pBA-P69-HA or pBA002/pBA-HC-Pro-HA. The empty vector pBA002 was used as a negative control. In 13 out of 16 clones analyzed, P69 mRNA cleavage

occurred at the expected position (nucleotide 224) located between the two nucleotides complementary to nucleotide 10 and 11 of the amiR-P69^{159} (Fig. 1e). Three other cleavage products with 5′ ends further downstream (at nucleotide 254, 285 and 403) were recovered, suggesting *A. thaliana* XRN4 exonuclease activity[34,35] (data not shown). No rapid amplification of 5′ complementary DNA ends (5′RACE) product was obtained from the negative control sample. Similar results were obtained in an HC-Pro mRNA cleavage experiment with 8 out of 14 clones analyzed having the correct cleavage at nucleotide 840 of the HC-Pro mRNA (complementary to nucleotides 10 to 11 of the triggering amiR-HC-Pro^{159}) whereas one clone showed cleavage at nucleotide 842 (Fig. 1e). The 5′ ends of the other 5 clones were detected at nucleotide 876, 878, 879, 913 and 1030 of the HC-Pro mRNA (data not shown). These data showed that both amiRNAs can mediate precise cleavage of their target viral RNAs.

Specificity of amiRNA

Using BLAST search we failed to find any *A. thaliana* genes having complementary sequences of more than 15-nt over the 21-nt sequence of amiR-P69^{159} or amiR-HC-Pro^{159}. The PATMATCH (ver 1.1) program on the TAIR website (http://www.arabidopsis.org/) also did not uncover any endogenous *A. thaliana* transcripts as possible targets when the parameter was set as 0 mismatch. However, 6 *A. thaliana* transcripts can potentially form imperfect pairing (mismatch and deletion) with amiR-P69^{159} and amiR-HC-Pro^{159} when three mismatches were allowed (see **Supplementary Fig. 1a,b** online).

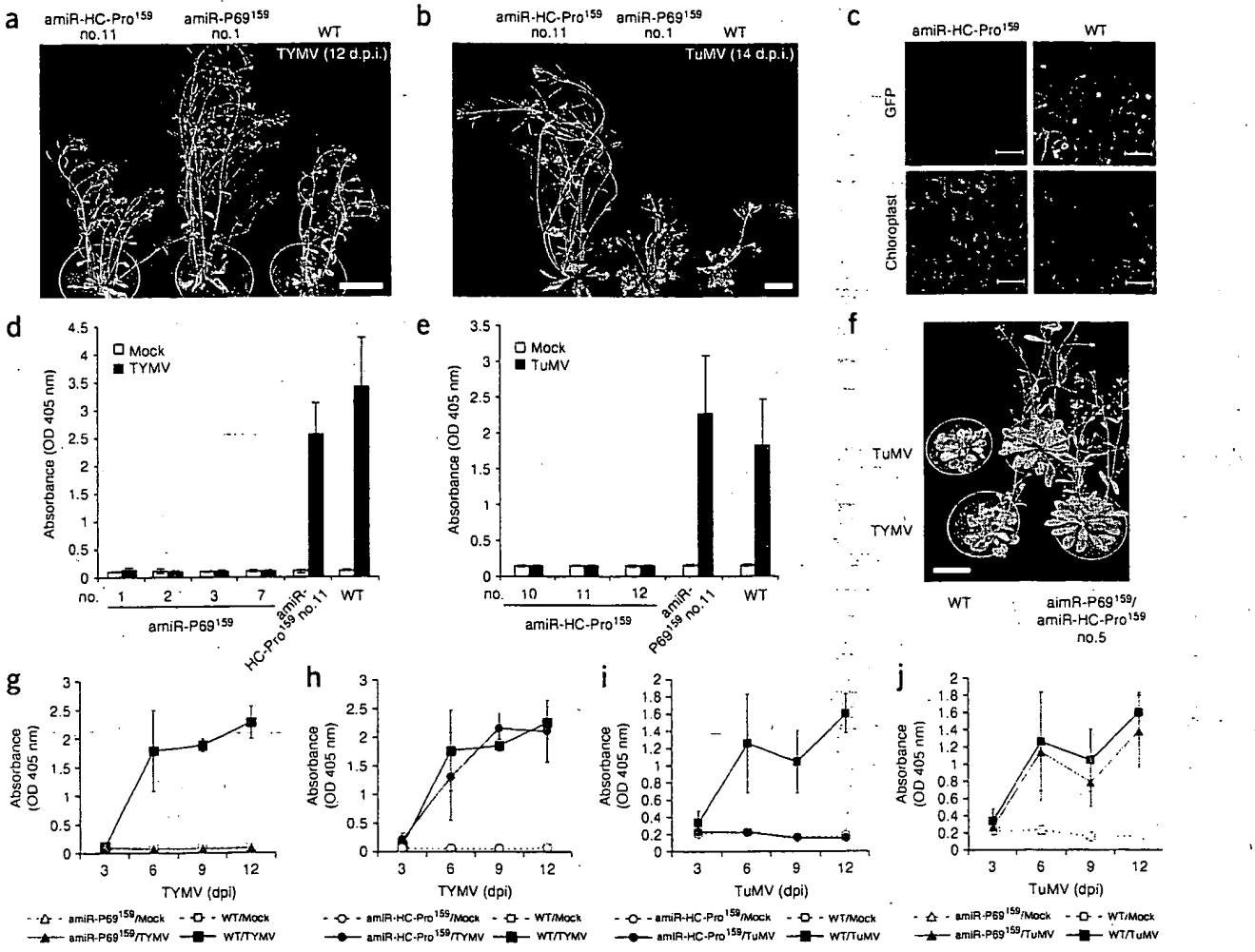

Figure 2 Transgenic plants expressing amiR-P69^{159} and amiR-HC-Pro^{159} are resistant to TYMV and TuMV infection, respectively. (**a**) Plants were inoculated with TYMV and photographs taken 12 d.p.i. Bar, 4 cm. (**b**) Plants were inoculated with TuMV and photographs taken 14 d.p.i. Bar, 3 cm. (**c**) TuMV-GFP infection and cell-to-cell movement of the chimeric virus on inoculated leaves. Entire inoculated leaves of wild-type and transgenic plants were examined by confocal microscopy. Inoculated wild-type leaves always displayed fluorescence due to replication of the GFP-virus, whereas transgenic leaves of amiR-HC-Pro^{159} plants never showed any fluorescence even when the entire leaf was examined. Bar, 50 μm. (**d**) ELISA detection of TYMV coat protein in different transgenic and wild-type plants. Readings were taken after 3 h of substrate hydrolysis. Bars represent standard deviations and $N = 22$. (**e**) ELISA detection of TuMV coat protein in different transgenic and wild-type plants at 14 d.p.i. Readings were taken after 30 min of substrate hydrolysis. Bars show standard deviations. $N = 12$. (**f**) Transgenic plants expressing amiR-P69^{159}/amiR-HC-Pro^{159} are resistant to TYMV and TuMV infection. Plants were inoculated with TYMV or TuMV and photographs taken 14 d.p.i. Bar, 4 cm. (**g,h**) Time course of TYMV titer in various transgenic lines (amiR-P69^{159} no. 1 and amiR-HC-Pro^{159} no. 11) and wild-type plants. Six d.p.i. transgenic amiR-HC-Pro^{159} no. 11 and wild-type plants were systemically infected by TYMV. Bars represent standard deviations and $N = 92$. (**i,j**) Time course of TuMV titers in various transgenic lines (amiR-P69^{159} no. 1 and amiR-HC-Pro^{159} no. 11) and wild-type plants. Bars represent standard deviation and $N = 41$.

Table 1 Infectivity assay of amiR-HC-Pro^{159} and amiR-P69^{159} transgenic plants challenged with TYMV inocula

	N° infected/inoculated plants					
	Experiment 1			Experiment 2		
Transgenic plant	Line	u[a]	R (%)[b]	Line	u	R (%)
amiR-P69^{159}	1[c]	0/3	100	1-1[d]	0/32	100
	2	0/6	100	2-5	0/22	100
	3	0/6	100	3-1	0/32	100
	7	0/6	100	7-1	0/32	100
amiR-HC-Pro^{159}	10	5/6	16.7	10-4	30/31	3.2
	11	6/6	0	11-3	32/32	0
	12	5/5	0	12-4	29/30	3.3
WT		16/17	5.9		61/61	0

[a]Upper noninoculated leaves were analyzed by ELISA. The nominator indicates the number of ELISA-positive plants and the denominator the total number of plants in the experiment. [b]R, number of resistant plants as a percentage of the total plant population. [c]The amiR-P69^{159} lines (nos. 1, 2, 3 and 7) and amiR-HC-Pro^{159} lines (nos. 10, 11 and 12) are T_2 progeny containing a mixture of homozygotes and hemizygotes with respect to the transgene. [d]The amiR-P69^{159} lines (nos. 1-1, 2-5, 3-1 and 7-1) and amiR-HC-Pro^{159} lines (nos. 10-4,11-3 and 12-4) are homozygous T_3 progeny. WT, wild type.

To check if the two amiRNAs can also downregulate *A. thaliana* transcripts with such imperfect matches, we monitored their expression levels in wild-type and transgenic plants by RT-PCR. We also examined possible effects on genome-wide expression by hybridizations to Affymetrix ATH1 arrays. Our analysis showed that none of the *A. thaliana* genes expressed in wild type were downregulated by either of the amiRNAs (see **Supplementary Table 1** online). Expression of five of the putative target genes was not affected by the amiRNAs (see **Supplementary Fig. 1c,d** online). The sixth putative target gene (AT1G69320) was not expressed either in wild-type plants or in transgenic plants by genome array analysis or by RT-PCR. This is likely due to its low transcript abundance (see **Supplementary Table 1** online). In addition to this molecular analysis, we found that transgenic plants expressing the amiRNAs displayed normal morphology and growth rate. The flowering time was unaltered, the flowers were fertile and the siliques contained seeds of the normal amount. Although these results suggest that amiR-P69^{159} and amiR-HC-Pro^{159} can specifically target viral RNA but not endogenous transcripts, we can not exclude the possibility that transcripts expressed only under specific conditions, for example, abiotic stress, might be affected.

TYMV resistance of amiR- P69^{159} plants

The cleavage of P69 mRNA mediated by amiR-P69^{159} suggested the possibility of using this amiRNA to mediate cleavage of viral RNA to confer resistance. We selected four amiR-P69^{159} transgenic lines (nos. 1, 2, 3 and 7) and challenged progeny plants with TYMV or buffer. Wild-type plants and three amiR-HC-Pro^{159} lines (nos. 10, 11 and 12) were used as controls.

Figure 2 shows responses of wild-type and transgenic plants to virus challenge. Twelve days post-inoculation (d.p.i.), wild-type plants and amiR-HC-Pro^{159} plants (line no. 11) showed diffused chlorotic local lesions on inoculated leaves and yellow mosaics on systemic leaves (**Fig. 2a** and **Supplementary Fig. 2a** online) characteristic of TYMV-induced symptoms[14]. Moreover, these infected plants developed shorter inflorescence internodes (see **Supplementary Fig. 2b** online), the inflorescences displayed early senescence and flowers had pollination defects. By contrast, amiR-P69^{159} plants (line no. 1) appeared normal, like mock-inoculated plants of all genotypes (wild type and transgenic) (**Fig. 2a** and **Supplementary Fig. 2a,b** online). Similar results were also obtained for amiR-P69^{159} transgenic line nos. 2, 3 and 7 after TYMV inoculation confirming that TYMV resistance can be seen in all four independent lines.

Extracts of systemic leaves from individual plants were assayed by enzyme-linked immunosorbent assays (ELISA) using polyclonal antibodies to the TYMV coat protein. The TYMV coat protein was undetectable in inoculated amiR-P69^{159} plants indicating virus resistance. By contrast, TYMV coat protein was present at high levels in the susceptible wild-type and amiR-HC-Pro^{159} plants (**Fig. 2d**) consistent with the appearance of virus symptoms (**Fig. 2a** and **Supplementary Fig. 2a,b** online). TYMV-inoculated wild-type and amiR-HC-Pro^{159} plants contained high TYMV coat protein levels, which were not detected in mock-inoculated plants of all genotypes and in TYMV-inoculated amiR-P69^{159} plants (see **Supplementary Fig. 2c** online).

In wild-type plants, coat protein was not detectable at 3 d.p.i. but accumulated rapidly to high levels at 6 d.p.i. and then the level reached a plateau thereafter (**Fig. 2g,h**). TYMV-inoculated amiR-HC-Pro^{159} plants continued to accumulate TYMV coat protein until 12 d.p.i. before leveling off. No accumulation of TYMV coat protein was found in amiR-P69^{159} plants at all time points, indicating virus resistance.

We also monitored symptoms development and TYMV coat protein accumulation on upper noninoculated leaves in two independent experiments (**Table 1**). In the first experiment, T_2 progeny (homozygotes and hemizygotes) of amiR-P69^{159} plants (nos. 1, 2, 3 and 7) and of amiR-HC-Pro^{159} plants (nos. 10, 11 and 12) were analyzed along with wild-type plants. Most of the wild-type plants (16 out of 17), all of the amiR-HC-Pro^{159} plants derived from two independent lines (nos. 11 and 12) and 5 out of 6 plants of amiR-HC-Pro^{159} line no. 10 showed systemic yellow mosaic symptom and accumulated TYMV coat protein. The percent resistance is around 0 to 16.7%. By contrast, all amiR-P69^{159} lines showed 100% resistance to TYMV. In the second experiment, T_3 progeny (homozygotes) of amiR-P69^{159} plants (line nos. 1-1, 2-5, 3-1 and 7-1) and of amiR-HC-Pro^{159} plants (line nos. 10-4, 11-3 and 12-4) were challenged with TYMV. The percent resistances of wild-type and amiR-HC-Pro^{159} plants were around 0–3.3%, but T_3 progeny of

Table 2 Infectivity assay of amiR-HC-Pro^{159} and amiR-P69^{159} transgenic lines challenged with TuMV inocula

		N° infected/inoculated plants					
		Experiment 1		Experiment 2		Experiment 3	
Transgenic plant	Line	u[a]	R (%)[b]	u	R (%)	u	R (%)
amiR-P69^{159}	1[c]	11/12	8.3	8/8	0	18/19	5.3
	2	ne[d]		8/8	0	16/17	5.9
	3	ne		5/6	16.7	ne	
	7	ne		5/5	0	ne	
amiR-HC-Pro^{159}	10	ne		0/12	100	0/24	100
	11	0/12	100	0/12	100	0/17	100
	12	ne		0/9	100	ne	
WT		11/12	8.3	25/33	24.2	41/41	0

[a]Upper noninoculated leaves were analyzed by ELISA. The nominator indicates the number of ELISA-positive plants and the denominator the total number of plants in the experiment. [b]R, number of resistant plants as a percentage of the total plant population. [c]The amiR-P69^{159} lines (nos. 1, 2, 3 and 7) and amiR-HC-Pro^{159} lines (nos. 10, 11 and 12) are T_2 progeny containing a mixture of homozygotes and hemizygotes with respect to the transgene. [d]ne, not examined. WT, wild type.

Table 3 Infectivity assay of amiR-P69^{159}/amiR-HC-Pro^{159} transgenic plants challenged with inocula of TYMV, TuMV or both viruses

		Nº infected/inoculated plants							
		Single infection[a]				Co-infection[b]			
	Line	u_{TuMV}[c]	R[d] (%)	u_{TYMV}	R (%)	u_{TuMV}	R (%)	u_{TYMV}	R (%)
amiR-P69^{159}/amiR-HC-Pro^{159}	2[e]	0/17	100	0/17	100	0/35	100	0/35	100
	5	0/16	100	0/17	100	0/34	100	0/34	100
	9	0/23	100	0/25	100	0/43	100	0/43	100
amiR-P69^{159}	7-1[f]	23/23	0	0/25	100	35/36	2.8	0/36	100
amiR-HC-Pro^{159}	10-4	0/23	100	23/23	0	0/32	100	32/32	0
WT		16/16	0	19/20	5	33/37	10.8	37/37	0

[a]Single infection with TuMV or TYMV inocula. [b]Co-infection with mixed TuMV and TYMV inocula. [c]Upper noninoculated leaves were analyzed by ELISA. The nominator indicates the number of ELISA-positive plants and the denominator the total number of plants in the experiment. [d]R, number of resistant plants as a percentage of the total plant population. [e]The amiR-P69^{159}/amiR-HC-Pro^{159} lines (nos. 2, 5 and 9) are T_2 progeny containing a mixture of homozygotes and hemizygotes with respect to the transgene. [f]amiR-P69^{159} line no. 7-1 and amiR-HC-Pro^{159} line no. 10-4 are homozygous T_3 progeny. WT, wild type.

amiR-P69^{159} plants displayed 100% resistance to TYMV. Together, the results show that the virus resistance trait can be transmitted to the next generation.

TuMV resistance of amiR-HC-Pro^{159} plants

Next, we inoculated the same set of transgenic plants with TuMV using wild-type plants as controls. Fourteen days after inoculation, vegetative growth of amiR-P69^{159} (line no.1) and wild-type plants showed severe developmental abnormalities, including stunting and reduced internodal distances (**Fig. 2b** and **Supplementary Fig. 3a** online). TuMV-infected amiR-P69^{159} and wild-type plants showed narrow sepals that failed to encase developing flowers. Moreover, the flowers were often sterile because of short anthers that failed to pollinate (see **Supplementary Fig. 3b** online), and siliques were small and appeared abnormal (see **Supplementary Fig. 3c** online). These symptoms were characteristics of plants infected with TuMV[15]. By contrast, transgenic amiR-HC-Pro^{159} plants (line no. 11) were resistant to TuMV infection and displayed normal inflorescence, flower and silique development, like mock-inoculated plants of all genotypes.

amiR-HC-Pro^{159} and wild-type plants were also challenged with a TuMV virus carrying a GFP gene. GFP signal was seen on inoculated and systemic leaves of wild-type but not those of amiR-HC-Pro^{159} plants (**Fig. 2c**). These results indicate the amiRNA-mediated resistance can block viral RNA replication in infected cells, and viruses can not move from cell to cell nor translocate systemically to upper leaves.

TuMV coat protein was not detected in mock-inoculated plants of all genotypes and in TuMV-inoculated amiR-HC-Pro^{159} plants indicating TuMV resistance. On the other hand, TuMV coat protein was present at high levels in TuMV-infected wild-type and amiR-P69^{159} plants (**Fig. 2e** and **Supplementary Fig. 3d** online) consistent with the appearance of virus symptoms (**Fig. 2b** and **Supplementary Fig. 3a-c** online).

In a time course experiment, amiR-P69^{159} and wild-type plants showed no detectable TuMV coat protein at 3 d.p.i. but it accumulated rapidly to high levels at 6 d.p.i. The TuMV titer decreased slightly at 9 d.p.i. but higher TuMV titer was detected at 12 d.p.i. (**Fig. 2i,j**). This result indicates that amiR-P69^{159} and wild-type plants were susceptible to TuMV infection. No accumulation of TuMV coat protein was found in amiR-HC-Pro^{159} plants at all time points, indicating TuMV resistance.

We monitored symptoms of upper noninoculated leaves and performed ELISA assays of leaf extracts in three independent experiments (**Table 2**). Plants of T_2 progeny (homozygotes and hemizygotes) of amiR-P69^{159} (line nos. 1, 2, 3 and 7) and amiR-HC-Pro^{159} (line nos. 10, 11 and 12) and wild-type control plants were analyzed. The percent resistance of wild-type and amiR-P69^{159} plants was ~0–24.2%. By contrast, all of the amiR-HC-Pro^{159} lines showed 100% resistance to TuMV in all three experiments. These results confirm the resistance of amiR-HC-Pro^{159} plants to TuMV.

In addition, we found that amiR-TuCP^{159} transgenic plants (line nos. 3, 11 and 15), which produced amiR-TuCP^{159} (5′-ACUCUCUGC UCGUAUCUUGGC-3′) targeting the TuMV coat protein sequences, showed complete resistance to TuMV (**Fig. 1f** and **Supplementary Table 2** online).

Transgenic plants resistant to both viruses

Transgenic plants expressing either amiR-P69^{159} or amiR-HC-Pro^{159} were resistant only to the specific virus targeted by the amiRNA. However, we observed breakdown of this specific resistance in a few transgenic plants co-inoculated with both viruses (see **Supplementary Table 3** online). This occasional breakdown is not surprising because when produced at sufficiently high levels the gene silencing suppressor of the nontargeted virus (P69 of TYMV or HC-Pro of TuMV) would interfere with the host miRNA machinery thereby blocking the targeting amiRNA activity. To generate transgenic plants with double resistance against both viruses, we constructed a dimeric amiRNA precursor (pre-amiR-P69^{159}/amiR-HC-Pro^{159}) by ligating pre-amiR-P69^{159} and pre-amiR-HC-Pro^{159} and expressing the dimer in a single Pol II transcription unit (**Fig. 1b**). Expression of both amiRNAs was detected in three independent transgenic lines (nos. 2, 5 and 9) carrying the dimeric pre-amiRNA (**Fig. 1f**). No viral symptoms were detected in these lines upon infection with either TuMV or TYMV or when co-inoculated with both viruses (**Fig. 2f**). These double resistance results were confirmed by ELISA analysis (**Table 3**).

Maintenance of virus resistance of amiRNA plants at 15 °C

Sense viral RNA-mediated resistance to cymbidium ringspot virus breaks down at 15 °C because of the sensitivity of post-transcriptional gene silencing to low temperatures[36]. To see whether the amiRNA plants would maintain their virus resistance at 15 °C, we grew wild-type and transgenic plants at 15 °C for 3 weeks. We found that

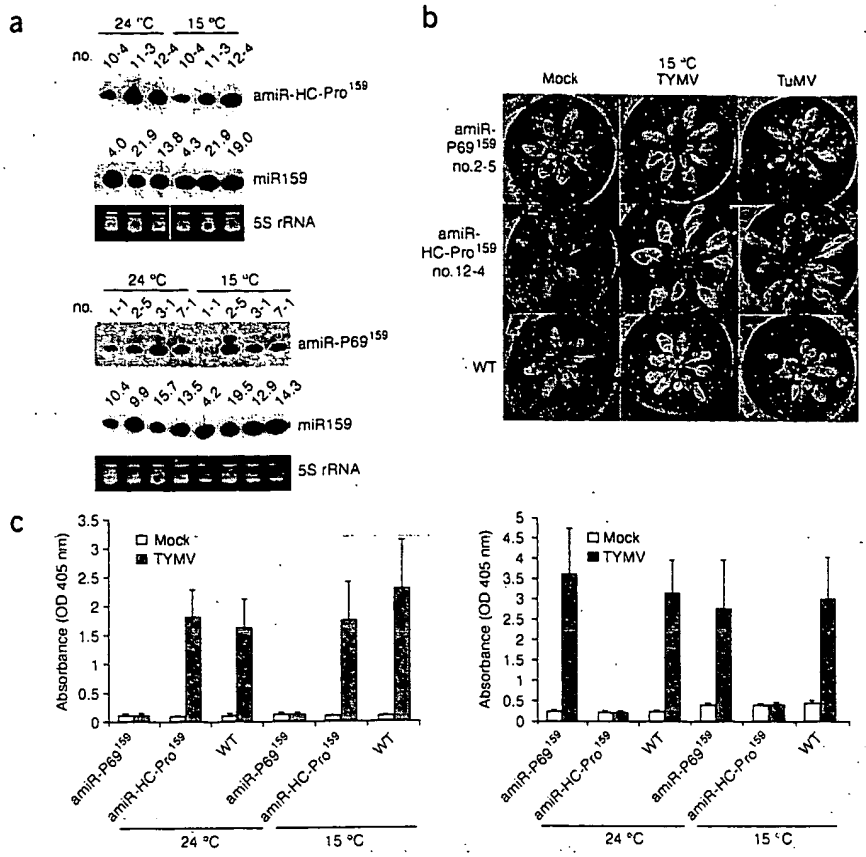

Figure 3 Effect of temperature on amiRNA production and virus resistance. (a) Expression of amiRNAs at 24 °C and 15 °C. Homozygous T_3 amiR-P69[159] and amiR-HC-Pro[159] transgenic plants were grown at 24 °C and 15 °C. Each lane contained 10 μg total RNA. 5S rRNA and tRNAs were used as loading controls. Transgenic line numbers are given on the top panels and numbers between the two panels represent signal strengths of amiRNA relative to miR159. (b) Symptom development and virus resistance phenotype of amiR-P69[159] and amiR-HC-Pro[159] transgenic plants at low temperatures. (c) amiR-P69[159] and amiR-HC-Pro[159] transgenic plants were resistant to TYMV (left panel) and TuMV (right panel), respectively, at low temperatures. Two transgenic amiR-HC-Pro[159] lines (nos. 10-4 and 11-3), two transgenic amiR-P69[159] lines (nos. 1-1 and 2-5) and wild-type plants were used. For each line, 12 individual plants were inoculated with TuMV or TYMV whereas 4 individual plants were inoculated with buffer as controls (Mock). After 2 weeks systemic leaves were collected for ELISA analyses using an antibody against TuMV coat protein or TYMV coat protein. Bars represent standard deviation and $N = 24$.

amiRNA levels at 15 °C were comparable to those at 24 °C (**Fig. 3a**). In addition, expression of endogenous miRNAs (miR165, miR164, miR159 and miR167) and trans-acting (ta-) siRNA (si255) was also not significantly affected at 15 °C (see **Supplementary Fig. 4** online). TYMV symptoms were more severe at 15 °C than at 24 °C. Severe yellowing and necrosis were visible on inoculated leaves of amiR-HC-Pro[159] and wild-type plants at 10 d.p.i. (**Fig. 3b**). On the other hand, only mild chlorosis appeared on TuMV-inoculated leaves of amiR-P69[159] and wild-type plants at the same temperature. For both types of transgenic plants, amiRNA-mediated specific virus resistance was maintained at 15 °C (**Fig. 3b,c**).

DISCUSSION

We show here that *A. thaliana* transgenic plants carrying a 35S-pre-amiRNA can express mature, 21-nt amiRNAs at high levels by a process that requires DCL1. Moreover, the amiRNAs can mediate target viral RNA cleavage to confer virus resistance. The resistance is highly specific to the amiRNA/virus pair and therefore can not be explained by the induction of some general host resistance mechanism by the amiRNAs. The resistance is detected at the cell level and is hereditable.

The amiRNA-mediated approach has several advantages. First, no viral cDNA fragment is used and any conserved or specific 21-nt antisense sequence from the viral RNA genome can be chosen[26]. In addition, by computer prediction, it should be possible to select a sequence with no extensive homology to any *A. thaliana* genes. Second, the 21-nt sequences of miR159 and miR159* (the complementary strand to miR159 in pre-miR159) can be easily replaced with any artificial sequences targeting any viral RNAs by PCR. Third, a binary plasmid carrying the 35S-pre-amiRNA can be first assayed by transient expression in *N. benthaminiana* leaves for amiRNA expression and cleavage efficiency of target mRNA. As the amiRNA gene is dominant, the resistance phenotype can be screened at the T_1 or even T_0 generation.

Comparison of the four different TYMV strains (BL, J04373, X07441 and X16378) showed that the 21-nt target sequence of amiR-P69[159] is fully conserved, suggesting that the amiR-P69[159] plants should be resistant to all the strains (see **Supplementary Fig. 5** online). Similarly, the amiR-HC-Pro[159] plants should be resistant to at least 36 out of the 78 TuMV strains, whose HC-Pro genes show full sequence complementarity to the 21-nt sequence of amiR-HC-Pro[159] (see **Supplementary Fig. 5a,b** online).

It is generally recognized that not all siRNA species against a given mRNA target are equally effective and some siRNAs show limited efficacy because of extensive positional effects, for example, secondary structure, along the mRNA[37]. A similar situation may also apply to amiRNA-mediated cleavage of target mRNAs or viral RNAs. Although we have not extensively investigated this possibility we found that amiRNA directed against a 21-nt sequence of the viral RNA encoding the TuMV coat protein was as effective as that against the HC-Pro sequence supporting the general utility of this method.

Low temperatures are known to inhibit accumulation of siRNAs in insect, plant and mammalian cells[36,38,39] and both virus- and transgene-triggered RNA-silencing become attenuated[36]. It is, therefore, not surprising that siRNA-mediated virus resistance breaks down at low temperatures[36]. By contrast, amiRNA expression levels are similar between 15 °C and 24 °C and the amiRNA plants continue to resist virus at 15 °C, suggesting that target RNA cleavage still occurs at this temperature. In *Brassicaceae*, cold-season bi-annuals such as turnips require 15–18 °C for optimum growth. As both TYMV and TuMV infect Brassica crops even at these low temperatures, the amiRNA-mediated strategy should prove useful for engineered virus resistance of low-temperature crop plants.

A number of environmental concerns have been raised regarding the large scale use of virus-resistant transgenic plants[5] irrespective of

whether the resistance is mediated by RNA or protein. Potential risks include[5,40–43]: (i) possible recombination between the virus-derived transgene and nontarget viruses; (ii) possible transmission by unrelated viruses, through trans-encapsidation or enhanced seed or pollen transmission; (iii) possible synergy with unrelated viruses; (iv) possible gene flow from transgenic pollen to weedy relatives; and (v) possible production of new allergens or toxic proteins in transgenic plants. With the exception of iv, these potential risks can be minimized by the amiRNA-mediated approach, which uses only a short, 21-nt sequence.

The importance of suppressors in viral pathogenesis has prompted us to exemplify the efficacies of the amiRNA-mediated virus-specific resistance strategy by first targeting suppressor-encoding sequences of two different RNA viruses. Subsequently, we found that transgenic plants expressing amiR-TuCP^{159}, which targets the TuMV coat protein sequence, are also resistant to TuMV infection. These observations, along with the generality of miRNA action, suggest that the amiRNA strategy should be broadly applicable to other viruses as well. Under field conditions, virus may evade the amiRNA surveillance mechanism and overcome the specific resistance by mutations. However, in the case of suppressor-specific amiRNAs, mutations within conserved sequences may attenuate suppressor function and weaken virus virulence[44]. Moreover, this potential problem of possible resistance breakdown can be mitigated by coexpressing several amiRNAs targeting different sequences of the same virus.

As mixed infection is common in the field, we have challenged amiRNA transgenic plants with both TYMV and TuMV. We observed a breakdown of specific resistance for some transgenic plants in co-infection experiments. Several factors, including the relative rate of virus replication and the efficiency of viral RNA cleavage, are expected to influence the outcome of such experiments. A more rapid replication of the nontargeted virus and subsequent accumulation of its silencing suppressor would inhibit the host miRNA machinery and block cleavage of the targeted viral RNA by its cognate amiRNA. Therefore, it is not surprising to see a breakdown of specific virus resistance in some transgenic plants. However, any possible breakdown of specific virus resistance because of a prior infection by an unrelated virus could be obviated by expressing in the same plant amiRNAs targeting two different viruses. Indeed, we show here that transgenic plants expressing both amiR-P69^{159} and amiR-HC-Pro^{159} were resistant to co-infection by TYMV and TuMV. Taken together, our observations indicate the possibility to engineer broad spectrum resistance to several viruses by co-expression of appropriately designed multiple amiRNAs.

METHODS

Construction of artificial pre-amiRNAs. A 273-bp fragment containing the entire sequence of the *A. thaliana* miR159a (see below) was cloned by PCR amplification using primers miR159-F1 (5′-CACCACAGTTTGCTTATGTCG GATCC-3′) and miR159-*Xma*I-R1 (5′-TGAC*CCGGG*ATGTAGAGCTCCCTT CAATCC-3′). The miR159-*Xma*I-R1 contains 18 of 21 nucleotides of the mature miR159 (underlined) and an introduced *Xma*I site (italic). The PCR fragment was cloned into pENTR vector (Invitrogen) according to the manufacturer's instructions to obtain pENTR-pre-miR159a. Mutagenesis of pre-miR159a was performed by PCR with amiR-HC-Pro^{159}-F1 and amiR-HC-Pro^{159}-R1 primers. The amiR-HC-Pro^{159}-F1 primer (5′-AAGA*TAGATCTTG* ATCTGACGATGGAAGCAGTCGAGTGCGTGAGCAAGTCATGAGTTGAGCA GGGTA-3′) contains a *Bgl*II site (italic) and the amiR-HCPro^{159*} sequence (underlined). The amiR-HC-Pro^{159}-R1 (5′-AAGA*CCCGGGATG*CAGTCGA GTGCGTGAGCAAGTGAAGAGTAAAAGCCATTA-3′) contains an *Xma*I site (italic) and the mature amiR-HC-Pro^{159} reverse complementary sequence (underlined).

PCR amplification of the miR159a precursor using the above primers and pENTR-pre-miR159a DNA as a template generated a DNA fragment that was subsequently digested with *Bgl*II and *Xma*I. The *Bgl*II-*Xma*I fragment was inserted into pENTR-pre-miR159a to generate pENTR-pre-amiR-HC-Pro^{159}. The point mutations introduced rendered the miRNA:miRNA* pair fully complementary. Gateway system (Invitrogen) procedures were used to transfer the amiR-HC-Pro^{159} precursor to the plant binary Gateway destination vector pBA-DC-myc[45] generating pBA-pre-amiR-HC-Pro^{159}, in which the pre-amiR-HC-Pro^{159} sequence is placed downstream of a 35S promoter.

In the case of amiR-P69^{159} two forward oligonucleotides amiR-P69^{159}-F1 and F2 and two reverse oligonucleotides amiR-P69^{159}-R1 and R2, were designed to change the miR159a sequence to a synthetic sequence targeting the P69 mRNA coding sequence from TYMV. The primer amiR-P69^{159}-F1 (5′-GGAAGCCACAAGACAATCGAGACTTTCATGAGTTGAGCAGGGTA-3′) contains the synthetic amiR-P69^{159*} sequence (underlined). The primer amiR-p69^{159}-F2 (5′-TCGA*TAGATCTT*GATCTGACGATGGAAGCCACAAGA CAATCGAGA-3′) contains a partial amiR-P69^{159}-F1 sequence (bold) and a *Bgl*II site (italic).

The primer amiR-P69^{159}-R1 (5′-CCACAAGACAATCGAGACTTTGAAG AGTAAAAGCCATTAA-3′) contains the synthetic amiR-P69^{159} sequence (underlined). The primer amiR-P69^{159}-R2 (5′-CCCTTTGA*CCCGGGA*TGC CACAAGACAATCGAGACTTT-3′) contains a partial amiRP69^{159}-R1 sequence (bold) and an *Xma*I site (italic).

Two rounds of PCR were performed to amplify a 227-bp DNA fragment that contains the amiR-P69^{159} and amiR-P69^{159*} sequences. Plasmid pENTR-pre-miR159a (as a template) and primers amiR-P69^{159}-F1 and amiR-P69^{159}-R1 were used in the first round PCR. In the second round, the PCR product of the first round was used as a template along with primers amiR-P69^{159}-F2 and amiR-P69^{159}-R2 to produce the 227-bp DNA fragment. After digestion with *Bgl*II and *Xma*I, the DNA fragment was cloned into *Bgl*II-*Xma*I–digested pENTR-pre-miR159a vector to generate pENTR-pre-amiR-P69^{159}. Gateway system procedures were used again to transfer the amiR-P69^{159} precursor to pBA-DC-myc generating pBA-pre-amiR-P69^{159}. In this vector the pre-amiR-P69^{159} sequence was placed downstream of a 35S promoter.

To construct amiRNA against the TuMV coat protein sequence, we designed amiRTuCP-F1; (5′-AAGA*TAGATCTT*GATCTGACGATGGAAGGCCAAGAT ACGAGCAGAGAGTCATGAGTTGAGCAGGGTA-3′) contains synthetic amiR-TuCP^{159*} sequence (underlined) and a *Bgl*II site (italic) and amiR-TuCP^{159}-R1 (5′-AAGAC*CCGGGA*TGGCCAAGATACGAGCAGAGAGTGAAGAGTAAAAG CCACCA-3′) contains synthetic amiR-TuCP^{159} sequence (underlined) and an *Xma*I site (italic) to change the miR159a sequence to a synthetic sequence targeting the TuMV coat protein sequence (8988 nt–9008 nt). The PCR fragment was first digested with *Bgl*II and *Xma*I before being cloned into *Bgl*II-*Xma*I–digested pENTR vector to generate pENTR-pre-amiR-TuCP^{159}. The pre-amiR-TuCP^{159} fragment was transferred to a binary vector containing a 35S promoter by Gateway recombination to generate pBA-pre-amiR-TuCP^{159}.

To construct the dimeric pre-amiR-P69^{159}-amiR-HC-Pro^{159}, we ligated the two PCR fragments of amiR-P69^{159} and amiR-HC-Pro^{159} with compatible cohesive ends obtained by previous digestions with *Spe*I and *Avr*II. The ligation product was used as a template for a second round of PCR with amiR-P69^{159}-F2 and amiR-HC-Pro^{159}-R1 primers. The fragment obtained from the second PCR was digested with *Bgl*II and *Xma*I and cloned into pENTR vector to generate pENTR-pre-amiR-P69^{159}-amiR-HC-Pro^{159}. The dimeric amiRNA precursor was placed downstream of a 35S promoter by transfer into a binary vector using Gateway recombination to generate pBA-pre-amiR-P69^{159}–amiR-HC-Pro^{159}.

Construction of cDNA encoding viral suppressors. Full length cDNAs encoding P69 and HC-Pro were cloned from infectious clones of TYMV[46] and TuMV (Yeh, S.D., unpublished data), respectively, by PCR. For the P69 cDNA, the primers were P69-F1 (5′-CACCATGAGTAACGGCCTTCC-3′) and P69-R1 (5′-ATCGGTGTCGGGGGCGCTGCCGTAGTC-3′). For the HC-Pro gene, the primers were HC-F1 (5′-CACCATGAGTGCAGCAGGAGCCAAC-3′), and HC-R1 (5′-TCCGACACGGTAGTGTTTTAAGCTTGA-3′). The P69 cDNA and the HC-Pro cDNA were cloned into the pENTR/D vector (Invitrogen) before being transferred to the pBA-DC-HA vector[45] by recombination using

the LR Clonase enzyme (Invitrogen) and generating pBA-P69-HA and pBA-HC-Pro-HA, respectively. Both viral suppressor genes were fused at the 3′ end with DNA sequences encoding hemagglutinin (HA) and the fusion gene placed downstream of a 35S promoter.

Plant material and growth conditions. Plants of *A. thaliana* ecotype Columbia (Col-0) were transformed with *Agrobacterium tumefaciens* containing the pBA-amiR-P69^{159} or pBA-amiR-HC-Pro^{159} plasmid by the floral dip method[47]. T_2 transgenic plants (a mixture of homozygotes and hemizygotes) were analyzed for transgene and miRNA levels and four independent lines of each construct were used for virus challenge experiments. In addition, homozygous T_3 progeny plants were used for some experiments. Homozygous amiR-P69^{159} plants (no. 2-5) and amiR-HC-Pro^{159} (no. 12-4) were crossed with *dcl1-9*. *dcl1-9* mutant carrying 35S-pre-amiRNA transgene were selected from T_2 progeny and analyzed. Seeds were surface sterilized and chilled at 4 °C for 2 d before either growth on Murashige and Skoog (MS) medium with/without antibiotics or planting on Florobella potting compost/sand mix (3:1). Plants were maintained in a growth room (16 h light/8 h darkness, 20 to 25 °C). For low temperature treatments, seedlings were grown on MS medium or soil at 15 °C in a 16 h light/8 h darkness cycle for 3 weeks.

Transient expression by agro-infiltration of *N. benthamiana*. Four constructs, pBA-pre-amiR-HC-Pro^{159}, pBA-pre-miR-P69^{159}, pBA-P69-HA and pBA-HC-Pro-HA, were used to infiltrate *N. benthamiana* leaves by agro-infiltration[16,48]. Two days after infiltration, total RNA was extracted from the infiltrated leaves using the RNeasy Plant Mini Kit (QIAGEN) and analyzed by 5′RACE.

Analysis of *in vivo* miRNA-directed cleavage. To identify products of miRNA-directed cleavage, we used the First Choice RLM-RACE Kit (Ambion) in 5′RACE experiments. We used 2 μg total RNA for direct ligation to the RNA adaptor without further processing of the RNA sample. Subsequent steps were done according to the manufacturer's directions. PCR fragments obtained from 5′RACE experiments were cloned into the pPCR-Script AMP SK(+) vector (Stratagene) and individual clones were analyzed by DNA sequencing.

Northern blot hybridizations. Total RNA was extracted from leaves using the Trizol reagent (Invitrogen). Ten μg total RNA was resolved in a 15% polyacrylamide/1× TBE (8.9 mM Tris, 8.9 mM boric acid, 20 mM EDTA)/8 M urea gel and blotted to a Hybond-N$^+$ membrane (Amersham). DNA oligonucleotides with the exact reverse-complementary sequence to miRNAs were end-labeled with ^{32}P-γ-ATP and T4 polynucleotide kinase (New England Biolabs) to generate high specific activity probes. Hybridization was carried out using the ULTRAHyb-Oligo solution according to the manufacturer's directions (Ambion), and signals were detected by autoradiography. In each case, the probe contained the exact antisense sequence of the expected miRNA to be detected.

Microarray analysis. Microarray analyses using the Affymetrix ATH1 platform were performed with three biological replicates using wild-type plants and amiR-P69^{159} and amiR-HC-Pro^{159} transgenic plants. Seedlings were grown on 1× MS medium with 1% sucrose for 14 d. One μg of total RNA was used for reverse transcription using MessageAmp II aRNA kits (Ambion) and 15 μg of labeled cRNA for hybridization. GeneChip hybridization and scanning were performed at the Genomic Resource Center, Rockefeller University, New York (http://www.rockefeller.edu/genomics).

Statistical analysis of microarray data. Statistical analysis of microarray data was performed by Genespring GX 7.3.1 software (Agilent). Normalized expression estimates were obtained using GC robust multiarray average (gcRMA) and present calls for genes in control (wild type) were obtained. All present genes were filtered by 1.5-fold change of expression level in the amiRNA transgenic lines. The Welch-*t*-test (variances not assumed equal) was used for parametric test. The $P \leq 1\%$ of Benjamini and Hochberg False Discovery Rate was adjusted for multiple testing correction.

Viruses and challenge inoculations of plants. *N. benthamiana* leaves were inoculated with TuMV YC5 strain (GenBank AF530055)[49] and chimeric TuMV-GFP contains a GFP gene inserted in between the NIb and the coat protein gene (Yeh, S.D., unpublished data). Two weeks later infected leaf tissues (1 g) containing 900 ng/mg tissue of TuMV viral RNA were extracted in 20 ml of 50 mM potassium phosphate buffer (pH 7.0), and the extract used as a TuMV inoculum. Leaves of 4-week-old plants of wild-type *A. thaliana* (col-0) were inoculated with TYMV Blue Lake strain (TYMV BL) (GenBank AF035403)[46] and 1 week later leaf tissues (1 g) containing 690 ng/mg tissue of TYMV viral RNA were extracted with 10 ml of 50 mM potassium phosphate buffer (pH 7.0). The extract was used as a TYMV inoculum. T_2 (amiR-P69^{159} nos. 1, 2, 3 and 7; amiR-HC-Pro^{159} nos. 10, 11 and 12) or T_3 (amiR-P69^{159} nos. 1-1, 2-5, 3-1 and 7-1; amiR-HC-Pro^{159} nos. 10-1, 11-3 and 12-4) plants of different transgenic lines expressing either amiR-P69^{159} or amiR-HC-Pro^{159} were grown in a greenhouse for 4 weeks (5- to 6-leaf stage). Plants were dusted with 600-mesh carborundum on the first to fourth leaf and then gently rubbed with 200 μl TuMV or TYMV inoculum. wild-type (col-0) plants were used as controls. Equal volumes of TuMV and TYMV inocula were mixed and used for co-infection experiments. All inoculated plants were kept in a greenhouse (23–28 °C) and development of symptoms was monitored daily for 2 weeks for TuMV experiments and 1 week for TYMV experiments. TuMV-GFP inoculated leaves were examined 5–7 d.p.i. with an LSM 510 confocal microscope (Zeiss).

ELISA and time course of virus accumulation. Leaf tissues (10 mg), from different systemic leaves of each plant infected with TuMV or TYMV were collected at 0, 3, 6, 9 and 12 d.p.i., and assayed by indirect ELISA using a polyclonal antiserum to the TuMV coat protein[49] or the TYMV coat protein (Loewe Biochemica). Goat anti-rabbit immunoglobulin G conjugated with alkaline phosphatase (Amersham Biosciences) was used as a secondary antibody and *p*-nitrophenyl phosphate (Sigma) was used as a substrate for color development. Results were recorded by measuring absorbance at 405 nm using a VERSAmax Tunable Microplate Reader (Molecular Devices).

Western blot analyses. Systemic leaves from inoculated plants were homogenized in 20 volumes (wt/vol) of denaturing buffer (50 mM Tris-HCl, pH 6.8, 4% SDS, 2% 2-mercaptoethanol, 10% glycerol and 0.001% bromophenol blue). After incubation at 100 °C for 5 min, extracts were clarified by centrifugation at 8,000*g* for 3 min. Total proteins were separated by SDS gel electrophoresis and western blots were analyzed using polyclonal antiserum to TuMV coat protein or TYMV coat protein. Gels were stained with Coomassie brilliant blue R250 and levels of the large subunit of RUBISCO (molecular mass, 55 kDa) were used as loading controls.

Note: Supplementary information is available on the Nature Biotechnology website.

ACKNOWLEDGMENTS

S.-S.L. was supported by a fellowship from Ministry of Education, Taiwan. K.-C.C. and H.-W.W. are visiting students from the National Chung-Hsing University, Taiwan. We thank Jun Chen for TYMV, Chin-Chih Chen for TuMV and TuMV-GFP; Mengdai Xu for technical assistance, Chan-Sen Wang and Xuning Wang for assistance with microarray analysis and statistical treatment of the results; and Enno Krebbers, Richard Broglie, Karen Broglie and Barbara Mazur for helpful suggestions and stimulating discussions. This work was supported by a grant from DUPONT to N.-H.C.

AUTHOR CONTRIBUTIONS

N.-H.C. and J.L.R. first conceived the idea of using amiRNAs to regulate gene expression. Q.-W.N., S.-S.L. and J.L.R. designed the amiRNAs. Q.-W.N. generated the transgenic plants. S.-S.L, Q.-W.N., K.-C.C. and H.-W.N. performed the virus challenge and related experiments. S.-D.Y. provided specific strains of TuMV and TuMV-GFP and advice on experimental design. All authors discussed the results and commented on the manuscript, which was written by N.-H.C. and S.-S.L.

COMPETING INTERESTS STATEMENT

The authors declare competing financial interests (see the *Nature Biotechnology* website for details).

Published online at http://www.nature.com/naturebiotechnology/
Reprints and permissions information is available online at http://npg.nature.com/reprintsandpermissions/

1. Kang, B.C., Yeam, I. & Jahn, M.M. Genetics of plant virus resistance. *Annu. Rev. Phytopathol.* 43, 581–621 (2005).
2. Carrington, J.C., Kasschau, K.D. & Johansen, L.K. Activation and suppression of RNA silencing by plant viruses. *Virology* 281, 1–5 (2001).

3. Sanford, J.C. & Johnston, S.A. The concept of parasite-derived resistance-Deriving resistance genes from the parasite's own genome. *J. Theor. Biol.* **113**, 395–405 (1985).
4. Abel, P.P. *et al.* Delay of disease development in transgenic plants that express the *Tobacco mosaic virus* coat protein gene. *Science* **232**, 738–743 (1986).
5. Tepfer, M. Risk assessment of virus-resistant transgenic plants. *Annu. Rev. Phytopathol.* **40**, 467–491 (2002).
6. Palukaitis, P. & Zaitlin, M. Replicase-mediated resistance to plant virus disease. *Adv. Virus Res.* **48**, 349–377 (1997).
7. Baulcombe, D.C. Mechanisms of pathogen-derived resistance to viruses in transgenic plants. *Plant Cell* **8**, 1833–1844 (1996).
8. Waterhouse, P.M., Graham, M.W. & Wang, M.B. Virus resistance and gene silencing in plants can be induced by simultaneous expression of sense and antisense RNA. *Proc. Natl. Acad. Sci. USA* **95**, 13959–13964 (1998).
9. Smith, H.A., Swaney, S.L., Parks, T.D., Wernsman, E.A. & Dougherty, W.G. Transgenic plant virus resistance mediated by untranslatable sense RNAs: expression, regulation, and fate of nonessential RNAs. *Plant Cell* **6**, 1441–1453 (1994).
10. Helliwell, C.A. & Waterhouse, P.M. Constructs and methods for hairpin RNA-mediated gene silencing in plants. *Methods Enzymol.* **392**, 24–35 (2005).
11. Xie, Z. *et al.* Genetic and functional diversification of small RNA pathways in plants. *PLoS Biol.* **2**, 642–652 (2004).
12. Mourrain, P. *et al. Arabidopsis* SGS2 and SGS3 genes are required for post-transcriptional gene silencing and natural virus resistance. *Cell* **101**, 533–542 (2000).
13. Dalmay, T., Horsefield, R., Braunstein, T.H. & Baulcombe, D.C. SDE3 encodes an RNA helicase required for post-transcriptional gene silencing in *Arabidopsis*. *EMBO J.* **20**, 2069–2078 (2001).
14. Chen, J., Li, W.X., Xie, D., Peng, J.R. & Ding, S.W. Viral virulence protein suppresses RNA silencing-mediated defense but upregulates the role of microrna in host gene expression. *Plant Cell* **16**, 1302–1313 (2004).
15. Kasschau, K.D. *et al.* P1/HC-Pro, a viral suppressor of RNA silencing, interferes with *Arabidopsis* development and miRNA function. *Dev. Cell* **4**, 205–217 (2003).
16. Llave, C., Kasschau, K.D. & Carrington, J.C. Virus-encoded suppressor of post-transcriptional gene silencing targets a maintenance step in the silencing pathway. *Proc. Natl. Acad. Sci. USA* **97**, 13401–13406 (2000).
17. Bartel, D.P. MicroRNAs: genomics, biogenesis, mechanism, and function. *Cell* **116**, 281–297 (2004).
18. Jones-Rhoades, M.W., Bartel, D.P. & Bartel, B. MicroRNAs and their regulatory roles in plants. *Annu. Rev. Plant Biol.* **57**, 19–53 (2006).
19. Vaucheret, H., Vazquez, F., Crete, P. & Bartel, D.P. The action of ARGONAUTE1 in the miRNA pathway and its regulation by the miRNA pathway are crucial for plant development. *Genes Dev.* **18**, 1187–1197 (2004).
20. Prod'homme, D., Jakubiec, A., Tournier, V., Drugeon, G. & Jupin, I. Targeting of the *Turnip yellow mosaic virus* 66K replication protein to the chloroplast envelope is mediated by the 140K protein. *J. Virol.* **77**, 9124–9135 (2003).
21. Mitchell, E.J. & Bond, J.M. Variation in the coat protein sequence of British isolates of *Turnip yellow mosaic virus* and comparison with previously published isolates. *Arch. Virol.* **150**, 2347–2355 (2005).
22. Tomimura, K., Gibbs, A.J., Jenner, C.E., Walsh, J.A. & Ohshima, K. The phylogeny of *Turnip mosaic virus*; comparisons of 38 genomic sequences reveal a Eurasian origin and a recent 'emergence' in east Asia. *Mol. Ecol.* **12**, 2099–2111 (2003).
23. Sanchez, F., Martinez-Herrera, D., Aguilar, I. & Ponz, F. Infectivity of *Turnip mosaic potyvirus* cDNA clones and transcripts on the systemic host *Arabidopsis thaliana* and local lesion hosts. *Virus Res.* **55**, 207–219 (1998).
24. Morch, M.D., Boyer, J.C. & Haenni, A.L. Overlapping open reading frames revealed by complete nucleotide sequencing of *Turnip yellow mosaic virus* genomic RNA. *Nucleic Acids Res.* **16**, 6157–6173 (1988).
25. Riechmann, J.L., Lain, S. & Garcia, J.A. Highlights and prospects of potyvirus molecular biology. *J. Gen. Virol.* **73**, 1–16 (1992).
26. Schwab, R., Ossowski, S., Riester, M., Warthmann, N. & Weigel, D. Highly specific gene silencing by artificial microRNAs in *Arabidopsis*. *Plant Cell* **18**, 1121–1133 (2006).
27. Alvarez, J.P. *et al.* Endogenous and synthetic microRNAs stimulate simultaneous, efficient, and localized regulation of multiple targets in diverse species. *Plant Cell* **18**, 1134–1151 (2006).
28. Simon-Mateo, C. & Garcia, J.A. MicroRNA-guided processing impairs *Plum pox virus* replication, but the virus readily evolves to escape this silencing mechanism. *J. Virol.* **80**, 2429–2436 (2006).
29. Dickins, R.A. *et al.* Probing tumor phenotypes using stable and regulated synthetic microRNA precursors. *Nat. Genet.* **37**, 1289–1295 (2005).
30. Boden, D. *et al.* Enhanced gene silencing of HIV-1 specific siRNA using microRNA designed hairpins. *Nucleic Acids Res.* **23**, 1154–1158 (2004).
31. Stegmeier, F., Hu, G., Rickles, R.J., Hannon, G.J. & Elledge, S.J. A lentiviral microRNA-based system for single-copy polymerase II-regulated RNA interference in mammalian cells. *Proc. Natl. Acad. Sci. USA* **102**, 13212–13217 (2005).
32. Zeng, Y., Wagner, E.J. & Cullen, B.R. Both natural and designed micro RNAs can inhibit the expression of cognate mRNAs when expressed in human cells. *Mol. Cell* **9**, 1327–1333 (2002).
33. Sun, D., Melegari, M., Sridhar, S., Rogler, C.E. & Zhu, L. Multi-miRNA hairpin method that improves gene knockdown efficiency and provides linked multi-gene knockdown. *Biotechniques* **41**, 59–63 (2006).
34. Gazzani, S., Lawrenson, T., Woodward, C., Headon, D. & Sablowski, R. A link between mRNA turnover and RNA interference in *Arabidopsis*. *Science* **306**, 1046–1048 (2004).
35. Souret, F.F., Kastenmayer, J.P. & Green, P.J. AtXRN4 degrades mRNA in *Arabidopsis* and its substrates include selected miRNA targets. *Mol. Cell* **15**, 173–183 (2004).
36. Szittya, G. *et al.* Low temperature inhibits RNA silencing-mediated defence by the control of siRNA generation. *EMBO J.* **22**, 633–640 (2003).
37. Overhoff, M. *et al.* Local RNA target structure influences siRNA efficacy: a systematic global analysis. *J. Mol. Biol.* **348**, 871–881 (2005).
38. Kameda, T., Ikegami, K., Liu, Y., Terada, K. & Sugiyama, T. A hypothermic-temperature-sensitive gene silencing by the mammalian RNAi. *Biochem. Biophys. Res. Commun.* **315**, 599–602 (2004).
39. Fortier, E. & Belote, J.M. Temperature-dependent gene silencing by an expressed inverted repeat in *Drosophila*. *Genesis* **26**, 240–244 (2000).
40. Rubio, T., Borja, M., Scholthof, H.B. & Jackson, A.O. Recombination with host transgenes and effects on virus evolution: an overview and opinion. *Mol. Plant Microbe Interact.* **12**, 87–92 (1999).
41. Hammond, J., Lecoq, H. & Raccah, B. Epidemiological risks from mixed virus infections and transgenic plants expressing viral genes. *Adv. Virus Res.* **54**, 189–314 (1999).
42. Aaziz, R. & Tepfer, M. Recombination in RNA viruses and in virus-resistant transgenic plants. *J. Gen. Virol.* **80**, 1339–1346 (1999).
43. Falk, B.W. & Bruening, G. Will transgenic crops generate new viruses and new diseases? *Science* **263**, 1395–1396 (1994).
44. Lin, S.S., Wu, H.W., Jan, F.J., Hou, R.F. & Yeh, S.D. Modifications of the HC-Pro of *Zucchini yellow mosaic potyvirus* for generation of attenuated mutants for cross protection against severe infection. *Phytopathology* (in press).
45. Zhang, X., Garreton, V. & Chua, N.H. The AIP2 E3 ligase acts as a novel negative regulator of ABA signaling by promoting ABI3 degradation. *Genes Dev.* **19**, 1532–1543 (2005).
46. Skotnicki, M.L., Mackenzie, A.M. & Gibbs, A.J. *Turnip yellow mosaic virus* variants produced from DNA clones encoding their genomes. *Arch. Virol.* **127**, 25–35 (1992).
47. Chung, M.H., Chen, M.K. & Pan, S.M. Floral spray transformation can efficiently generate *Arabidopsis* transgenic plants. *Transgenic Res.* **9**, 471–476 (2000).
48. Voinnet, O., Lederer, C. & Baulcombe, D.C. A viral movement protein prevents spread of the gene silencing signal in *Nicotiana benthamiana*. *Cell* **103**, 157–167 (2000).
49. Chen, C.C. *et al.* Identification of *Turnip mosaic virus* isolates causing yellow stripe and spot on Calla Lily. *Plant Dis.* **87**, 901–905 (2003).

The EMBO Journal Vol.17 No.22 pp.6739–6746, 1998

Viral pathogenicity determinants are suppressors of transgene silencing in *Nicotiana benthamiana*

Gianinna Brigneti, Olivier Voinnet, Wan-Xiang Li[1], Liang-Hui Ji[1], Shou-Wei Ding[1] and David C.Baulcombe[2]

The Sainsbury Laboratory, John Innes Centre, Colney Lane, Norwich NR4 7UH, UK and [1]Molecular Virology Laboratory, Institute of Molecular Agrobiology, National University of Singapore, 1 Research Link, Singapore 117604

[2]Corresponding author
e-mail: david.baulcombe@bbsrc.ac.uk

G.Brigneti and O.Voinnet contributed equally to this work

Post-transcriptional gene silencing (PTGS) of a green fluorescent protein (GFP) transgene is suppressed in *Nicotiana benthamiana* plants infected with potato virus Y (PVY) or with cucumber mosaic virus (CMV), but not in plants infected with potato virus X (PVX). By expressing PVY and CMV-encoded proteins in a PVX vector we have shown that the viral suppressors of gene silencing are the HCPro of PVY and the 2b protein of CMV. The HCPro acts by blocking the maintenance of PTGS in tissues where silencing had already been set, whereas the 2b protein prevents initiation of gene silencing at the growing points of the plants. Combined with previous findings that viruses are both activators and targets of PTGS, these data provide compelling evidence that PTGS represents a natural mechanism for plant protection against viruses.
Keywords: cucumber mosaic virus/gene silencing/potato virus X/potato virus Y/virus resistance

Introduction

Post-transcriptional gene silencing (PTGS) in transgenic plants involves sequence-specific degradation of RNA. The targeted RNA species are similar to the transcribed part of a silencer transgene and, in plants exhibiting PTGS, there is only a low level of the transgene RNA even if transcription is at a high level (Depicker and Van Montagu, 1997). In addition, if the silencer transgene is similar to an endogenous gene, there is only a low level of the corresponding endogenous gene RNAs (Matzke and Matzke, 1995). PTGS can also be targeted against viral RNA, (Lindbo *et al.*, 1993; Smith *et al.*, 1994; Guo and Garcia, 1997) and extrapolating from this finding, it has been proposed that PTGS is a manifestation of a natural virus resistance mechanism in plants (Baulcombe, 1996; Pruss *et al.*, 1997). According to this idea, PTGS is activated in plants when the transgene, or its RNA, is perceived as a virus (Ratcliff *et al.*, 1997).

In support of the proposed relationship between PTGS and natural virus resistance, it has been shown that tobamo-, potex- and geminiviruses are activators as well as targets of gene silencing, provided they share sequence homology with a nuclear gene (Kumagai *et al.*, 1995; English *et al.*, 1996; Kjemtrup *et al.*, 1998; M.T.Ruiz *et al.*, 1998). Furthermore, caulimo- and nepoviruses induce a PTGS-like resistance mechanism even if there is no sequence similarity between the virus and nuclear genes (Covey *et al.*, 1997; Ratcliff *et al.*, 1997). This mechanism causes the systemically infected leaves to be symptom-free, to have only low levels of the virus and to have RNA sequence-specific resistance against challenge virus infection (Ratcliff *et al.*, 1997).

If there is a natural PTGS-like virus resistance in plants, it is likely that viruses would evolve strategies to avoid or suppress this mechanism. This idea was first developed based on the analysis of plants infected with two viruses in which the disease symptoms were more severe than in plants infected with either of the two viruses alone (Pruss *et al.*, 1997). In plants infected with a potyvirus this synergism was due to suppression of a host defense mechanism by the P1-HC-protease (P1-HCPro) (Pruss *et al.*, 1997). Following from this discovery, it was suggested that P1-HCPro is targeted against a PTGS-like resistance mechanism.

A second candidate suppressor of a PTGS-like resistance mechanism is the 2b protein encoded in cucumber mosaic virus (CMV) (Ding *et al.*, 1995). This protein is required for long distance transport of CMV (Ding *et al.*, 1995) and is now thought to act by suppressing a host resistance mechanism (L.H.Ji, W.X.Li and S.W.Ding, in preparation). In the absence of this suppressor, the resistance mechanism would prevent entry, translocation or exit of CMV from the phloem of infected plants. It is conceivable that this resistance could rely on a PTGS-like mechanism.

Here, we test the hypothesis that the P1-HCPro and 2b proteins are suppressors of PTGS. Plants exhibiting PTGS of a green fluorescent protein (GFP) transgene were infected with a potyvirus (potato virus Y, PVY) or with CMV. We also infected silenced plants with potato virus X (PVX) and with chimeric constructs carrying coding sequences from PVY and CMV in a PVX vector. If PVY or CMV produce suppressors of a PTGS-like resistance mechanism we predicted that infection by PVY, CMV or the PVX vectors would interfere with PTGS. The outcome of these experiments was consistent with this prediction and reveals that HCPro and the 2b protein suppress different stages of PTGS. The results implicate a PTGS-like mechanism as a limiting factor in the accumulation and spread of PVY, PVX and CMV. Moreover, as these are unrelated viruses, it is likely that this mechanism is a generalized anti-viral defense in plants.

Results

Reversion of GFP silencing by wild-type PVY

From the analysis of plants infected with a potyvirus and a second virus, it had been shown that potyviruses encode

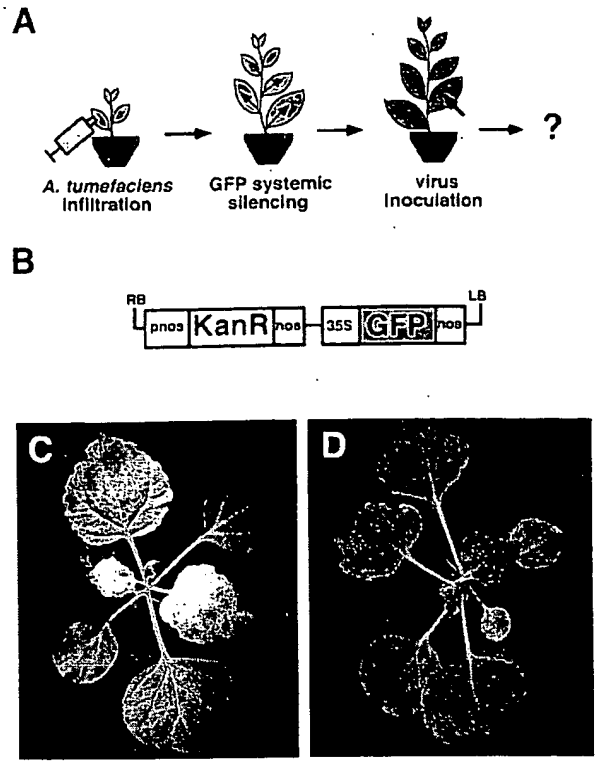

Fig. 1. PTGS of a GFP transgene induced by infiltration with *A.tumefaciens*. (A) Schematic representation of the experimental system. GFP silencing was induced in transgenic *N.benthamiana* (line 16c) by infiltration with a hypervirulent strain of *A.tumefaciens* carrying a binary-Ti plasmid shown in (B). Complete GFP silencing was achieved at 10 days post-infiltration and plants appeared uniformly red under UV illumination. It was at this stage that plants were ready for virus inoculation. (B) Structure of the binary-Ti plasmid cassette used to generate transgenic *N.benthamiana* plants (line 16c) expressing GFP and to induce GFP silencing in plants from line 16c by *A.tumefaciens* (strain cor308) infiltration. The right and left borders of the T-DNA (RB and LB) flank a kanamycin resistance gene (KanR) in a nos promoter (pnos) and nos terminator (nos) cassette. (C) *Nicotiana benthamiana* plant (line 16c) showing high levels of GFP expression under UV illumination. (D) *Nicotiana benthamiana* plant (line 16c) after induction of gene silencing by infiltration with a hypervirulent strain of *A.tumefaciens* carrying the binary-Ti plasmid shown in (B). The bright red colour is due to chlorophyll fluorescence under UV illumination.

a suppressor of a host plant defense against virus infection (Pruss *et al.*, 1997). To investigate the relationship of this defense mechanism to PTGS we inoculated PVY, the type-member of the potyviridae, to transgenic *Nicotiana benthamiana* exhibiting PTGS of a GFP transgene. We predicted that there would be reversion of GFP silencing in the PVY-infected tissues if the suppressed defense mechanism is related to PTGS.

Our experimental system involves lines of *N.benthamiana* carrying a GFP transgene (Voinnet and Baulcombe, 1997; M.T.Ruiz *et al.*, 1998). These plants accumulate a high level of GFP mRNA and appear uniformly green fluorescent under UV illumination (Figure 1C), whereas non-transformed plants appear red due to chlorophyll (M.T.Ruiz *et al.*, 1998). PTGS of the GFP transgene (Figure 1A) was induced by infiltration of lower leaves of 3-week-old seedlings with a strain of *Agrobacterium tumefaciens*, as described previously (Voinnet and Baulcombe, 1997). This strain carried a binary-Ti plasmid containing the same GFP expression cassette that was used for plant transformation (Figure 1B). We showed previously that PTGS of GFP is initiated in the infiltrated zone and that a systemic GFP silencing signal spreads through the plant. Eventually the plant appears completely red under UV light (Figure 1C and D) (Voinnet and Baulcombe, 1997). We have also shown that this systemic gene silencing is sequence-specific and acts at the post-transcriptional level (Voinnet *et al.*, 1998).

To test for a suppressor of gene silencing, PVY was inoculated two weeks after infiltration when systemic gene silencing was complete in all tissues of the plants (Figure 1A), except in the extreme meristematic zones which always remain non-silenced (Voinnet *et al.*, 1998). By 2 weeks post-inoculation, the GFP-silenced plants showed the systemic mild mottle and leaf curling symptoms of PVY, indicating that the virus had spread from the inoculated leaf. Under UV light, there were large regions of GFP fluorescence coinciding with the viral symptoms (Figure 2A–C). Northern analysis of RNA extracted from these plants showed that the effects on GFP fluorescence were parallel to the levels of GFP mRNA. Thus, in mock-inoculated GFP-silenced plants (Figure 2D, track 10) the GFP mRNA levels were below the limit of Northern blot detection, whereas in plants infected with PVY, the levels were similar to those in non-silenced plants (Figure 2D, tracks 5, 6 and 11). One of the samples from a PVY-infected plant had only low level of GFP mRNA (Figure 2D, track 7). However in this sample there was also only a low level of PVY RNA indicating a relationship between the levels of GFP mRNA and of PVY. We could rule out that these increased GFP mRNA levels were due to a non-specific enhancement of transgene expression because PVY infection in non-silenced plants had no effect on the level of GFP mRNA (Figure 2D, track 8) or on GFP fluorescence (data not shown). We could also rule out, based on the effects of PVX, that reversion of silencing was a non-specific effect of virus infection. The symptoms of PVX are a mild mosaic like those of PVY. However the GFP-silenced plants remained red-fluorescent after PVX infection (data not shown) and contained low levels of GFP mRNA (Figure 2D, tracks 1, 2 and 3). Therefore, from the analyses of RNA and GFP-fluorescence, these results are consistent with a suppressor of PTGS encoded in the PVY genome.

Reversion of GFP silencing by PVX–PVY recombinant viruses

The N-terminal P1 and HCPro potyviral proteins have been implicated in suppression of host defense (Pruss *et al.*, 1997). In order to test the role of these proteins in the suppression of gene silencing, a series of PVX vectors carrying PVY gene sequences were generated (Figure 3) and inoculated to *N.benthamiana* plants exhibiting systemic PTGS of GFP. The PVX vectors are named according to the PVY-encoded protein produced in the infected plants. Thus, the pTXYHC vector produces HCPro: pTX refers to the backbone of these constructs which is a full-length cDNA of PVX (pTXS; Kavanagh *et al.*, 1992) and Y refers to PVY. The plasmids carrying these constructs are pTXY**, where ** identifies the PVY protein. The

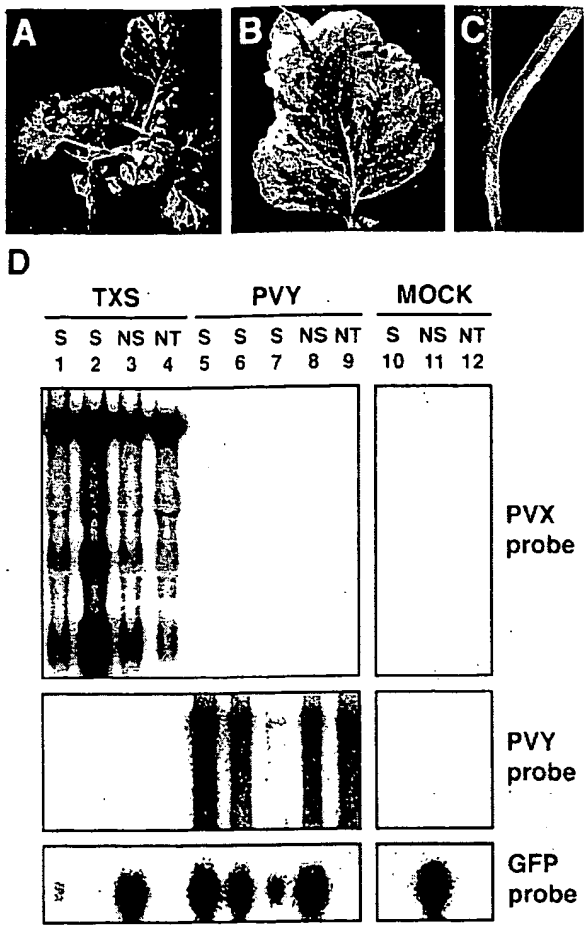

Fig. 2. Suppression of PTGS by PVY. (A) GFP-silenced *N.benthamiana* (line 16c) infected with PVY under UV illumination (15 days post-inoculation). The green fluorescence reveals that PTGS of GFP was lost in the PVY-infected tissue. Close-up views of a leaf and stem from the same plant are shown in (B) and (C), respectively. (D) Northern analysis of RNA extracted at 15 days post-inoculation from non-transformed (NT) and 16c *N.benthamiana* inoculated with PVX (TXS), PVY or mock-inoculated. Silenced (S) and non-silenced (NS) plants of line 16c were used in the experiment. Five micrograms of total RNA per sample were fractionated by electrophoresis on 0.9% (w/v) agarose–formaldehyde gels, blotted onto a nylon membrane and hybridized with probes specific for either PVX, PVY or GFP, as indicated.

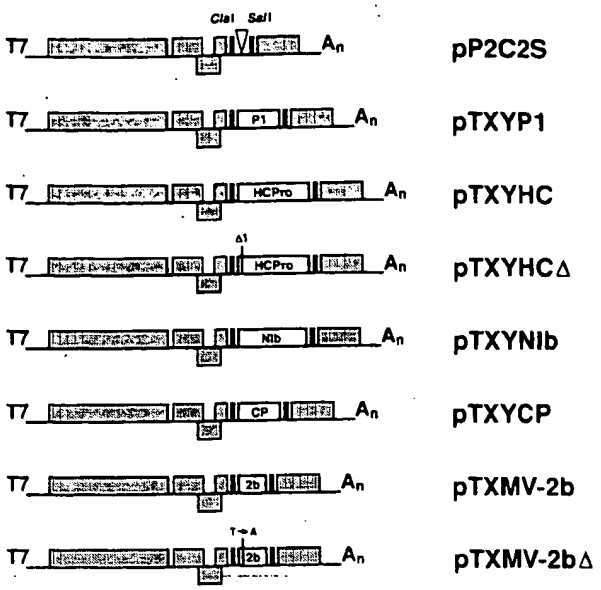

Fig. 3. Schematic representation of the PVX vector and chimeric constructs incorporating PVY and CMV coding sequences. Individual sequences were inserted into the pP2C2S PVX vector using the *ClaI* and *SalI* cloning sites (Baulcombe *et al.*, 1995). Expression of the insert and the PVX coat protein is controlled by duplicated PVX coat protein promoters indicated by a solid bar. The inserted PVY sequences are labeled: P1, 31 kDa N-terminal protein; HCPro, helper component protease; NIb, nuclear inclusion b; CP, coat protein. 2b refers to the CMV RNA 2-encoded protein required for long distance movement of the virus. Mutant versions of the HCPro and the 2b ORFs were also introduced into the PVX vector. In the pTXYHCΔ construct there was a −1 frame-shift in the first codon of the HCPro open reading frame (Δ1). The pTXMV-2bΔ construct had a single nucleotide substitution (T→A) that converted the fourth codon (TTG) of the 2b ORF to a stop codon (TAG).

viruses produced when the transcripts of these plasmids were inoculated are simply TXY**.

Most of these TXY** viruses induced mosaic symptoms, like the wild-type PVX (data not shown). However, TXYHC produced symptoms that were much more severe than those of wild-type PVX, inducing necrosis in stems and leaves, in addition to stunting of the infected plants (Figure 4A and C), as described previously for a PVX construct expressing the HCPro of tobacco etch virus (TEV) (Pruss *et al.*, 1997).

The TXYP1 and TXYCP viruses were similar to PVX (TXS) in that they had no effect on GFP silencing. Under UV illumination, at 2 weeks post inoculation, GFP-silenced plants infected with these constructs remained red, indicating that there had been no suppression of GFP gene silencing. Correspondingly, the GFP mRNA levels remained low in these plants (Figure 4F, tracks 1–4 and 10–13). However, in TXYHC-infected plants, there were large green fluorescent regions coinciding with the viral symptoms (Figure 4A–E). This effect was evident in all infected tissues, including stems (Figure 4E) and leaves (Figure 4C and D) that were already developed at the time of virus inoculation. Northern blot analysis showed that GFP mRNA levels had increased in these green fluorescent tissues and that the amount of GFP mRNA correlated with the relative amounts of TXYHC present in the sample (Figure 4F, tracks 5–9). We can rule out the possibility that the effect of TXYHC on gene silencing was an RNA-mediated effect because TXYHCΔ, with a frame-shift mutation at the 5′ end of the HCPro insert, did not suppress GFP gene silencing (Figure 4G, tracks 1–4). The symptoms of TXYHCΔ were mild, like those of wild-type PVX.

To rule out that suppression of GFP silencing was a secondary effect of the severe symptoms caused by TXYHC, we inoculated GFP-silenced plants with TXY-NIb. Like TXYHC, TXYNIb is highly necrogenic and causes death of the infected plant by 3 weeks post inoculation (data not shown). Analysis of TXYNIb-infected plants showed that GFP fluorescence and mRNA levels remained low in the severely symptomatic tissues (Figure 4G, tracks 5–7). From this, we conclude that HCPro of PVY is a direct suppressor of gene silencing and host defense in infected plants.

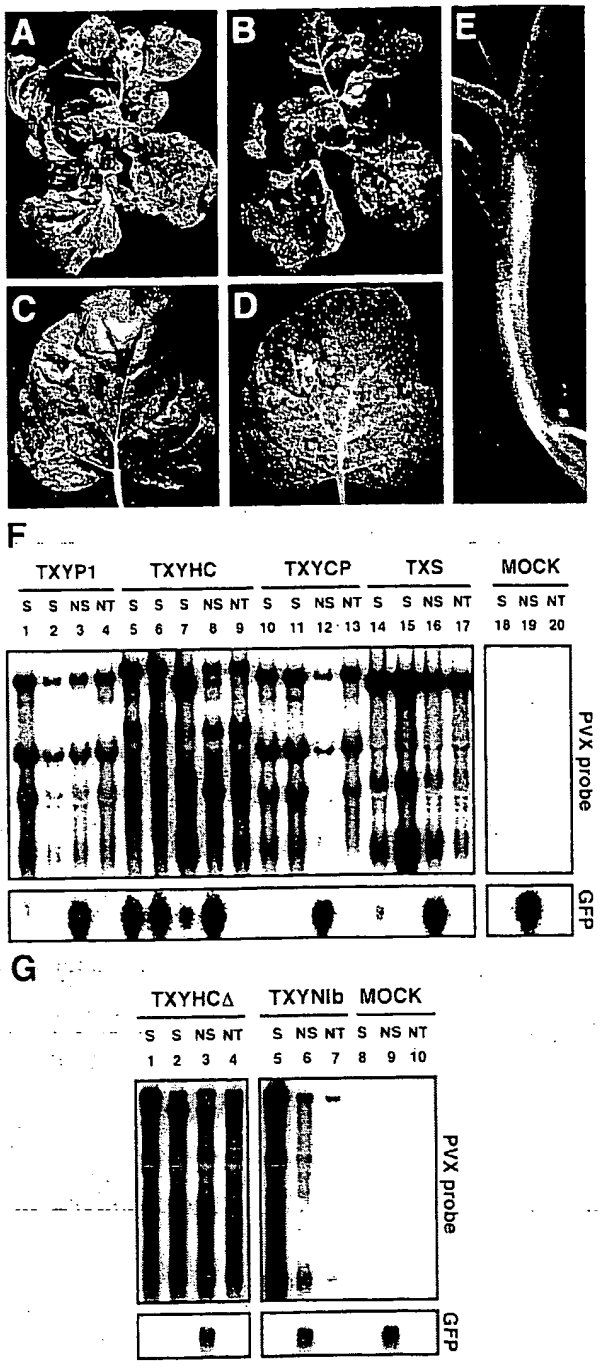

Fig. 4. Suppression of PTGS by TXYHC. (**A**) GFP-silenced *N.benthamiana* (line 16c) under white light showing symptoms of TXYHC infection (15 days post-inoculation). The same plant, shown under UV illumination in (**B**), revealing that PTGS of GFP was suppressed in all symptomatic tissues infected with the chimaeric virus. (**C**) Close-up of a leaf from the same plant under white light. (**D**) Close-up of the same leaf under UV illumination showing the co-localization of GFP expression with viral symptoms. (**E**) Close-up of the stem. (**F** and **G**) Northern analyses of RNA extracted at 15 days post-inoculation from non-transformed (NT) and *N.benthamiana* (line 16c) inoculated with PVX (TXS), TXY** recombinant viruses or mock-inoculated. Silenced (S) and non-silenced (NS) plants of line 16c were used in the experiments. Five micrograms (F) or 1 μg (G) of total RNA per sample were fractionated by electrophoresis on 0.9% (w/v) agarose–formaldehyde gels, blotted onto nylon membranes and hybridized with probes specific for PVX or GFP RNAs, as indicated.

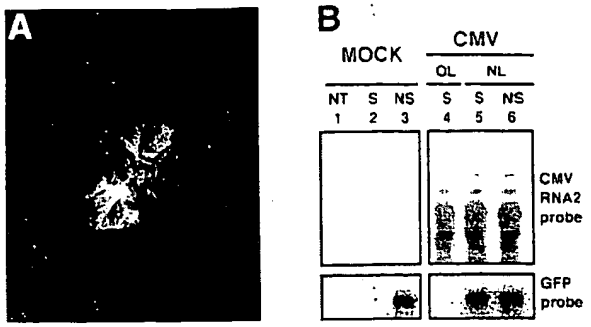

Fig. 5. Suppression of PTGS by CMV. (**A**) GFP-silenced *N.benthamiana* (line 16c) infected with CMV (21 days post-inoculation). GFP expression was restored in the newly emerging tissue after systemic CMV infection had been established. (**B**) Northern analysis of RNA extracted at 15 days post CMV inoculation from silenced (S) and non-silenced (NS) *N.benthamiana* plants of line 16c and from non-transformed plants. These plants were either infected with CMV or were mock inoculated. The RNA samples were taken either from old leaves (OL) that had emerged before systemic CMV infection or from new leaves (NL) emerging after CMV had spread systemically. Five micrograms of total RNA per sample were fractionated by electrophoresis on a 0.9% (w/v) agarose–formaldehyde gel, blotted onto a nylon membrane and hybridized with probes specific for RNA2 of CMV or for GFP RNA, as indicated. The multiple RNA species hybridizing to the CMV probe may represent degraded or subgenomic RNAs and have been described previously (Baulcombe *et al.*, 1986).

Reversion of GFP silencing by wild-type CMV

To determine whether viruses other than potyviruses can suppress gene silencing, we carried out experiments similar to those described above but with CMV instead of PVY. CMV was selected for these experiments because, like potyviruses, it encodes a suppressor of host defense (L.H.Ji, W.X.Li and S.W.Ding, in preparation). Three weeks post-inoculation there were mosaic symptoms on the upper leaves of the plants. Under UV light, the symptomatic leaves of the GFP-silenced plants remained red-fluorescent if they had emerged from the growing points before virus infection. However, the leaves emerging from the growing points after systemic spread of the virus became bright green-fluorescent (Figure 5A). There was no effect of CMV on the GFP fluorescence of non-silenced plants (data not shown). Northern analysis revealed that the GFP fluorescence in the CMV-infected plants was correlated with the levels of GFP RNA: the red fluorescent leaves of the silenced plants had GFP RNA levels that were below the limit of detection (Figure 5B, track 4) whereas in the newly emerging tissues, which were green fluorescent, GFP RNA levels were similar to those in non-silenced plants (Figure 5, tracks 5 and 6). The levels of GFP RNA on non-silenced plants were unaffected by CMV infection (Figure 5B, tracks 3 and 6). From these results, we conclude that CMV encodes a suppressor of PTGS. However, because CMV and PVY do not suppress silencing in the same parts of the plant, these viruses must block different stages in the gene silencing mechanism.

Reversion of GFP silencing by PVX–CMV recombinant viruses

The putative CMV-encoded suppressor of host defense is the 2b protein (Ding *et al.*, 1995). By analogy with the

potyviral HCPro, we considered that the ability of the 2b protein to suppress a plant defense mechanism could be due to its ability to suppress PTGS. To test this hypothesis, we inoculated a PVX vector expressing the CMV 2b protein (TXMV-2b; Figure 3) to GFP-silenced *N.benthamiana*. We also infected GFP-silenced plants with TXYMV-2bΔ in which a single nucleotide substitution (U to A) converted the fourth codon (UUG) of the 2b open reading frame (ORF) to a stop codon (UAG) (Figure 3).

By 3 weeks post-inoculation, TXMV-2b produced symptoms that were much more severe than those produced by wild-type PVX or by TXMV-2bΔ (Figure 6A). Instead of the normal mild mosaic symptoms of PVX, TXMV-2b induced necrosis on the systemically infected leaves and stem, leading to death of the plants (Figure 6A). However, at 14 days post-inoculation, before the systemic necrosis had developed, the newly emerging leaves of TXMV-2b-infected plants were green fluorescent under UV illumination. As in the CMV-infected plants, the leaves that had emerged prior to virus infection, although symptomatic, remained red fluorescent (Figure 6B–F). The phenotype of TXMV-2b-infected plants was associated with corresponding changes in the levels of GFP RNA. In the older, red-fluorescent leaves, the level of GFP RNA remained below the level of detection as in mock-infected leaves (Figure 6I, tracks 2 and 4). In contrast, in the new green-fluorescent leaves the GFP RNA had increased to the levels of non-silenced plants (Figure 6I, tracks 3, 5 and 6).

From the symptoms of TXMV-2bΔ, we ruled out the possibility that the suppression of GFP silencing was an RNA-mediated effect of the 2b sequence. GFP silenced plants infected with this construct remained totally red-fluorescent (Figure 6G and H) and contained low levels of GFP mRNA as in the GFP-silenced plants that had been mock-inoculated (Figure 6I, tracks 2 and 7–9). We also ruled out the possibility that the suppression of GFP silencing was due to a non-specific enhancement of transgene expression by the 2b protein by showing that TXMV-2b had no effect on GFP RNA or the green fluorescence of the non-silenced GFP lines (data not shown). Therefore, from the similarity of the CMV and TXMV-2b effects, we conclude that the 2b protein is the major suppressor of gene silencing encoded in the CMV genome.

Discussion

In this study, we identified two viral suppressors of PTGS in CMV and PVY. Our findings confirm the previously made suggestion that PTGS in plants is a natural protection mechanism against viruses (Baulcombe, 1996; Pruss *et al.*, 1997; M.T.Ruiz *et al.*, 1998). Furthermore, by implicating PTGS in resistance against diverse types of RNA virus, our findings indicate that this mechanism has general significance in plant–virus interactions.

Suppressors at different stages of PTGS

The two viral suppressors of PTGS in plants identified in this work are HCPro encoded by the PVY genome and

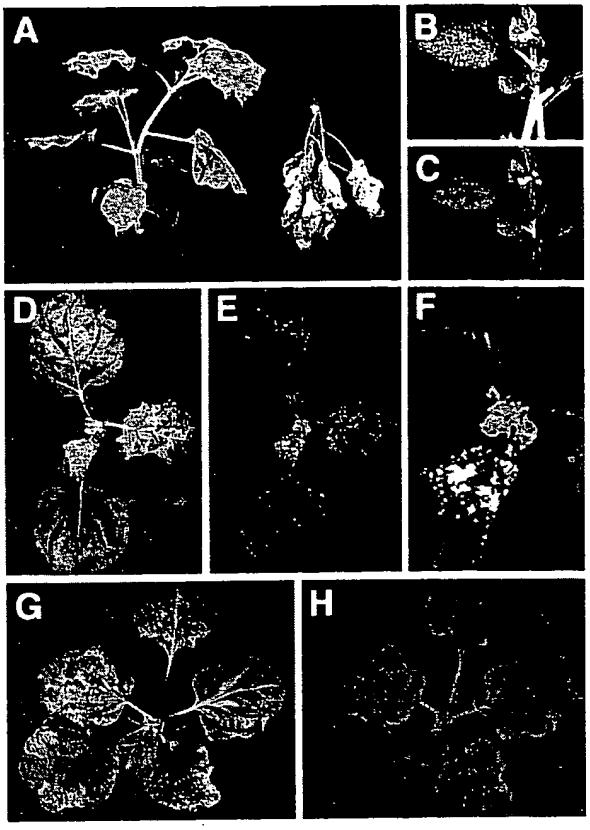

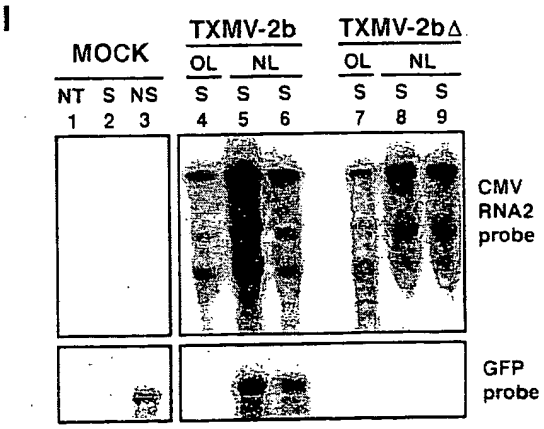

Fig. 6. Suppression of PTGS by the 2b protein of CMV (**A**) Non-transformed *N.benthamiana* plants inoculated with TXMV-2bΔ (left) and TXMV-2b (right). The photograph was taken at 21 days post-inoculation and both plants were the same age when inoculated. (**B**) GFP-silenced *N.benthamiana* (line 16c) showing symptoms of TXMV-2b infection at 21 days post-inoculation. (**C**) The same plant shown under UV illumination revealing the PTGS of GFP persisted in symptomatic leaves that had emerged from meristems before systemic infection but that it is suppressed in the post emergence leaves. (**D** and **E**) Aerial views of the plant shown in (B) under white light and UV illumination. (**F**) The apical zone from the image in (E). (**G** and **H**) GFP-silenced *N.benthamiana* (line 16c) showing symptoms of TXMV-2bΔ under white light (G) and UV illumination (H). (**I**) Northern analysis of RNA extracted at 15 days post-inoculation from either NT, non-silenced (NS) or silenced (S) *N.benthamiana* (line 16c) inoculated with TXMV-2b and TXMV-2bΔ. The RNA samples were taken either from old leaves (OL) that had emerged before systemic virus infection or from new leaves (NL) emerging after the virus had spread systemically. Five micrograms of total RNA per sample were fractionated by electrophoresis on a 0.9% (w/v) agarose–formaldehyde gel, blotted onto a nylon membrane and hybridized with probes specific for RNA2 of CMV or for GFP RNA as indicated.

the 2b protein encoded by the RNA 2 of CMV. Expression of either of these proteins from a PVX vector suppressed PTGS of a GFP transgene (Figures 4 and 6). This effect was clearly protein- rather than RNA-mediated because there was no suppression of PTGS when the PVX vector carried modified forms of the HCPro and the 2b coding sequences (Figures 4G and 6G). We can rule out that suppression of PTGS was due to a non-specific stimulation of the GFP transgene expression because GFP fluorescence and RNA levels remained unaffected in a non-silenced line infected with PVY, TXYHC or CMV (Figures 3D, 4F and 5B). We can also rule out the possibility that the results obtained are an artefact associated with a virus vector because P1-HCPro of TEV expressed in transgenic plants is also a suppressor of PTGS (Anandalakshmi *et al.*, 1998; Kasschau and Carrington, 1998).

In a previous analysis of GFP silencing, we showed that initiation, systemic spread of a silencing signal and maintenance are separate stages of the PTGS mechanism (Voinnet *et al.*, 1998). Here, from the GFP phenotype in virus-infected plants, we have shown that these stages are differentially targeted by the two viral suppressors. In plants infected with PVY or TXYHC there was suppression of PTGS in all of the symptomatic tissues, including the older leaves that would have received the systemic signal and initiated PTGS before the viruses had established infection (Figures 2 and 4). Based on these observations, we conclude that HCPro must be blocking at least the maintenance stage of PTGS, although our data do not rule out the possibility that initiation and systemic spread are also affected. The extent of suppression of PTGS was correlated with the level of PVY or TXYHC RNA (Figure 2D, lane 7), which suggests that high levels of the HCPro are required for suppression of PTGS.

Suppression of PTGS in CMV- or PVX-2b-infected plants was unlike the HCPro-mediated effect, because the only affected leaves were those that emerged from the growing points after the viruses had spread systemically (Figures 5 and 6). From this pattern, we conclude that the 2b protein affects the cells in, or near to, the growing points of the plants. The growing points do not normally exhibit PTGS, even when there is extensive silencing in the rest of the plant (Voinnet *et al.*, 1998). Therefore, it is possible that the 2b protein prevents entry of the gene silencing signal to the cells emerging from the growing points. Alternatively, it could be that the signal enters these cells but that the 2b protein prevents initiation of the PTGS mechanism.

Viral symptom determinants and suppressors of gene silencing

From the results presented here and elsewhere, it is shown that the HCPro and the 2b proteins have several activities. First, these proteins are pathogenicity factors of the respective viruses (Cronin *et al.*, 1995; Ding *et al.*, 1995). They also enhance the accumulation and symptoms of PVX when they are expressed from PVX vectors (Pruss *et al.*, 1997) and, as shown here, they suppress PTGS. In addition, in protoplasts from transgenic plants expressing HCPro, there is enhanced accumulation of PVX, TMV or CMV (Pruss *et al.*, 1997).

Although it remains formally possible that these are unrelated effects of the two proteins, a more likely explanation is that they are all associated with the suppression of a PTGS-like resistance mechanism. From the findings that PVY, CMV and the various PVX constructs are all affected by this mechanism, we propose that it is activated or given specificity by different types of RNA virus. We envisage that this mechanism could target degradation of RNA species that are similar to the inoculated virus. The effect of the mechanism would be to restrict viral RNA accumulation in infected cells. In addition, as shown in PTGS (Palauqui *et al.*, 1997; Voinnet and Baulcombe, 1997), we consider it possible that there is a sequence-specific signal molecule that spreads away from the cells in which the process is initiated. The potential to transmit a signal out of the initially infected cell could mean that this PTGS-like resistance mechanism has the ability to activate viral RNA degradation in non-infected cells located beyond the front of infection. Consequently, the PTGS-like mechanism could be responsible for suppression of virus movement as well as restriction of viral accumulation in infected cells.

It is unlikely that an effect of a PTGS-like resistance mechanism is specific to the potex, cucumo- and potyviral groups. These groups represent extremes in the evolution of positive strand RNA viruses having either monopartite or multipartite genome organization and similarity to either the picorna- or sindbis-virus groups (Matthews, 1991). Therefore, the shared property of these viruses as activators of the PTGS-like resistance mechanism is probably common to most groups of positive strand RNA viruses in plants. Moreover, if a PTGS-like mechanism is implicated in virus resistance, it is expected that other virus-encoded proteins will function as suppressors of gene silencing. From the results presented here, we predict that many viral proteins that were originally identified as pathogenicity determinants, like the 2b protein or HCPro, will eventually be identified as suppressors of PTGS.

The lack of an effect of PVX on the GFP silenced plants shows that this virus does not produce a suppressor of PTGS. However, the increase in symptoms and virus accumulation in plants infected with TXYHC and PTXMV-2b implies that PVX does activate the PTGS-like resistance. To reconcile these observations, we propose that PVX has the potential to partially evade rather than to suppress the PTGS-like resistance mechanism. Evasion might involve very rapid replication and spread of the virus so that the resistance mechanism is out-competed. Alternatively, PVX might be compartmentalized, so that it avoids the PTGS-like mechanism.

Several virological phenomena could be explained by the proposed involvement of a PTGS-like resistance mechanism in plants and the corresponding suppressors of gene silencing encoded in different viruses. Most obviously, there are various synergistic interactions between viruses resulting in disease that is much more severe in plants infected with two viruses than in plants infected with either virus alone (Pio-Riberio *et al.*, 1978; Vance, 1991; Murphy and Kyle, 1995). As with the PVX–PVY synergism, these interactions could be explained by the production of a suppressor of gene silencing by either or both of the interacting viruses.

The phenomenon of cross protection (Matthews, 1991) could also be explained, at least in part, by the involvement of a PTGS-like resistance mechanism. Cross protection is

an induced resistance mechanism in virus-infected plants that affects a second virus (the challenge strain) inoculated days or weeks after the initial inoculation. This resistance is specific for challenge strains that are similar to the inducing strain. Perhaps the inducing strain would initiate or provide the specificity determinant for the PTGS-like resistance mechanism so that the challenge strain, having sequence similarity to the inducer, would be suppressed. We have already demonstrated that cross protection associated with nepoviral recovery is similar to PTGS (Ratcliff *et al.*, 1997). However, based on our findings that diverse viruses may activate a PTGS-like resistance mechanism, it now appears likely that many other examples of cross protection may also fit into the same category.

Viral adaptations to gene silencing

The general principles of suppression and evasion of the PTGS-like resistance mechanism will probably apply to many plant–virus interactions. Evasive or strongly suppressive viruses will be highly pathogenic, whereas the others will be weak or non-pathogens. The probable central role of this mechanism in plant virus interactions means that there will be strong selective pressures on the virus to evade or suppress the mechanism. Similarly, there will be corresponding selective pressures on the plant side to ensure that the mechanism is effective against many viruses. These selective pressures will probably cause a high level of polymorphism in both the plant and the viral genes involved in the mechanism. Clearly, identification of other viral suppressors and further investigation of this proposed adaptive mechanism will certainly provide support for a previously uncharacterized, generalized virus resistance mechanism in plants. In addition, it is hoped that identification of viral suppressors of PTGS will provide an experimental handle for the characterization of host components involved in PTGS. It may also be possible to use the suppressors of PTGS to investigate the relationship of superficially similar gene silencing phenomena in plants, fungi, ciliates and nematodes (Cogoni and Macino, 1997; Fire *et al.*, 1998; F.Ruiz *et al.*, 1998).

Materials and methods

Plant material

Transgenic *N.benthamiana* plants carrying the GFP ORF were described previously (M.T.Ruiz *et al.*, 1998). The line used in this study, 16c, carries one copy of the transgene at a single locus in homozygous conditions (M.T.Ruiz *et al.*, 1998).

Agrobacterium induction of post-transcriptional gene silencing

GFP-expressing seedlings from line 16c were infiltrated with an hypervirulent strain of *A.tumefaciens* (strain cor308) (Hamilton *et al.*, 1995) carrying a binary-Ti plasmid vector into which a functional 35S-GFP cassette had been inserted. This cassette is the same as the one used for plant transformation (Figure 2B). Infiltration of *A.tumefaciens* was based on a previously described method (English *et al.*, 1997).

Wild-type and recombinant viruses

A PVY isolate belonging to the necrotic strain group was maintained in *Nicotiana clevelandii* plants. Wild-type PVX (pTXS) (Kavanagh *et al.*, 1992) and the PVX vector (pP2C2S) (Baulcombe *et al.*, 1995) have been described previously. pP2C2S was used to deliver PVY proteins into plant cells (Figure 1). PVY cDNA fragments encoding the 31 kDa protein (P1), helper component (HC), nuclear inclusion b (NIb) and coat protein (CP) were PCR-amplified from cDNA and individually cloned, in-frame, into the PVX vector under the control of a duplicated PVX CP promoter. An additional recombinant virus that carried a frameshift version of the HC coding sequence was also generated and termed pTXYHCΔ. The mutation in this construct consisted of the deletion of the first nucleotide of the HCPro coding sequence, creating a −1 frameshift. The sequence of the PVY mature proteins and the primer design for cloning purposes were based mainly in the published full-length sequences of the virus (Robaglia *et al.*, 1989; Thole *et al.*, 1993).

Wild-type CMV was maintained in *N.benthamiana* plants. As described above, the PVX vector (pP2C2S) was used to deliver CMV sequences into plant cells (Figure 1). pTXMV-2b contained a 500 bp DNA fragment derived from nucleotides 2410–2908 of CMV RNA 2 and thus the complete 2b coding sequence (CMV RNA 2, nucleotides 2410–2712; Ding *et al.*, 1995). This inserted CMV sequence was rendered non-coding in pTXYMV-2bΔ by a single nucleotide substitution (T to A) that converted the fourth codon (TTG) of the 2b ORF to a stop codon (TAG).

In vitro transcription

In vitro transcription reactions to produce infectious PVX and PVX derivatives RNAs were performed as described previously (Chapman *et al.*, 1992).

Northern blot analysis

RNA was extracted from systemically infected leaves 15 to 21 days post-inoculation as described previously (Mueller *et al.*, 1995). RNA samples (1–5 μg) were electrophoresed on a 0.9% (w/v) agarose formaldehyde gels, transferred to Hybond-N membranes and hybridized with ^{32}P-labeled RNA or cDNA probes specific for the respective viruses or for the GFP transgene RNA.

GFP imaging

Visual detection of GFP fluorescence in whole plant was performed using a 100 W hand-held long-wave ultraviolet lamp (UV products, Upland, CA, Black Ray model B 100AP). Plants were photographed with a Kodak Ektachrome Panther (400 ASA) film through a Wratten 8 filter. Exposure times varied up to 70 s depending on the intensity of the fluorescence and the distance of the camera and lamp from the plant.

Acknowledgements

We are grateful to the Gatsby Charitable Foundation for continuing support. We are also grateful to Vicki Vance, James Carrington, Andrew Maule and our colleagues in the Sainsbury Laboratory for helpful discussions.

References

Anandalakshmi,R., Pruss,G.J., Ge,X., Marathe,R., Smith,T.H. and Vance,V.B. (1998) A viral suppressor of gene silencing in plants. *Proc. Natl Acad. Sci. USA*, **95**, in press.

Baulcombe,D.C. (1996) Mechanisms of pathogen-derived resistance to viruses in transgenic plants. *Plant Cell*, **8**, 1833–1844.

Baulcombe,D.C., Saunders,G.R., Bevan,M.W., Mayo,M.A. and Harrison,B.D. (1986) Expression of biologically active viral satellite RNA from the nuclear genome of transformed plants. *Nature*, **321**, 446–449.

Baulcombe,D.C., Chapman,S.N. and Santa Cruz,S. (1995) Jellyfish green fluorescent protein as a reporter for virus infections. *Plant J.*, **7**, 1045–1053.

Chapman,S.N., Kavanagh,T.A. and Baulcombe,D.C. (1992) Potato virus X as a vector for gene expression in plants. *Plant J.*, **2**, 549–557.

Cogoni,C. and Macino,G. (1997) Conservation of transgene-induced post-transcriptional gene silencing in plants and fungi. *Trends Plant Sci.*, **2**, 438–443.

Covey,S.N., Al-Kaff,N.S., Langara,A. and Turner,D.S. (1997) Plants combat infection by gene silencing. *Nature*, **385**, 781–782.

Cronin,S., Verchot,J., Haldeman-Cahill,R., Schaad,M.C. and Carrington,J.C. (1995) Long-distance movement factor: a transport function of the potyvirus helper component proteinase. *Plant Cell*, **7**, 549–559.

Depicker,A. and Van Montagu,M. (1997) Post-transcriptional gene silencing in plants. *Curr. Opin. Cell Biol.*, **9**, 372–382.

Ding,S.W., Li,W.-X. and Symons,R.H. (1995) A novel naturally occurring hybrid gene encoded by a plant RNA virus facilitates long distance virus movement. *EMBO J.*, **14**, 5762–5772.

English,J.J., Mueller,E. and Baulcombe,D.C. (1996) Suppression of virus accumulation in transgenic plants exhibiting silencing of nuclear genes. *Plant Cell*, **8**, 179–188.

English,J.J., Davenport,G.F., Elmayan,T., Vaucheret,H. and Baulcombe, D.C. (1997) Requirement of sense transcription for homology-dependent virus resistance and *trans*-inactivation. *Plant J.*, **12**, 597–603.

Fire,A., Xu,S., Montgomery,M.K., Kostas,S.A., Driver,S.E. and Mello,C.C. (1998) Potent and specific genetic interference by double-stranded RNA in *Caenorhabditis elegans*. *Nature*, **391**, 806–811.

Guo,H.S. and Garcia,J.A. (1997) Delayed resistance to plum pox potyvirus mediated by a mutated RNA replicase gene: involvement of a gene-silencing mechanism. *Mol. Plant–Microbe Interact.*, **10**, 160–170.

Hamilton,C.M., Frary,A., Lewis,C. and Tanksley,S.D. (1995) Stable transfer of intact high molecular weight DNA into plant chromosomes. *Proc. Natl Acad. Sci. USA*, **93**, 9975–9979.

Kasschau,K.D. and Carrington,J.C. (1998) A counter-defensive strategy of plant viruses: suppression of post-transcriptional gene silencing. *Cell*, **95**, in press.

Kavanagh,T., Goulden,M., Santa Cruz,S., Chapman,S., Barker,I. and Baulcombe,D. (1992) Molecular analysis of a resistance-breaking strain of potato virus X. *Virology*, **189**, 609–617.

Kjemtrup,S., Sampson,K.S., Peele,C.G., Nguyen,L.V., Conkling,M.A., Thompson,W.F. and Robertson,D. (1998) Gene silencing from plant DNA carried by a geminivirus. *Plant J.*, **14**, 91–100.

Kumagai,M.H., Donson,J., Della-Cioppa,G., Harvey,D., Hanley,K. and Grill,L.K. (1995) Cytoplasmic inhibition of carotenoid biosynthesis with virus-derived RNA. *Proc. Natl Acad. Sci. USA*, **92**, 1679–1683.

Lindbo,J.A., Silva-Rosales,L., Proebsting,W.M. and Dougherty,W.G. (1993) Induction of a highly specific antiviral state in transgenic plants: implications for regulation of gene expression and virus resistance. *Plant Cell*, **5**, 1749–1759.

Matthews,R.E.F. (1991) *Plant Virology*. Academic Press, San Diego, CA.

Matzke,M.A. and Matzke,A.J.M. (1995) How and why do plants inactivate homologous (trans)genes? *Plant Physiol.*, **107**, 6679–6685.

Mueller,E., Gilbert,J.E., Davenport,G., Brigneti,G. and Baulcombe,D.C. (1995) Homology-dependent resistance: transgenic virus resistance in plants related to homology-dependent gene silencing. *Plant J.*, **7**, 1001–1013.

Murphy,J.F. and Kyle,M.M. (1995) Alleviation of restricted systemic spread of pepper mottle potyvirus in *Capsicum annuum* cv. Avelar by coinfection with a cucumovirus. *Phytopathology*, **85**, 561–566.

Palauqui,J.-C., Elmayan,T., Pollien,J.-M. and Vaucheret,H. (1997) Systemic acquired silencing: transgene-specific post-transcriptional silencing is transmitted by grafting from silenced stocks to non-silenced scions. *EMBO J.*, **16**, 4738–4745.

Pio-Riberio,G., Wyatt,S.D. and Kuhn,C.W. (1978) Cowpea stunt: a disease caused by a synergistic interaction of two viruses. *Phytopathology*, **68**, 1260–1265.

Pruss,G., Ge,X., Shi,X.M., Carrington,J.C. and Vance,V.B. (1997) Plant viral synergism: the potyviral genome encodes a broad-range pathogenicity enhancer that transactivates replication of heterologous viruses. *Plant Cell*, **9**, 859–868.

Ratcliff,F., Harrison,B.D. and Baulcombe,D.C. (1997) A similarity between viral defense and gene silencing in plants. *Science*, **276**, 1558–1560.

Robaglia,C., Durand-Tardif,M., Tronchet,M., Astier-Manifacier,S. and Casse-Delbart,F. (1989) Nucleotide sequence of potato virus Y (N strain) genomic RNA. *J. Gen. Virol.*, **70**, 935–947.

Ruiz,F., Vassie,L., Klotz,K., Sperling,L. and Madeddu,L. (1998a) Homology-dependent gene silencing in *Paramecium*. *Mol. Biol. Cell*, **9**, 931–943.

Ruiz,M.T., Voinnet,O. and Baulcombe,D.C. (1998b) Initiation and maintenance of virus-induced gene silencing. *Plant Cell*, **10**, 937–946.

Smith,H.A., Swaney,S.L., Parks,T.D., Wernsman,E.A. and Dougherty, W.G. (1994) Transgenic plant virus resistance mediated by untranslatable sense RNAs: Expression, regulation and fate of nonessential RNAs. *Plant Cell*, **6**, 1441–1453.

Thole,V., Dalmay,T., Burgyan,J. and Balazs,E. (1993) Cloning and sequencing of potato virus Y (Hungarian isolate) genomic RNA. *Gene*, **123**, 149–156.

Vance,V. (1991) Replication of potato virus X RNA is altered in coinfections with potato virus Y. *Virology*, **182**, 486–494.

Voinnet,O. and Baulcombe,D.C. (1997) Systemic signalling in gene silencing. *Nature*, **389**, 553.

Voinnet,O., Vain,P., Angell,S. and Baulcombe,D.C. (1998) Systemic spread of sequence-specific transgene RNA degradation is initiated by localised introduction of ectopic promoterless DNA. *Cell*, **95**, in press.

Received August 21, 1998; revised and accepted September 24, 1998

Silencing on the Spot. Induction and Suppression of RNA Silencing in the *Agrobacterium*-Mediated Transient Expression System[1]

Lisa K. Johansen and James C. Carrington*

Institute of Biological Chemistry, Washington State University, Pullman, Washington 99164–6340

The *Agrobacterium*-mediated transient expression assay in intact tissues has emerged as a rapid and useful method to analyze genes and gene products in plants. In many cases, high levels of active protein can be produced without the need to produce transgenic plants. In this study, a series of tools were developed to enable strong or weak induction of RNA silencing and to suppress RNA silencing in the absence of stable transgenes. Transient delivery of a gene directing production of a double-stranded green fluorescent protein (GFP) transcript rapidly induced RNA silencing of a codelivered GFP reporter gene, effectively preventing accumulation of GFP protein and mRNA. RNA silencing triggered by the strong dsGFP inducer was partially inhibited by the tobacco etch virus silencing suppressor, P1/HC-Pro. In the absence of the strong double-stranded GFP inducer, the functional GFP gene served as a weak RNA silencing inducer in the transient assay, severely limiting accumulation of the GFP mRNA over time. The weak silencing induced by the GFP gene was suppressed by P1/HC-Pro. These results indicate RNA silencing can be triggered by a variety of inducers and analyzed entirely using transient gene delivery systems. They also indicate that RNA silencing may be a significant limitation to expression of genes in the *Agrobacterium*-mediated transient assay but that this limitation can be overcome by using RNA silencing suppressors.

RNA silencing in plants (also known as post-transcriptional gene silencing) is the remarkable process, whereby foreign RNA molecules are recognized and degraded in a sequence-specific manner (Meins, 2000; Sijen and Kooter, 2000). The foreign RNAs can derive from a highly expressed or aberrant transgene or from an infectious virus. In fact, RNA silencing is an adaptive defense response that can limit virus infection and the severity of symptoms (Marathe et al., 2000). RNA silencing in plants is closely related to the process of RNA interference in animals, which has been studied most intensively in *Caenorhabditis elegans* and *Drosophila* (Hunter, 2000). In many organisms, RNA silencing has proven to be a highly effective tool for producing epigenetic knockout phenotypes in whole organisms (Baulcombe, 1999; Bosher and Labouesse, 2000).

Through genetic and biochemical analyses in a variety of systems, the molecular basis for RNA silencing is partially understood (Bass, 2000; Carrington, 2000). A key early step in RNA silencing is formation of double-stranded (ds) RNA. In the case of most plant viruses, dsRNA is formed during the intermediate steps of genome replication, and this may explain why viruses are often potent inducers of RNA silencing (Baulcombe, 1999). RNA silencing triggered by transgenes, but not some viruses, requires an RNA-dependent RNA polymerase (RdRp)-like protein that is hypothesized to catalyze synthesis of RNA complementary to the target species (Dalmay et al., 2000; Mourrain et al., 2000). Double-stranded RNA is then recognized by a dsRNA-specific nuclease and cleaved to produce small (21–23 nucleotides) RNA species (Hamilton and Baulcombe, 1999; Hammond et al., 2000; Zamore et al., 2000). The small RNAs are proposed to associate with one or more nuclease-like proteins and serve as guides for sequence-specific cleavage of silencing target RNAs (Bass, 2000). This explains how a given inducer molecule can trigger RNA degradation directed against itself and against any RNA with high levels of sequence identity.

The differential requirements for RNA silencing triggered by transgenes and by RNA viruses in plants, and the effects of various virus-encoded silencing suppressors support a model in which there are two induction pathways leading to RNA silencing in plants (Carrington, 2000; Dalmay et al., 2000; Voinnet et al., 2000). Silencing triggered by a transgene mRNA, or an RNA with limited amounts of ds secondary structure, depend on the "weak" inducer pathway that involves the RdRp. It is interesting that this pathway also leads to systemic RNA silencing in which tissues distal to the initial sites of silencing induction also acquire the silenced state (Voinnet et al., 2000). Systemic silencing involves a graft-transmissible signal that moves through the phloem (Fagard and Vaucheret, 2000). Silencing triggered by some replicating RNA viruses, and possibly by inducers with very long segments of dsRNA, may occur through a "strong" inducer pathway in which the requirement for the RdRp is bypassed. The strong

[1] This work was supported by the National Institutes of Health (grant nos. AI43288 and AI27832) and by the U.S. Department of Agriculture (grant no. 98–35303–6485).

* Corresponding author; e-mail carrington@wsu.edu; fax 509–335–2482.

inducers may be recognized directly by the dsRNase required for synthesis of the small RNAs (Zamore et al., 2000).

The *Agrobacterium tumefaciens*-mediated transient expression system is a versatile tool to rapidly introduce genes into plant tissue. This system enables gene expression within a short period of time and without the requirement for regenerating transgenic plants. A useful feature of this system is the ability to introduce multiple genes simultaneously into a patch of leaf tissue. This system will likely increase in utility, particularly for high-throughput functional genomic and proteomic analyses. The *Agrobacterium*-mediated expression system has also been used effectively as a means to deliver RNA silencing inducers and suppressors into transgenic plants that express a silencing reporter gene (for example, Brigneti et al., 1998; Voinnet et al., 1998, 2000; Llave et al., 2000).

In this study, we developed tools and procedures to enable analysis of RNA silencing using the *Agrobacterium*-mediated transient expression system in the absence of a stable transgene reporter. The response of a reporter gene in the presence of weak and strong RNA silencing inducers was analyzed as was the effect of co-introduction of a virus-encoded silencing suppressor. The results indicate that highly effective RNA silencing can be triggered rapidly with strong inducers. The results also indicate that RNA silencing may be an inevitable consequence of *Agrobacterium*-mediated transient delivery of functional genes under the control of a strong promoter but that this can be countered through use of silencing suppressors.

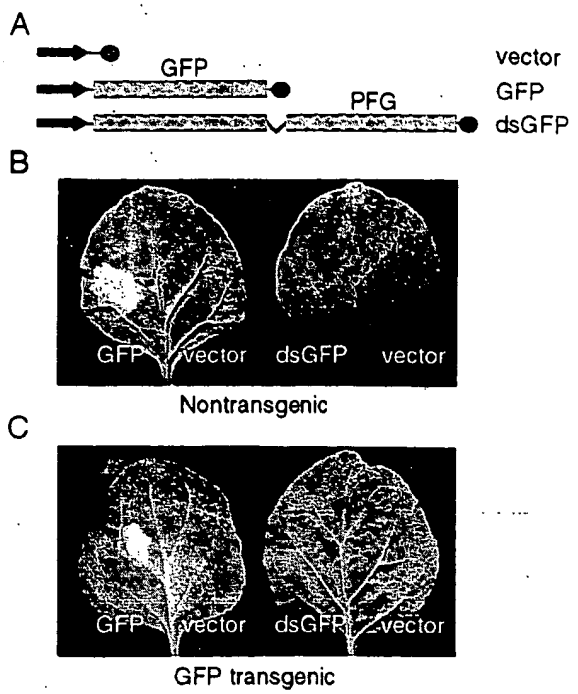

Figure 1. *Agrobacterium*-mediated transient expression in *N. benthamiana* leaves. A, Constructs used contained the 35S promoter (arrow) and terminator sequences (black circle). The GFP construct contained a functional copy of the soluble-modified GFP coding sequence, whereas the dsGFP construct contained both sense and antisense smGFP sequences separated by an intron. B and C, *Agrobacterium*-infiltrated non-transgenic (B) and GFP-transgenic (C) leaves were viewed at 6-d p.i. under long wavelength UV illumination. Spots in half leaves were infiltrated with *Agrobacterium* containing the indicated constructs.

RESULTS

Transient Delivery of RNA Silencing Inducers and Targets

Most studies to analyze RNA silencing in plants have depended on transgenic plants that express an active or silenced reporter gene. To enable analysis of RNA silencing that is independent of transgenes, an *Agrobacterium*-mediated transient system was devised to simultaneously introduce both silencing inducer and target RNAs in *Nicotiana benthamiana*. Two key constructs were used in most experiments. A 35S-green fluorescent protein (GFP) gene (referred to as the GFP construct) encoded the soluble-modified form of green fluorescent protein. A 35S-GFP/antisense GFP gene contained the full-length GFP coding sequence, an intron, and a full-length GFP sequence in the inverted orientation (Fig. 1A). Transcription of this gene and RNA processing was predicted to yield an intron spliced hairpin RNA that was referred to as the dsGFP RNA. Constructs directing synthesis of dsRNAs in transgenic plants were shown to be potent inducers of RNA silencing (Waterhouse et al., 1998; Chuang and Meyerowitz, 2000; Schweizer et al., 2000; Smith et al., 2000). An empty vector construct was also used in all experiments as a negative control.

Leaves of *N. benthamiana* plants were infiltrated with cultures of *Agrobacterium* containing vector, GFP, or dsGFP constructs, and GFP fluorescence was monitored using a handheld long wavelength UV light source. Noninfiltrated zones and zones infiltrated with cells containing the vector alone appeared red due to autofluorescence. Tissue infiltrated with bacteria containing the GFP gene appeared bright green (Fig. 1B). In contrast, tissue infiltrated with *Agrobacterium* containing the dsGFP construct appeared red and was indistinguishable from the vector-only infiltration sites. Similar results were obtained when *Agrobacterium* cultures containing the vector, GFP and dsGFP constructs were injected into leaves of GFP-expressing transgenic *N. benthamiana* plants. In these plants, GFP expressed from the injected construct was detected against a background of light green fluorescence from the transgene-expressed protein (Fig. 1C).

RNA Silencing by a Strong Inducer in the Transient System

A time-course analysis of GFP- and dsGFP-expressing tissue was done to examine the initiation of RNA silencing in the infiltrated tissues. High M_r and small RNAs were extracted from *Agrobacterium*-injected tissue and analyzed by blot hybridization with a radiolabeled probe specific for the GFP sequence. The small RNA fraction was prepared to analyze RNA silencing-associated 21- to 23-nucleotide RNA species. In cells undergoing RNA silencing, these small RNAs correspond to both sense and antisense fragments of the silencing target (Hamilton and Baulcombe, 1999). In non-transgenic tissue, the 35S-GFP mRNA was detected at 2-d postinfiltration (p.i.). After peaking at 3-d p.i., however, the level of GFP mRNA declined dramatically through 6-d p.i. (Fig. 2A). Relatively little small RNA with homology to the GFP sequence was detected during the time course. In contrast, neither a full-length dsGFP transcript nor a unit length GFP RNA was detected in non-transgenic tissue expressing the dsGFP gene (Fig. 2A). However, GFP-specific small RNA was detected at 2-d p.i. and accumulated over the 6-d time course in non-transgenic plants. In the GFP-expressing transgenic plants, the dsGFP gene also induced formation of GFP-related small RNAs as well as a moderate decline in the level of GFP transgene mRNA between 2- and 6-d p.i. (Fig. 2B). Transient expression of the dsGFP gene, therefore, was sufficient to induce RNA silencing in the injection zone of both non-transgenic and GFP-transgenic plants.

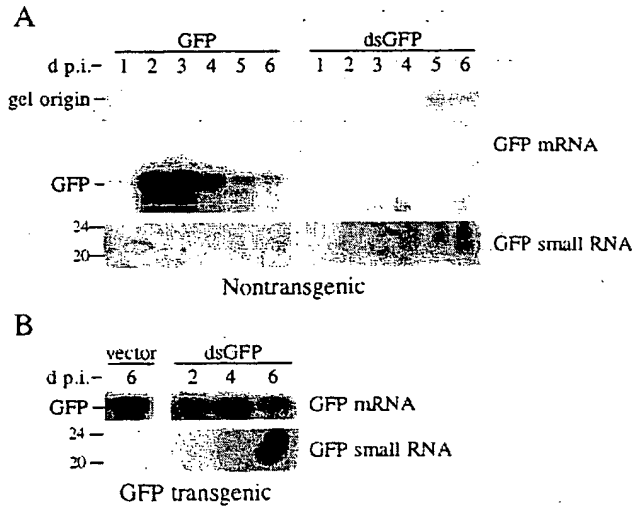

Figure 2. Analysis of GFP-related RNAs from tissue infiltrated with *Agrobacterium* containing the GFP and dsGFP genes. HMW RNA (5 μg) and small RNA (50 μg) samples were prepared at various times p.i. and subjected to RNA-blot analysis using a radiolabeled GFP sequence probe. A, Time course analysis of GFP-related RNAs in *Agrobacterium*-infiltrated non-transgenic leaf tissue expressing GFP or dsGFP genes. B, Limited time-course analysis of GFP-related RNAs in GFP-transgenic plants that were infiltrated with *Agrobacterium* containing empty vector or the dsGFP gene. The electrophoretic positions of GFP mRNA and oligonucleotide standards (20 and 24 nucleotides) are shown at the left.

To determine if transient dsGFP expression was sufficient to silence the *Agrobacterium*-injected GFP gene, coinfiltration experiments with both GFP and dsGFP constructs were done. In these and subsequent experiments, three *Agrobacterium* cultures were mixed in equal parts prior to all injections. One culture contained the GFP reporter gene. Depending on the experiment, the other two cultures contained empty vector, the dsGFP construct, or another test construct (see below). In all cases, however, the amount of injected *Agrobacterium* containing the GFP reporter was constant, regardless of whether or not additional cultures containing test constructs were added to the injection mix. In non-transgenic plants, infiltration of an *Agrobacterium* mixture containing the GFP gene and empty vector resulted in bright green fluorescence within 2 d of p.i. (Fig. 3, A and C). GFP fluorescence required a Vir^+ *Agrobacterium* strain, as tissue injected with a Vir^- strain containing the GFP construct failed to fluoresce (Fig. 3G). Infiltration of a mixture containing the GFP gene, dsGFP gene, and empty vector resulted in no GFP fluorescence (Fig. 3A). The same results were obtained when the mixtures were injected into GFP-expressing transgenic plants (Fig. 3, D and F). The suppression of GFP activity in tissue injected with the GFP plus dsGFP mixture required that the dsGFP construct be in a Vir^+ *Agrobacterium* strain (Fig. 3H). Furthermore, the GFP-inhibitory effect of the dsGFP construct was sequence-specific, as co-injection of *Agrobacterium* containing the GFP construct and a dsGUS construct resulted in strong GFP fluorescence (Fig. 3I).

The effect of co-introduction of GFP and dsGFP genes was investigated by analysis of GFP protein in the infiltrated tissue of transgenic and non-transgenic plants. As controls, tissues were infiltrated with *Agrobacterium* containing empty vector, GFP plus empty vector, and dsGFP plus empty vector. The GFP protein was detected in transgenic plants but not non-transgenic plants injected with *Agrobacterium* containing empty vector (Fig. 4, A and B, lanes 1–3). In non-transgenic tissue injected with the GFP gene plus empty vector, GFP protein accumulated to increasing levels over the 6-d time course (Fig. 4A, lanes 4–6), whereas in transgenic tissue GFP accumulated to levels higher than the endogenous (transgene-encoded) levels (Fig. 4B, compare lanes 4–6 with 1–3). However, in non-transgenic tissue infiltrated with the *Agrobacterium* mixture containing GFP and dsGFP genes, no GFP protein was detected at any time point (Fig. 4A, lanes 10–12). These data indicate that the dsGFP construct was inhibitory to accumulation of protein encoded by the injected GFP gene. Similarly, the levels of endogenous GFP in the transgenic plants decreased 5-fold, relative to tissue expressing the empty vector, over the time-course in

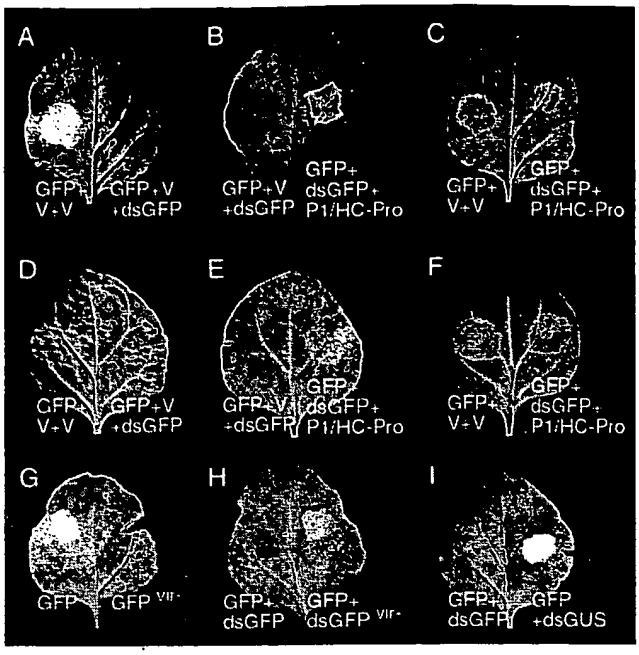

Figure 3. *Agrobacterium*-mediated transient expression of combinations of GFP, dsGFP, and P1/HC-Pro constructs. Non-transgenic (A–C and G–I) or GFP-transgenic (D–F) *N. benthamiana* leaves were infiltrated and analyzed as described in Figure 1. The vir− strain of *Agrobacterium* lacked DNA transfer properties and was used in a series of controls (G and H). All infiltrations with a mixture of three *Agrobacterium* cultures (A–F) were done using equivalent amounts of the individual components. In half leaves shown in A, C, D, and F, two equivalents of the empty vector (V) culture were used.

tissue infiltrated with the *Agrobacterium* mixtures containing the dsGFP gene alone or the dsGFP plus GFP genes (Fig. 4B, lanes 7–12).

Co-introduction of GFP and dsGFP genes was further investigated by analysis of GFP mRNA and small RNAs from the infiltrated tissues of non-transgenic plants. As in the previous experiment (Fig. 2A), infiltrated tissue expressing the GFP gene contained the GFP mRNA, which declined significantly between the 4- and 6-d-p.i. time points (Fig. 5, lanes 2–4). This decrease in GFP mRNA steady-state level over time contrasted with the increasing accumulation of GFP protein (Fig. 4A, lanes 4–6). The high steady-state level of protein likely resulted from the high stability of GFP. Little or no GFP-related small RNA was detected using these experimental conditions, even at 6-d p.i. (Fig. 5, lanes 2–4). However, these small RNAs were detected using higher specific activity probes and increasing exposure times (data not shown). No GFP mRNA was detected after co-introduction of the GFP and dsGFP genes, whereas small RNA accumulated to increasing levels throughout the time course (Fig. 5, lanes 8–10). The cumulative data from in situ visualization of fluorescence, and from analysis of GFP protein, GFP mRNA and GFP small RNA indicate that the dsGFP construct induced silencing rapidly and efficiently in the transient system, regardless of whether or not a homologous nuclear transgene was present.

Suppression of RNA Silencing by Tobacco Etch Virus (TEV) P1/HC-Pro in the Transient System

The TEV-encoded RNA silencing suppressor, P1/HC-Pro (Anandalakshmi et al., 1998; Brigneti et al., 1998; Kasschau and Carrington, 1998), was introduced into the GFP-based transient silencing system to address two issues. First, the ability of P1/HC-Pro to suppress RNA silencing from the "strong" inducer derived from the dsGFP gene was tested. In previous studies, P1/HC-Pro was shown to reverse RNA silencing triggered by a "weak" transgene inducer in transgenic plants (Llave et al., 2000). Second, the ability of P1/HC-Pro to inhibit decline of the GFP mRNA in tissues expressing the functional GFP gene was tested. If the decline was due to slow or weak induction of RNA silencing, then P1/HC-Pro was predicted to inhibit the decline. P1/HC-Pro is actually a polyprotein that undergoes autoproteolytic processing catalyzed by proteinase domains within the P1 and HC-Pro proteins (Carrington et al., 1990).

In contrast to the lack of GFP fluorescence in tissues injected with mixtures of *Agrobacterium* containing GFP plus dsGFP genes, tissues infiltrated with the triple mixture containing GFP, dsGFP, and P1/HC-Pro genes exhibited bright green fluorescence, regardless of whether the plants were non-transgenic or GFP-transgenic (Fig. 3, B, C, E, and F). In non-transgenic plants, the appearance of green fluor-

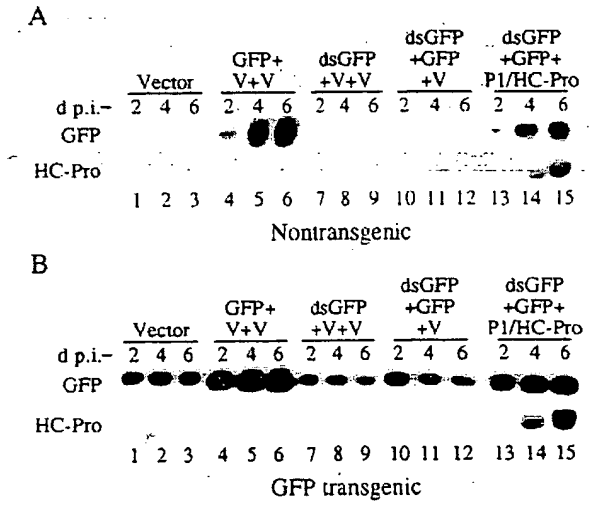

Figure 4. Immunoblot analysis of GFP and HC-Pro in *Agrobacterium*-infiltrated tissue. Time course analysis of GFP and HC-Pro protein in non-transgenic (A) or GFP transgenic (B) *N. benthamiana* plants infiltrated with *Agrobacterium* containing empty vector (lanes 1–3) or combinations of *Agrobacterium* containing empty vector (V), GFP, dsGFP, or P1/HC-Pro constructs (lanes 4–15). Normalized extracts (20 μg) were prepared at 2-, 4-, and 6-d p.i. and subjected to immunoblot analysis with anti-GFP or anti-HC-Pro sera.

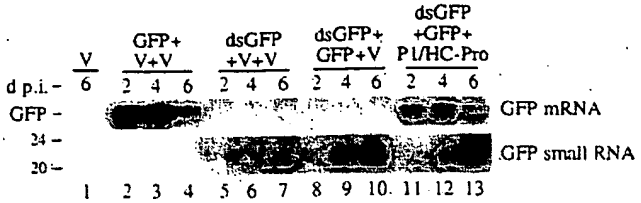

Figure 5. RNA-blot analysis of GFP-specific RNAs in *Agrobacterium*-infiltrated non-transgenic *N. benthamiana* tissue. HMW RNA (5 μg) and small RNA (50 μg) samples were prepared at various times p.i. and subjected to RNA-blot analysis using a radiolabeled GFP sequence probe. Samples were extracted from tissue that was infiltrated with *Agrobacterium* containing empty vector (V, lane 1) or combinations of *Agrobacterium* containing empty vector (v), GFP, dsGFP, or P1/HC-Pro constructs (lanes 2–13). The electrophoretic positions of oligonucleotide standards (20 and 24 nucleotides) are shown at the left.

escence in leaves injected with the triple mixture corresponded with accumulation of GFP protein in time-course experiments (Fig. 4A, lanes 13–15). HC-Pro was also detected in the immunoblot assay at 4- and 6-d p.i., although accumulation of HC-Pro was delayed relative to accumulation of GFP (Fig. 4A, lanes 13–15). In transgenic plants, the level of GFP protein that accumulated in tissues receiving the triple mixture was enhanced relative to tissues injected with the GFP plus dsGFP mixture (Fig. 4B, lanes 10–15). The enhancement (11.3-fold) was particularly evident at 6-d p.i. (Fig. 4B, compare lanes 12 and 15). In addition, the presence of P1/HC-Pro in non-transgenic tissues injected with the triple mixture resulted in accumulation of GFP mRNA (Fig. 5, lanes 11–13). However, as seen in tissues expressing GFP alone (Fig. 5, lanes 2–4), the GFP mRNA declined between 4- and 6-d p.i. Furthermore, the presence of P1/HC-Pro did not prevent accumulation of silencing-specific small RNAs (Fig. 5, lanes 11–13). At the 6-d p.i. time-point, in six independent experiments, the level of accumulation of GFP-related small RNAs in tissue injected with the triple mixture was equal to or greater than that detected in tissue expressing GFP plus dsGFP alone. These data suggest that P1/HC-Pro partially suppresses RNA silencing initiated by the strong inducer in the transient GFP expression system, although suppression likely occurs only at the early time points examined.

In addition to examination of the effect of P1/HC-Pro on dsGFP-induced RNA silencing, the effect of P1/HC-Pro on expression and accumulation of the GFP mRNA in the absence of dsGFP was tested. As in previous experiments (Figs. 2A and 5), tissue injected with *Agrobacterium* containing the GFP gene accumulated GFP mRNA to relatively high levels within 2-d p.i., but GFP mRNA levels declined at later time points (Fig. 6, lanes 1–3). In contrast, tissue injected with an *Agrobacterium* mixture containing GFP and P1/HC-Pro genes accumulated GFP mRNA to relatively high levels that did not decrease between 2- and 6-d p.i. (Fig. 6, lanes 10–12). These data indicate that the slow decline in GFP mRNA after *Agrobacterium*-mediated introduction of the GFP gene into leaf tissue is likely due to RNA silencing and that this is efficiently suppressed by P1/HC-Pro. This differs from the effect of P1/HC-Pro on dsGFP-mediated silencing of the GFP mRNA where the suppressor promotes accumulation of the GFP mRNA early (2-d p.i.) but not late (6-d p.i.) in the time course (Fig. 6, lanes 7–9).

DISCUSSION

RNA Silencing in the Transient Assay

The *Agrobacterium*-mediated transient expression system was used to deliver RNA silencing inducer, reporter, and suppressor constructs to intact tissues of *N. benthamiana*. This system enabled analysis of RNA silencing of a GFP construct based entirely on genes delivered in the transient assay. RNA silencing triggered by a strong inducer derived from the dsGFP construct occurred rapidly, regardless of whether or not the plant contained a GFP transgene. A key feature of this system is the ability to simultaneously introduce additional genes along with silencing reporter genes. For example, the effects of silencing suppressors can be tested by adding *Agrobacterium* cultures containing test constructs to the injection mix. The codelivery of multiple constructs is enabled by the extremely high efficiency of *Agrobacterium*-mediated gene transfer in *N. benthamiana* leaves. Microscopic examination of tissue injected with *Agrobacterium* containing the GFP construct suggests that virtually all cells express the gene (unpublished observations).

The finding that transient delivery of dsGFP triggered RNA silencing efficiently is fully consistent with several other studies using transgenic plants (Waterhouse et al., 1998; Chuang and Meyerowitz, 2000; Smith et al., 2000). The basis for this strong inducer activity relates to the probable role of dsRNA as the substrate for a nuclease that catalyzes cleavage to 21 to 23 nucleotide RNAs (Zamore et al., 2000). The

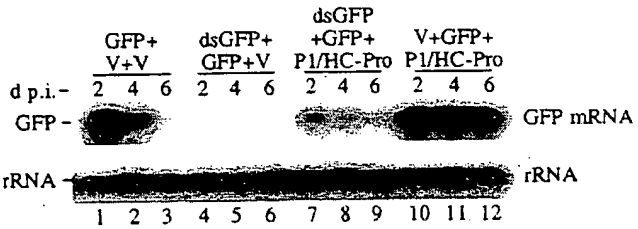

Figure 6. RNA-blot analysis of GFP-specific RNAs in *Agrobacterium*-infiltrated non-transgenic *N. benthamiana* tissue. HMW RNA samples (5 μg) were prepared at various times p.i. and subjected to RNA-blot analysis using a radiolabeled GFP sequence probe. Samples were extracted from tissue that was infiltrated with combinations of *Agrobacterium* containing empty vector (V), GFP, dsGFP, or P1/HC-Pro constructs. The blot was stripped and reprobed using radiolabeled DNA corresponding to ribosomal RNA.

small RNAs are proposed to guide a nucleolytic ribonucleoprotein complex to target RNAs. Thus, increasing amounts of dsRNA would lead to increasing amounts of small RNAs, which would lead to increasing amounts of a component of the sequence-specific nuclease. In clear support of this model, small RNAs were produced in relatively high quantities after introduction of the dsGFP construct. This was in stark contrast to the relatively low levels of small RNA in tissues expressing the functional GFP gene, at least during the time course examined.

Despite the relatively low levels of small RNA in the functional GFP-expressing tissue, RNA silencing was eventually detected in the absence of the dsGFP inducer. Similarly, Voinnet et al. (2000) found that infiltration of a GFP-expressing construct in GFP transgenic plants resulted intitally in strong fluorecence at the site of infiltration, followed by systemic silencing of the GFP transgene and small RNA accumulation. The results of experiments using P1/HC-Pro support the hypothesis that the decline in GFP steady-state level was due to RNA silencing. Co-introduction of GFP and P1/HC-Pro constructs resulted in maintenance of relatively high steady-state levels of GFP mRNA. As P1/HC-Pro has little or no effect on transcription (Kasschau and Carrington, 2001), maintenance of high GFP mRNA levels by P1/HC-Pro likely resulted from RNA silencing suppression.

These studies underscore the idea that there are two types of RNA silencing inducers (Dalmay et al., 2000; Voinnet et al., 2000). Strong inducers are those that contain extensive amounts of dsRNA, either because a gene directs synthesis of a transcript that adopts considerable double stranded structure or because a replicating virus produces dsRNA during the course of genome replication. Weak inducers are those that contain relatively little double stranded structure but that are eventually recognized by the silencing apparatus and targeted. An important step in targeting a weak inducer may be recognition by the cellular RdRp, which is proposed to catalyze synthesis of complementary RNA and which would lead to accumulation of dsRNA intermediates (Dalmay et al., 2000; Mourrain et al., 2000). How a weak inducer is initially recognized remains to be determined.

The effects of TEV P1/HC-Pro on RNA silencing induced by a β-glucuronidase (GUS) transgene was analyzed previously (Kasschau and Carrington, 1998; Llave et al., 2000). The GUS transgene in those studies likely resulted in formation of a weak inducer RNA in transgenic plants. Co-expression of P1/HC-Pro effectively suppressed both RNA silencing and formation of small RNAs (Kasschau and Carrington, 1998; Llave et al., 2000). In the dsGFP-induced system described here, P1/HC-Pro transiently suppressed RNA silencing induced by the dsGFP construct. However, RNA silencing triggered by the dsGFP construct in the presence of P1/HC-Pro eventually occurred in the 6-d time course experiments, resulting in declining GFP mRNA levels and accumulation of small RNAs. It is proposed that in the presence of low levels of dsRNA inducer, P1/HC-Pro effectively suppresses RNA silencing. However, as dsRNA inducer accumulates, the suppressing activity of P1/HC-Pro is overcome, and RNA silencing occurs. These data suggest that P1/HC-Pro inhibits a dsRNA-dependent step in the RNA silencing pathway.

Applications

There are three types of applications that arise from this work. First, the transient RNA silencing assay using various types of inducers and GFP as a reporter provides a rapid method to screen candidate genes, or random genes from a library, for effects of RNA silencing. Screens could be designed for positive or enhancing effects in the case of genes encoding RNA silencing activators or effectors. Alternatively, screens can be done for silencing suppressors that have a negative effect. Such a strategy for identification of positive and negative factors involved in RNA silencing will complement mutant screens.

Second, the transient delivery of dsRNA constructs provides a rapid method to potentially silence any gene in the *Agrobacterium* infiltration zone. Of course, the use of dsRNA-mediated transient silencing depends on the availability of an assay to monitor effects, and the range of processes that might be investigated using this approach in leaf tissue is limited. The transient RNA silencing system is further limited by potential residual effects of gene products that accumulate prior to induction of silencing. This point is illustrated by examination of the effects of dsGFP on endogenous GFP protein and mRNA levels in GFP-transgenic tissue (Figs. 2B and 4B). Although the dsGFP inducer triggered RNA silencing, residual GFP protein and GFP mRNA were still detected at 6-d p.i. In addition, the applicability of the transient system is limited to those species that are amenable to delivery and expression of T-DNA constucts by *Agrobacterium*.

Third, the effect of P1/HC-Pro on RNA silencing triggered by functional (weak silencing inducer) genes has broad use. The use of the *Agrobacterium* delivery system to introduce foreign genes into leaf tissue continues to grow. Further, we see tremendous potential for this system in functional genomics and proteomics programs, in which expression of wild-type or tagged proteins is followed by analysis of effects on global gene expression, metabolic pathways, or protein complex formation. Under the control of the 35S promoter, it is clear that the GFP gene is subject to RNA silencing after an initial burst of gene expression. It is reasonable to expect that many

genes, expressed in a similar manner, will follow the same pattern. Co-introduction of P1/HC-Pro with the GFP gene suppressed the RNA silencing response. It follows, therefore, that P1/HC-Pro will suppress RNA silencing triggered by other constructs and result in maintenance of high expression levels for extended periods.

MATERIALS AND METHODS

Plasmid Construction

The base vector for all constructs, pRTL2 (Restrepo et al., 1990), contained an enhanced 35S promoter from cauliflower mosaic virus, the TEV 5′-non-translated sequence, and the 35S terminator.

The GFP construct (pRTL2-smGFP) contained the coding region of the soluble-modified green fluorescent protein from *Aequorea victoria* (nucleotides 21–737) (Davis and Vierstra, 1998). An additional codon (GCA) was inserted immediately after the start codon to form a *Nco*I restriction site at the 5′ end of the open reading frame. The 3′ end of the GFP coding sequence contained the authentic stop codon followed by a *Kpn*I site. The GFP coding sequence was inserted between the *Nco*I and *Kpn*I sites of pRTL2.

The dsGFP construct (pRTL2-dsGFP) contained the entire GFP open reading frame, including the stop codon, a 120-nucleotide intron from the *RTM1* gene of Arabidopsis Col-0 (Chisholm et al., 2000), and the entire GFP coding region in the antisense orientation. The dsGFP construct was made by joining the *RTM1* intron to the 3′ end of the GFP coding sequence using PCR. This fragment was cloned into pRTL2-smGFP using *Kpn*I and *Xba*I restriction sites.

The dsGUS construct (pRTL2-dsGUS) contained the entire GUS coding region, followed by the *RTM1* intron, and then an antisense copy of the 3′-proximal 558 nucleotides of the GUS coding sequence. The intron-antisense GUS fragment was inserted into pRTL2-GUS (Restrepo et al., 1990) between the *Bgl*II and *Bam*HI sites.

Construction of the P1/HC-Pro construct (pRTL2–0027) was described previously (Carrington et al., 1990). This construct contained the sequence corresponding to nucleotides 12 to 2,681 of the TEV genome, which encodes the P1 and HC-Pro proteins and the N-terminal 82 amino acid residues of the P3 protein.

The expression cassette from each pRTL2-based construct was excised using *Pst*I and inserted into the plant transformation vector, pSLJ75515 (Jones et al., 1992). Each of these plasmids was introduced into *Agrobacterium tumefaciens* strain GV2260 or the avirulent strain C58C1^{P} by triparental mating.

Plant Material and *Agrobacterium* Infiltration

Transgenic *Nicotiana benthamiana* plants expressing GFP protein were provided by Dr. David C. Baulcombe (Sainsbury Laboratory) and were described previously (Schaad et al., 1997; Brigneti et al., 1998). *Agrobacterium* infiltration of leaves was done as described (Llave et al., 2000) except that the cultures were incubated overnight in infiltration medium at room temperature. *Agrobacterium* cultures were mixed prior to infiltration by combining equal volumes of individual cultures. A 3-cc syringe was used to infiltrate tissue from the underside of leaves.

GFP Imaging

Visual detection of GFP fluorescence was done using a long-wave UV lamp (Black Ray model B 100 AP). Plants were photographed with a 950 digital camera (Nikon, Tokyo) mounted with both UV and yellow filters. The images were processed electronically using Adobe Photoshop.

RNA Isolation and Blot Analysis

Total RNA from infiltrated spots was extracted by grinding leaf tissue in liquid nitrogen and resuspending the frozen powder in Trizol reagent (10 [v/w]) (Life Technologies/Gibco-BRL, Cleveland). After 5 min at room temperature, chloroform was added (0.2 [v/v]) and the solution was mixed thoroughly. The RNA was separated from the DNA and protein by centrifugation at 12,000*g* for 15 min at 4°C. The RNA phase was removed, and RNA was precipitated by the addition of isopropanol (0.5 [v/v]). The RNA pellet was dissolved in 1 mL of Qiagen buffer QRL1 (Qia RNA/DNA Midi Kit). Nine milliliters of QRV2 buffer was added to the solution. The RNA was applied to a Qiagen RNA/DNA column according to the manufacturer's directions. Low M_r (LMW) RNA was eluted with buffer QRW2, and high M_r (HMW) RNA was subsequently eluted with buffer QRU. The RNA was precipitated with ice-cold isopropanol (1 [v/v]) and recovered by centrifugation at 15,000*g* for 30 min at 4°C. The RNA pellets were resuspended in diethyl pyrocarbonate-treated water, and total RNA concentration was determined using a UV-1601 spectrophotometer (Shimadzu, Columbia, MD).

The LMW RNA (50 μg) was resolved by electrophoresis in a 15% (w/v) polyacrylamide-7 M urea gel in TBE buffer (45 mM Tris-borate, pH 8.0, 1 mM EDTA). The HMW RNA (5 μg) was resolved by electrophoresis in a 1.5% (w/v) agarose-formaldehyde gel using a buffer consisting of 20 mM HEPES, pH 7.8, 1 mM EDTA. The RNA in gels was transferred to HyBond-N membrane and subjected to UV crosslinking (1,200 μJ, Stratalinker, Stratagene, La Jolla, CA). The LMW and HMW RNA blots were prehybridized in solution (50% formamide [v/v], 10× Denhardt's solution, 0.5 mg/mL sheared salmon sperm DNA, 1% [w/v] SDS, 3× SSC, and 50 mM phosphate buffer) at 35°C and 42°C, respectively, for at least 3 h. GFP specific radioactive DNA probes were generated by a random priming technique. Hybridization of the LMW (35°C) and HMW (42°C) blots was done overnight in a rotating incubator and was followed by four washes (20 min each) in 2× SSC buffer and 0.2% (w/v) SDS at 50°C and 65°C, respectively. Radio-

activity on the blots was quantitated using a phosphoimager. Blots were then exposed to x-ray film.

Immunoblot Analysis

Leaf tissue from infiltration zones was ground in liquid nitrogen and resuspended (5 [v/w]) in dissociation buffer (40 mM sodium phosphate, pH 7.0, 10 mM EDTA, 0.1% [v/v] Triton X-100, 0.1% [w/v] *N*-lauryl sarcosine, 10 mM β-mercaptoethanol, 0.5 mM phenylmethylsulfonyl fluoride, 1 μg/mL aprotinin, and 1 μg/mL leupeptin). Total protein concentration was determined by the method of Bradford using the Protein Assay dye reagent (Bio-Rad Laboratories, Hercules, CA). Protein samples (20 μg) were subjected to SDS-PAGE and immunoblot analysis using anti-GFP (Promega, Madison, WI) or anti-HC-Pro-specific sera. Immunoreactions were detected using an alkaline phosphataselinked second antibody and a chemiluminescence procedure. Blots were exposed to x-ray film for different periods of time. Densitometry of bands was done using an Eagle Eye II system (Stratagene).

ACKNOWLEDGMENTS

We thank Christa Weathers for help in the initial *Agrobacterium* infiltration experiments and assistance in taking photographs of leaf tissue. We also thank Kristin Kasschau and Cesar Llave for helpful comments and advice during the course of this work.

Received December 19, 2000; returned for revision February 27, 2001; accepted March 16, 2001.

LITERATURE CITED

Anandalakshmi R, Pruss GJ, Ge X, Marathe R, Smith TH, Vance VB (1998) A viral suppressor of gene silencing in plants. Proc Natl Acad Sci USA 95: 13079–13084

Bass BL (2000) Double stranded RNA as a template for gene silencing. Cell 101: 235–238

Baulcombe DC (1999) Fast forward genetics based on virus-induced gene silencing. Curr Opin Plant Biol 2: 109–113

Bosher JM, Labouesse M (2000) RNA interference: genetic wand and genetic watchdog. Nat Cell Biol 2: E31–E36

Brigneti G, Voinnet O, Wan-Xiang L, Ding SW, Baulcombe DC (1998) Viral pathogenicity determinants are suppressors of transgene silencing. EMBO J 17: 6739–6746

Carrington JC (2000) RNA silencing: moving targets. Nature 408: 150–151

Carrington JC, Freed DD, Oh C-S (1990) Expression of potyviral polyproteins in transgenic plants reveals three proteolytic activities required for complete processing. EMBO J 9: 1347–1353

Chisholm ST, Mahajan SK, Whitham SA, Yamamoto ML, Carrington JC (2000) Cloning of the *Arabidopsis RTM1* gene, which controls restriction of long-distance movement of tobacco etch virus. Proc Natl Acad Sci USA 97: 489–494

Chuang CF, Meyerowitz EM (2000) Specific and heritable genetic interference by double stranded RNA in *Arabidopsis thaliana*. Proc Natl Acad Sci USA 97: 4985–4990

Dalmay T, Hamilton A, Rudd S, Angell S, Baulcombe DC (2000) An RNA-dependent RNA polymerase gene in *Arabidopsis* is required for posttranscriptional gene silencing mediated by a transgene but not by a virus. Cell 101: 543–553

Davis SJ, Vierstra RD (1998) Soluble, highly fluorescent variants of green fluorescent protein (GFP) for use in higher plants. Plant Mol Biol 36: 521–528

Fagard M, Vaucheret H (2000) Systemic silencing signals. Plant Mol Biol 43: 285–293

Hamilton AJ, Baulcombe DC (1999) A species of small antisense RNA in posttranscriptional gene silencing in plants. Science 286: 950–952

Hammond SM, Bernstein E, Beach D, Hannon GJ (2000) An RNA-directed nuclease mediates post-transcriptional gene silencing in *Drosophila* cells. Nature 404: 293–296

Hunter CP (2000) Gene silencing: shrinking the black box of RNAi. Curr Biol 10: 137–140

Jones JD, Shlumukov L, Carland F, English J, Scofield SR, Bishop GJ, Harrison K (1992) Effective vectors for transformation, expression of heterologous genes, and assaying transposon excision in transgenic plants. Transgenic Res 1: 285–297

Kasschau KD, Carrington JC (1998) A counter-defensive strategy of plant viruses: suppression of posttranscriptional gene silencing. Cell 95: 461–470

Kasschau KD, Carrington JC (2001) Long-distance movement and genome replication functions correlate with RNA silencing suppressor activity of potyvirus HC-Pro. Virology 284: (in press)

Llave C, Kasschau KD, Carrington JC (2000) Virus-encoded suppressor of posttranscriptional gene silencing targets a maintenance step in the silencing pathway. Proc Natl Acad Sci USA 97: 13401–13406

Marathe R, Anandalakshmi R, Smith TH, Pruss GJ, Vance VB (2000) RNA viruses as inducers, suppressors and targets of post-transcriptional gene silencing. Plant Mol Biol 43: 285–293

Meins F (2000) RNA degradation and models for posttranscriptional gene silencing. Plant Mol Biol 43: 261–273

Mourrain P, Beclin C, Elmayan T, Feuerbach F, Godon C, Morel JB, Jouette D, Lacombe AM, Nikic S, Picault N et al. (2000) *Arabidopsis* SGS2 and SGS3 genes are required for posttranscriptional gene silencing and natural virus resistance. Cell 101: 533–542

Restrepo MA, Freed DD, Carrington JC (1990) Nuclear transport of plant potyviral proteins. Plant Cell 2: 987–998

Schaad MC, Jensen P, Carrington JC (1997) Formation of plant RNA virus replication complexes on membranes: role of an endoplasmic reticulum-targeted viral protein. EMBO J 16: 4049–4059

Schweizer P, Pokorny J, Schulze-Lefert P, Dudler R (2000)

Technical advance: double-stranded RNA interferes with gene function at the single-cell level in cereals. Plant J 24: 895–903

Sijen T, Kooter JM (2000) Post-transcriptional gene-silencing: RNAs on the attack or on the defense? Bioessays 22: 520–531

Smith NA, Singh SP, Wang MB, Stoutjesdijk PA, Green AG, Waterhouse PM (2000) Total silencing by intron-spliced hairpin RNAs. Nature 407: 319–320

Voinnet O, Lederer C, Baulcombe DC (2000) A viral movement protein prevents spread of the gene silencing signal in *Nicotiana benthamiana*. Cell 103: 157–167

Voinnet O, Vain P, Angell S, Baulcombe DC (1998) Systemic spread of sequence-specific transgene RNA degradation in plants is initiated by localized introduction of ectopic promoterless DNA. Cell 95: 177–187

Waterhouse PM, Graham MW, Wang MB (1998) Virus resistance and gene silencing in plants can be induced by simultaneous expression of sense and antisense RNA. Proc Natl Acad Sci USA 95: 13959–13964

Zamore PD, Tuschl T, Sharp PA, Bartel DP (2000) RNAi: double-stranded RNA directs the ATP-dependent cleavage of mRNA at 21 to 23 nucleotide intervals. Cell 101: 25–33

Intestinal adenomas from $Apc^{Min/+}$;$Blm^{Cin/+}$ mice were evaluated for loss of heterozygosity (LOH) at the *Apc* locus, a feature typical of $Apc^{Min/+}$ adenomas (*24*, *25*). Five adenomas from $Apc^{Min/+}$;$Blm^{+/+}$ mice and 20 adenomas from $Apc^{Min/+}$;$Blm^{Cin/+}$ mice were analyzed (Fig. 2C). The mean ratio of the Apc^{+} to the Apc^{Min} allele in tumors from $Apc^{Min/+}$;$Blm^{Cin/+}$ mice was not different from that in tumors from $Apc^{Min/+}$;$Blm^{+/+}$ mice. Each was consistent with published values (*24*, *25*), demonstrating loss of the WT *Apc* allele in all tumors from *Blm* heterozygous mice.

We next investigated the mutational mechanisms responsible for loss of the normal *Apc* allele in the intestinal tumors by LOH analysis. *Apc* maps to chromosome 18 and is located on the genetic map at 15.0 centimorgans (*26*). We used quantitative polymerase chain reaction (PCR) with simple sequence length polymorphism markers (*19*) for three loci to examine allelic loss on chromosome 18 in our set of 25 tumors (Fig. 2C). Tumors in $Apc^{Min/+}$;$Blm^{+/+}$ mice and 18 of 20 tumors in $Apc^{Min/+}$;$Blm^{Cin/+}$ mice were characterized by LOH of *Apc* and all markers proximal and distal to *Apc* on chromosome 18 (Fig. 2C). Two tumors from $Apc^{Min/+}$;$Blm^{Cin/+}$ mice, of which one is shown, remained heterozygous at the proximal marker *D18Mit19* (Fig. 2C). These results indicate that *Apc* loss in $Apc^{Min/+}$ tumors with two WT *Blm* alleles is characterized by LOH of chromosome 18 but that in some $Blm^{Cin/+}$ tumors, loss of the normal *Apc* allele occurs by somatic recombination.

To test whether the tumors from $Apc^{Min/+}$;$Blm^{Cin/+}$ mice retained the WT *Blm* allele, we performed a quantitative PCR-based assay on 14 tumors. The ratio of the WT to the targeted allele in each tumor sample from $Apc^{Min/+}$;$Blm^{Cin/+}$ mice was not significantly different from that in adjacent normal tissue (Fig. 2D). Western blots of 10 tumor lysates from $Apc^{Min/+}$;$Blm^{Cin/+}$ mice evaluated with antiserum to COOH-terminus of BLM confirmed that BLM expression had been retained (fig. S3A). Similarly, immunofluorescence of MLV-induced lymphomas from $Blm^{Cin/+}$ mice demonstrated nuclear BLM staining (fig. S3B). These results suggest that mutation of the remaining WT *Blm* allele was not required for tumor formation in either T cells or intestinal tissues.

Mutation of one allele of *Blm* has measurable consequences for the phenotype of murine somatic cells and for the tumor susceptibility of the mouse. Our data demonstrate that *Blm* haploinsufficiency is sufficient to affect tumor formation in susceptible mice, and probably alter genomic stability. These effects have not been described in other targeted *Blm* mice (*12*, *13*). These data also suggest that *Blm* haploinsufficiency could promote tumor formation in tissues other than those studied here. Additionally, although none of the tumors in $Apc^{Min/+}$;$Blm^{Cin/+}$ mice were invasive at the 4-month end point of our experiments, it is possible that these tumors would progress to malignancy if given more time. Our results are also important for human populations: About 1 in 100 Ashkenazi Jews carry one mutant allele of *BLM* (*25*, *26*). An accompanying paper by Gruber *et al.* (*27*) demonstrates that carriers of BLM^{Ash} have a more than twofold increase in the occurrence of colorectal cancer. Together, these studies suggest that *Blm*/*BLM* mutation is an important modifier of intestinal cancer predisposition and that individuals carrying one mutant allele of *BLM* may have one of the noteworthy clinical hallmarks of BS—namely, increased cancer predisposition.

References and Notes

1. J. German, *Medicine* **72**, 393 (1993).
2. J. Groden, J. German, *Hum. Genet.* **90**, 360 (1992).
3. J. Groden, Y. Nakamura, J. German, *Proc. Natl. Acad. Sci. U.S.A.* **87**, 4315 (1990).
4. N. A. Ellis *et al.*, *Cell* **83**, 655 (1995).
5. N. A. Ellis, M. Proytcheva, M. M. Sanz, T.-Z. Ye, J. German, *Am. J. Hum. Genet.* **65**, 1368 (1999).
6. A. Bahr, F. De Graeve, C. Kedinger, B. Chatton, *Oncogene* **17**, 2565 (1998).
7. J. K. Karow, A. Constantinou, J. L. Li, S. C. West, I. D. Hickson, *Proc. Natl. Acad. Sci. U.S.A.* **97**, 6504 (2000).
8. H. Sun, J. K. Karow, I. D. Hickson, N. Maizels, *J. Biol. Chem.* **273**, 27587 (1998).
9. G. Langland *et al.*, *Cancer Res.* **62**, 2766 (2002).
10. L. Shahrabani-Gargir, *Genet. Test.* **2**, 293 (1998).
11. L. Li, C. Eng, R. J. Densnick, J. German, N. A. Ellis, *Mol. Genet. Metab.* **64**, 286 (1998).
12. N. Chester, F. Kuo, C. Kozak, C. D. O'Hara, P. Leder, *Genes Dev.* **12**, 3382 (1998).
13. G. Luo *et al.*, *Nature Genet.* **26**, 424 (2000).
14. J. Groden, unpublished data.
15. J. German, N. A. Ellis, M. Proytcheva, *Clin. Genet.* **49**, 223 (1996).
16. M. P. Rosin, J. German, *Hum. Genet.* **71**, 187 (1985).
17. M. M. Sanz, J. German, unpublished data.
18. R. H. Martin, A. Rademaker, J. German, *Am. J. Hum. Genet.* **55**, 1242 (1994).
19. Materials and methods are available as supporting material on *Science* Online.
20. A. M. Lowy *et al.*, *Gastroenterology* **121**, 435 (2001).
21. A. R. Moser, H. C. Pitot, W. F. Dove, *Science* **247**, 322 (1990).
22. L. K. Su *et al.*, *Science* **256**, 668 (1992).
23. C57BL/6J-$Apc^{Min/+}$ male mice (from the Jackson Laboratory) were mated to $Blm^{Cin/+}$ female mice (backcrossed to 129/SvEv to the N_3 generation) to obtain progeny that were $Apc^{Min/+}$;$Blm^{+/+}$ or $Apc^{Min/+}$;$Blm^{Cin/+}$. Mice were genotyped for the Apc^{Min} mutation, and tumors were quantified as previously described by C. L. Wilson *et al.* [*Proc. Natl. Acad. Sci. U.S.A.* **94**, 1402 (1997)].
24. D. B. Levy *et al.*, *Cancer Res.* **54**, 5953 (1994).
25. C. Luongo, A. R. Moser, S. Gledhill, W. F. Dove, *Cancer Res.* **54**, 5947 (1994).
26. C. Luongo *et al.*, *Genomics* **15**, 3 (1993).
27. S. S. Gruber *et al.*, *Science* **297**, 2013 (2002).

28. We thank the University of Cincinnati Comparative Pathology and Gene Targeting Facilities, J. Mante, and T. Reichling for assistance. Supported by the Ohio Cancer Research Foundation; the National Cancer Institute Mouse Models of Human Cancer Consortium (grant CA84291); the Center for Environmental Genetics at the University of Cincinnati (grant ES06096); the National Institutes of Health [grants CA63507 (J.G.) and CA88460 (K.H.G.)]; and the Howard Hughes Medical Institute.

Supporting Online Material

www.sciencemag.org/cgi/content/full/297/5589/2051/DC1
Materials and Methods
Figs. S1 to S3
Table S1

24 May 2002; accepted 19 August 2002

Cleavage of *Scarecrow-like* mRNA Targets Directed by a Class of *Arabidopsis* miRNA

Cesar Llave, Zhixin Xie, Kristin D. Kasschau, James C. Carrington*

Micro-RNAs (miRNAs) are regulatory molecules that mediate effects by interacting with messenger RNA (mRNA) targets. Here we show that *Arabidopsis thaliana* miRNA 39 (also known as miR171), a 21-ribonucleotide species that accumulates predominantly in inflorescence tissues, is produced from an intergenic region in chromosome III and functionally interacts with mRNA targets encoding several members of the *Scarecrow-like* (*SCL*) family of putative transcription factors. miRNA 39 is complementary to an internal region of three *SCL* mRNAs. The interaction results in specific cleavage of target mRNA within the region of complementarity, indicating that this class of miRNA functions like small interfering RNA associated with RNA silencing to guide sequence-specific cleavage in a developmentally controlled manner.

Micro-RNAs in eukaryotes are ~21- to 22-ribonucleotide RNAs that arise from short stem-loop precursors through the activity of the double-stranded ribonuclease Dicer (*1*–*6*). The miRNAs from *lin-4* and *let-7* genes are involved in translational control through interaction with 3′-proximal sequences in target mRNAs in *Caenorhabditis elegans* (*7*–*11*). However, the range of functions for other miRNAs in plants, animals, and microorganisms has yet to be determined.

Arabidopsis contains numerous small RNAs, many of which resemble miRNAs identified in animals (*12*, *13*). Several of

these, including miRNA 39, have sequence identity or complementarity to mRNAs for protein-coding genes. miRNA 39 accumulates predominantly in inflorescence tissue and was predicted to arise from a precursor gene in an intergenic region (IGR) in chromosome III (*12*, *13*). The miRNA 39 sequence and predicted stem-loop structure of the putative precursor are conserved in the genome of rice (*Oryza sativa*) (*13*). We detected miRNA 39–like species in *Arabidopsis*, rice, and *Nicotiana benthamiana* by blot assay (Fig. 1A). The *Arabidopsis*, rice, and *N. benthamiana* miRNA 39 accumulated to relatively high levels in inflorescence and flower tissues (Fig. 1A, lanes 3, 6, and 8) and to lower or nondetectable levels in leaf and stem tissue (Fig. 1A, lanes 1, 2, 4, 5, and 7).

The miRNA 39 sequence in *Arabidopsis* is perfectly complementary to an internal sequence in mRNAs of three members [*SCL6-II* (locus At2g45160), *SCL6-III* (locus At3g60630), and *SCL6-IV* (locus At4g00150)] of the *Scarecrow-like* family of putative transcription factors (*12*, *13*). Four *SCL* genes in rice have complementarity to miRNA 39 (*13*). Members of the *SCL* family control a wide range of developmental processes, including radial patterning in roots and hormone signaling (*14*–*17*). No other small RNAs related to sequences from the 3′-proximal regions of *SCL6-III* or *SCL6-IV* genes were detected in *Arabidopsis* leaf, stem, or inflorescence tissues by blot assay [fig. S1A (*18*)], indicating that miRNA 39 was not part of a larger small interfering RNA (siRNA) population resulting from general RNA silencing triggered against broader segments of the *SCL* mRNAs. Blot assays indicated that *SCL6-III* and *SCL6-IV* genes were expressed in leaf, stem, and inflorescence tissues (Fig. 1B), although *SCL6-III* and *SCL6-IV* mRNAs were most abundant in inflorescence tissue (Fig. 1B, lanes 5, 6, 13, and 14). In addition to full-length mRNAs [designated SCL6-III(a) and SCL6-IV(a) RNAs], shorter RNAs [SCL6-III(b) and SCL6-IV(b)] of ~1.4 and ~1.3 kilobases (kb), respectively, were detected with a 3′-proximal probe in extracts from inflorescence tissue but not in extracts from stems or leaves (Fig. 1B, lanes 5, 6, 13, and 14).

The 5′ ends of SCL6-III(b) and SCL6-IV(b) RNAs were mapped by 5′ RACE (rapid amplification of cDNA ends) to positions corresponding to the middle of the respective sequences complementary to miRNA 39 (Fig. 1B). The 5′-RACE reactions involved ligation of an adapter to the 5′ end without enzymatic pretreatment, suggesting that both RNAs contained a ligation-competent 5′ monophosphate rather than a conventional 5′ cap. These results are consistent with a model in which the SCL6-III(b) and SCL6-IV(b) RNAs arise by sequence-specific cleavage of the full-length mRNAs at a site directed by miRNA 39. In effect, miRNA 39 may function like a single siRNA (*19*), produced in trans from a miRNA 39 precursor gene, that guides cleavage of target *SCL* mRNAs. As siRNA-guided cleavage of silencing targets occurs at positions centered in the middle of siRNA-target RNA duplexes (*20*), both siRNA-guided and miRNA 39–guided cleavage might occur by a common mechanism within a sequence-specific nucleolytic complex termed RISC (RNA-induced silencing complex) (*21*, *22*). This model predicts that accumulation of SCL6-III(b) and SCL6-IV(b) RNAs will correlate with accumulation of miRNA 39, which is consistent with the tissue-specific distribution patterns of miRNA 39 and SCL6-III(b) and SCL6-IV(b) RNAs (*12*) (Fig. 1, A and B).

We tested the hypothesis that miRNA 39 functions to direct cleavage of *SCL* mRNAs with an *Agrobacterium*-mediated delivery (Agro-inoculation) system to coexpress miRNA 39 and SCL6-IV target mRNA in *N. benthamiana* leaf tissue. We reasoned that a miRNA 39 precursor could be produced through transcription of the miRNA 39–containing IGR, either with an endogenous miRNA 39 promoter or with a 35*S* promoter, followed by Dicer-like processing (*13*) of the precursor in *N. benthamiana*. Three constructs with the complete miRNA 39–containing IGR, or empty vector as a control, were coexpressed with the *SCL6-IV* construct (*35S:SCL6-IV*). Two of the constructs (*35S:IGR-mi39* and *35S:AS-IGR-mi39*) contained

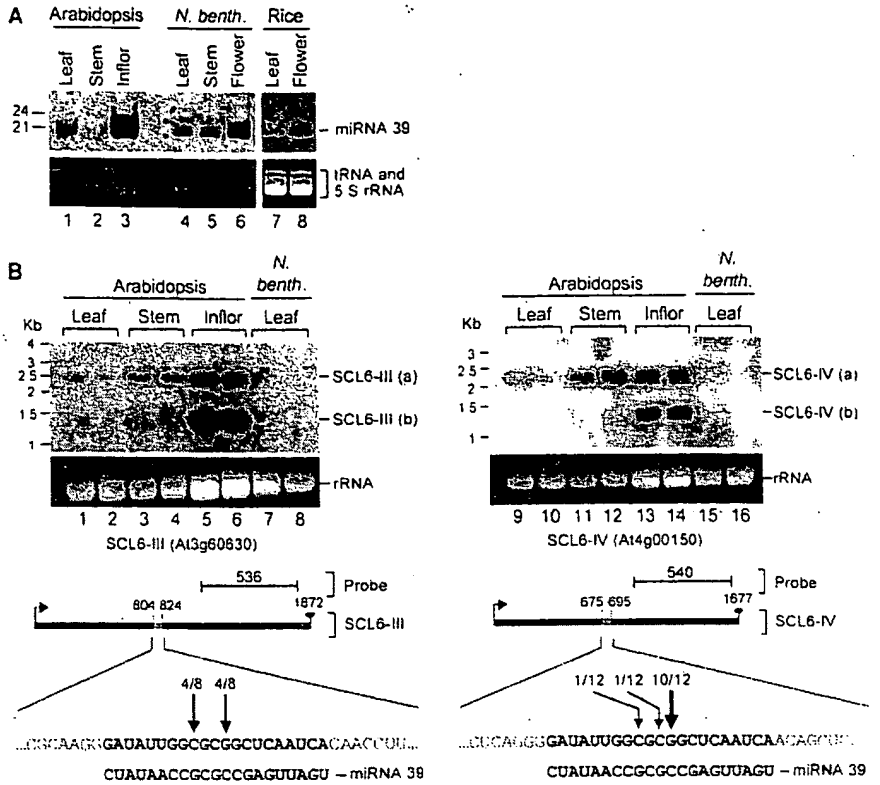

Fig. 1. Expression of *SCL* genes and miRNA 39. (**A**) RNA blot analysis of miRNA 39 from *Arabidopsis* and *N. benthamiana* leaf, stem, and inflorescence/flower tissue and from rice (*O. sativa*) leaf and flower tissue. (**B**) RNA blot analysis of *SCL6-III* (left) and *SCL6-IV* (right) mRNAs. Normalized (10 μg per lane) RNA samples from *Arabidopsis* leaf, stem, and inflorescence tissue were analyzed in duplicate. The proportion of total RNA represented by the large cytoplasmic ribosomal RNA (rRNA) (shown in ethidium bromide–stained gels) differs between tissue types in *Arabidopsis*, which accounts for the more abundant rRNA in the inflorescence samples. The protein-coding regions (nucleotide numbering begins at the start codon) and the locations of the sequences complementary to miRNA 39 are shown in the expanded diagrams. *SCL6-III*– and *SCL6-IV*–specific probes detected both full-length mRNA [SCL6-III(a) and SCL6-IV(a)] and shorter RNA [SCL6-III(b) and SCL6-IV(b)] in inflorescence tissue. The positions corresponding to the 5′ ends of the SCL6-III(b) and SCL6-IV(b) RNAs determined by 5′ RACE, and the number of 5′-RACE clones corresponding to each site, are indicated by arrows.

Center for Gene Research and Biotechnology, and Department of Botany and Plant Pathology, Oregon State University, Corvallis, OR 97331, USA.

*To whom correspondence should be addressed. E-mail: carrington@orst.edu

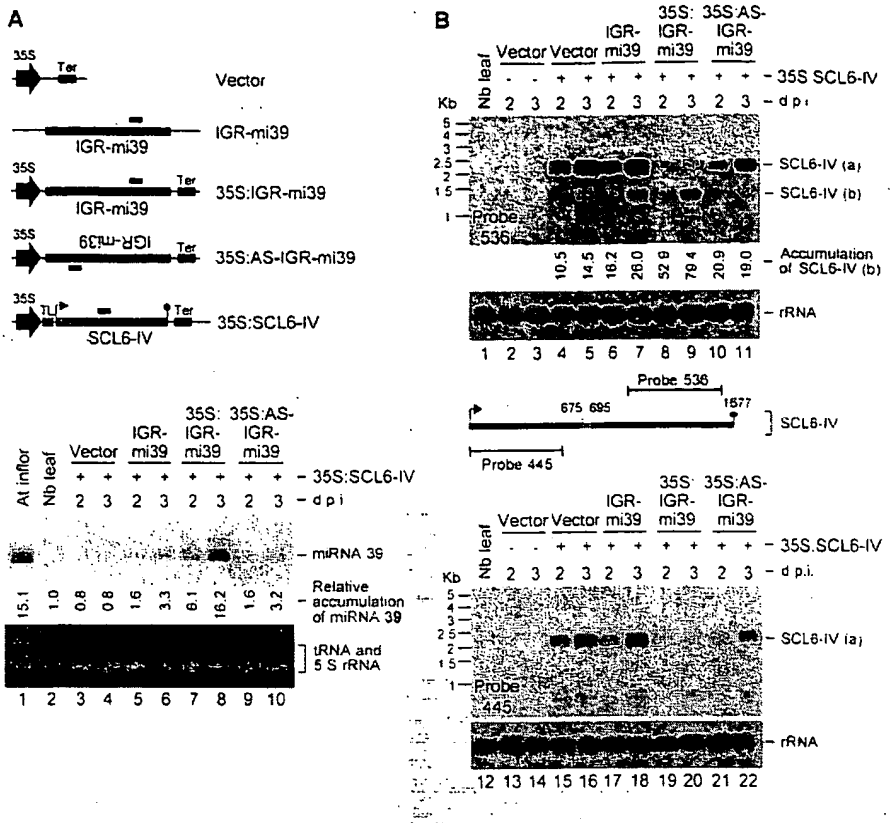

Fig. 2. Cleavage of *SCL6-IV* mRNA is directed by miRNA 39. (A) Constructs containing the miRNA 39–containing IGR and the *SCL6-IV* coding sequence were co–Agro-inoculated in *N. benthamiana* leaves, and normalized extracts were tested for miRNA 39 by RNA blot assay 2 and 3 days postinoculation (d p.i.). (B) Analysis of SCL6-IV (a) and (b) RNA forms in normalized extracts from co–Agro-inoculated tissue by RNA blot assay with probes corresponding to 3′ (top) or 5′ (bottom) regions of the *SCL6-IV* coding sequence. The amount of SCL6-IV(b) RNA, expressed as a percentage of total SCL6-IV RNA [(a) + (b)], is indicated for each sample. The blots were stripped and reanalyzed with a cytoplasmic rRNA probe. The position of sequence complementary to miRNA 39 is indicated in gray in the diagram. The size of the SCL6-IV(b) RNA (~1.3 kb) corresponds to the 3′-proximal SCL6-IV sequence (~1.0 kb) plus the 3′-untranslated sequence (~0.3 kb). At, *A. thaliana*; Nb, *N. benthamiana*.

a 35*S* promoter for production of synthetic IGR transcripts of sense (relative to miRNA 39) or antisense orientation, respectively, and one (*IGR-mi39*) contained the IGR sequence without a 35*S* promoter (Fig. 2A). A basal level of endogenous miRNA 39 was detected in nontreated leaves (Fig. 2A, lane 2) and in leaves that were co–Agro-inoculated with *35S:SCL6-IV* and the empty vector (lanes 3 and 4). High levels of miRNA 39 were produced after co–Agro-inoculation with the sense-oriented *35S:IGR-mi39* construct (Fig. 2A, lanes 7 and 8), indicating that the synthetic RNA transcript was recognized accurately by a Dicer-like enzyme (*13*). Data showing that miRNA 39 accumulation in these experiments was not the result of generalized RNA silencing of *SCL* genes or the 35*S* promoter–driven constructs are provided in the SOM text (*18*). Only low levels of miRNA 39 above background were detected in tissues expressing the antisense-oriented *35S:AS-IGR-mi39* (Fig. 2A, lanes 9 and 10) or IGR-mi39 constructs (lanes 5 and 6). The low levels of miRNA 39 directed by the *IGR-mi39* construct suggest that the IGR sequence contains relatively weak regulatory sequences for transcription of the miRNA 39 precursor gene, or that the miRNA 39 precursor gene is suppressed, in *N. benthamiana* leaf tissue.

Coexpression of *35S:IGR-mi39* and *35S:SCL6-IV* resulted in internal cleavage of the *SCL6-IV* mRNA (Fig. 2B, top, lanes 8 and 9).

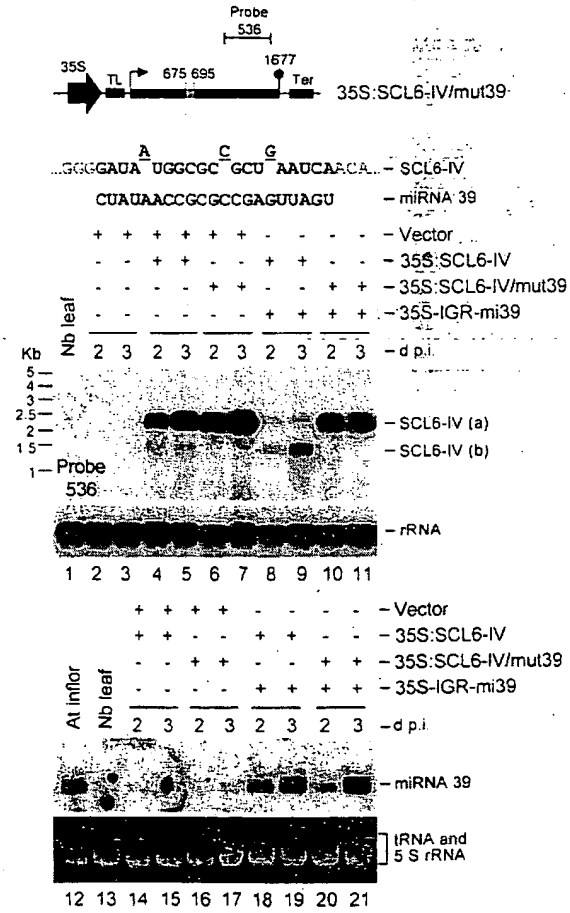

Fig. 3. Cleavage of *SCL6-IV* mRNA requires sequence complementarity to miRNA 39. Mutations (underlined) were introduced into the *35S:SCL6-IV/mut39* construct, and wild-type and mutant constructs were co–Agro-inoculated with the *35S:IGR-mi39* construct in *N. benthamiana*. SCL6-IV RNA forms (top) and miRNA 39 (bottom) in extracts at 2 and 3 d p.i. were analyzed by blot assay. The SCL6-IV RNA blot was hybridized with a probe corresponding to the 3′ end of the *SCL6-IV* coding region and then reanalyzed with a cytoplasmic rRNA probe.

About 53 and 79% of the *SCL6-IV*–related RNA detected 2 and 3 days postinfiltration, respectively, corresponded to the SCL6-IV(b) RNA product. Relatively small proportions of *SCL6-IV* mRNA were cleaved after coexpression with empty vector (Fig. 2B, top, lanes 4 and 5), *IGR-mi39* (lanes 6 and 7), and *35S:AS-IGR-mi39* constructs (lanes 10 and 11), which can be explained by the basal or low levels of miRNA 39 in these samples. No cleavage products were detected with the SCL6-IV 5′-end probe (Fig. 2B), suggesting that the 5′ fragment was less stable than the 3′ fragment [SCL6-IV(b)]. Identical results were obtained when the *SCL6-III* mRNA was used as a target in coexpression assays (*23*).

To determine whether cleavage of *SCL6-IV* mRNA depends on perfect complementarity with miRNA 39, we introduced three mismatches into the sequence complementary to miRNA 39 in *SCL6-IV* RNA (construct *35S:SCL6-IV/mut39*) (Fig. 3). Whereas the wild-type *SCL6-IV* mRNA was cleaved efficiently in the presence of the miRNA 39–producing *35S:IGR-mi39* construct (Fig. 3, lanes 8, 9, 18, and 19), the *SCL6-IV/mut39* mRNA was completely resistant to cleavage (lanes 10, 11, 20, and 21). Furthermore, the low level of cleavage of *SCL6-IV* mRNA in the presence of the empty vector construct was inhibited by the mutations (Fig. 3, lanes 4 to 7), confirming that this activity was due to low levels of endogenous miRNA 39 in *N. benthamiana* tissue.

The finding of miRNA-directed cleavage of several *SCL* mRNA targets in *Arabidopsis* indicates that there are at least two functional classes of miRNAs. Members of the small temporal RNA (stRNA)–like class, including *C. elegans lin-4* and *let-7* miRNAs, downregulate translation of target mRNAs but do not direct RNA target degradation or site-specific cleavage (*7*, *8*, *10*, *11*). The stRNA class members do not interact with perfect complementarity to their natural targets, which may explain why they do not exhibit siRNA-like activity (*24*). In contrast, members of a class represented by *Arabidopsis* miRNA 39 interact with perfect complementarity and appear to mimic siRNA function to guide cleavage. We propose that miRNA 39 incorporates into a RISC-like complex identical or similar to the RISC complex that mediates target cleavage during RNA silencing (*21*, *22*). Support for this concept also comes from the finding that engineered miRNA-target combinations with perfect complementarity result in target RNA cleavage (*25*, *26*). Finally, miRNA 39–guided cleavage of mRNAs has several possible consequences, including developmentally coordinated inactivation of *SCL* mRNAs. Internal cleavage might also generate RNA products with novel characteristics or coding potential for truncated SCL proteins. Given the numbers of miRNAs that were recently discovered in eukaryotes (*4–6*, *12*, *13*, *27*, *28*), additional members will likely be added to each class.

References and Notes

1. E. Bernstein, A. A. Caudy, S. M. Hammond, G. J. Hannon, *Nature* **409**, 363 (2001).
2. G. Hutvágner *et al.*, *Science* **293**, 834 (2001).
3. R. F. Ketting *et al.*, *Genes Dev.* **15**, 2654 (2001).
4. M. Lagos-Quintana, R. Rauhut, W. Lendeckel, T. Tuschl, *Science* **294**, 853 (2001).
5. N. C. Lau, E. P. Lim, E. G. Weinstein, D. P. Bartel, *Science* **294**, 858 (2001).
6. R. C. Lee, V. Ambros, *Science* **294**, 862 (2001).
7. R. C. Lee, R. L. Feinbaum, V. Ambros, *Cell* **75**, 843 (1993).
8. B. Wightman, I. Ha, G. Ruvkun, *Cell* **75**, 855 (1993).
9. E. G. Moss, R. C. Lee, V. Ambros, *Cell* **88**, 637 (1997).
10. B. J. Reinhart *et al.*, *Nature* **403**, 901 (2000).
11. F. J. Slack *et al.*, *Mol. Cell* **5**, 659 (2000).
12. C. Llave, K. D. Kasschau, M. A. Rector, J. C. Carrington, *Plant Cell* **14**, 1605 (2002).
13. B. J. Reinhart, E. G. Weinstein, M. W. Rhoades, B. Bartel, D. P. Bartel, *Genes Dev.* **16**, 1616 (2002).
14. L. DiLaurenzio *et al.*, *Cell* **86**, 423 (1996).
15. A. L. Silverstone, C. N. Ciampaglio, T. Sun, *Plant Cell* **10**, 155 (1998).
16. C. Bolle, C. Koncz, N. H. Chua, *Genes Dev.* **14**, 1269 (2000).
17. Y. Helariutta *et al.*, *Cell* **101**, 555 (2000).
18. Materials and methods are available as supporting material on *Science* Online.
19. A. J. Hamilton, D. C. Baulcombe, *Science* **286**, 950 (1999).
20. S. M. Elbashir, W. Lendeckel, T. Tuschl, *Genes Dev.* **15**, 188 (2001).
21. S. M. Hammond, E. Bernstein, D. Beach, G. J. Hannon, *Nature* **404**, 293 (2000).
22. S. M. Hammond, S. Boettcher, A. A. Caudy, R. Kobayashi, G. J. Hannon, *Science* **293**, 1146 (2001).
23. C. Llave, J. C. Carrington, unpublished data.
24. G. Ruvkun, *Science* **294**, 797 (2001).
25. M. T. McManus, C. P. Petersen, B. B. Haines, J. Chen, P. A. Sharp, *RNA* **8**, 842 (2002).
26. G. Hutvágner, P. D. Zamore, *Science* **297**, 2056 (2002); published online 1 August 2002 (10.1126/science.1073827).
27. Z. Mourelatos *et al.*, *Genes Dev.* **16**, 720 (2002).
28. E. C. Lai, *Nature Genet.* **30**, 363 (2002).

29. We thank L. Johansen, M. Rector, and B. Shaffer for valuable comments and technical support. We are also grateful to J. Valkonen and J. Kreuze for helpful suggestions on 5′-RACE procedures and D. Olszyk for providing rice tissue. C.L. was the recipient of a postdoctoral fellowship from the Ministerio de Educación y Cultura (Spain). This work was supported by grant MCB-0209836 from the National Science Foundation, grants AI27832 and AI43288 from NIH, and grant NRI 2002-35319-11560 from the U.S. Department of Agriculture.

Supporting Online Material

www.sciencemag.org/cgi/content/full/297/5589/2053/DC1
Materials and Methods
SOM Text
Fig. S1
Table S1
References

18 July 2002; accepted 31 July 2002

A microRNA in a Multiple-Turnover RNAi Enzyme Complex

György Hutvágner and Phillip D. Zamore*

In animals, the double-stranded RNA-specific endonuclease Dicer produces two classes of functionally distinct, tiny RNAs: microRNAs (miRNAs) and small interfering RNAs (siRNAs). miRNAs regulate mRNA translation, whereas siRNAs direct RNA destruction via the RNA interference (RNAi) pathway. Here we show that, in human cell extracts, the miRNA *let-7* naturally enters the RNAi pathway, which suggests that only the degree of complementarity between a miRNA and its RNA target determines its function. Human *let-7* is a component of a previously identified, miRNA-containing ribonucleoprotein particle, which we show is an RNAi enzyme complex. Each *let-7*–containing complex directs multiple rounds of RNA cleavage, which explains the remarkable efficiency of the RNAi pathway in human cells.

Two types of 21- to 23-nucleotide (nt) RNAs are produced by the multidomain ribonuclease (RNase) III enzyme Dicer: small interfering RNAs (siRNAs) from long double-stranded RNA (*1*, *2*) and microRNAs (miRNAs) from ~70-nt hairpin precursor RNAs whose expression is often developmentally regulated (*3–8*). siRNAs direct the cleavage of complementary mRNA targets, a process known as RNA interference (RNAi) (*9*). Target RNA cleavage is catalyzed by the RNA-induced silencing complex (RISC), which acts as an siRNA-directed endonuclease, cleaving the target RNA across from the center of the complementary siRNA strand (*10*, *11*). Assembly of the RISC is adenosine triphosphate (ATP) dependent and precedes target recognition (*10*, *12*). Unlike siRNAs, miRNAs are single stranded and pair with target mRNAs that contain sequences only partially complementary to the miRNA and repress mRNA translation without altering mRNA stability (*13–19*). Although at least 135 miRNAs have been identified collectively from *Caenorhabditis elegans*, *Drosophila melanogaster*, and humans, none is fully complementary to

Department of Biochemistry and Molecular Pharmacology, University of Massachusetts Medical School, Lazare Research Building, Room 825, 364 Plantation Street, Worcester, MA 01605, USA.

*To whom correspondence should be addressed. E-mail: phillip.zamore@umassmed.edu.